

University of Kent

School of Biosciences

**Characterising the structure and
activity of the Ebola virus Delta Peptide**

Biochemistry MSc Research

Eleanor Towler

2021

Supervisor: Dr Jose Ortega-Roldan

Word count: 21,763

Declaration

No part of this thesis has been submitted in support of an application for any degree or qualification of the University of Kent or any other University or institute of learning.

Eleanor Towler

December 2021

Acknowledgements

I would like to thank my supervisor Dr. Jose Ortega-Roldan of the University of Kent School of Biosciences for his support and guidance throughout this project. I would also like to thank all the members of the Ortega lab for their continuous help and kindness, and for teaching me new techniques. This project wouldn't have been possible without all of your assistance and advice.

Collaborations with other laboratories have also greatly assisted me. I would particularly like to thank Dr. Gary Thompson from the Wellcome Trust Biomolecular NMR Facility for his teaching and knowledge of the NMR spectrometer. Diego Cantoni for his work on the UV microscopy membrane insertion assay and the short DP fragment dye leakage assay. Kevin Howland of the Biomolecular Science Facility of the University of Kent for use of the HPLC and mass spectrometer.

Finally, my wonderful family and friends who have provided me with endless support and encouragement throughout my studies.

Contents

| | |
|--|----|
| I. List of figures..... | 5 |
| II. List of tables..... | 6 |
| III. Abbreviations..... | 6 |
| IV. Abstract | 8 |
| <u>Chapter 1- Introduction</u> | |
| 1.1. Ebola virus background and history..... | 8 |
| 1.2. Ebola virus transmission..... | 10 |
| 1.3. Clinical presentation of disease..... | 11 |
| 1.4. Proteins of the Ebola virus..... | 13 |
| 1.5. Viroporins..... | 14 |
| 1.6. DP structure..... | 15 |
| 1.7. DP function..... | 17 |
| 1.8. Project outline..... | 18 |
| <u>Chapter 2- Delta peptide growth and purification optimisation</u> | |
| 2.1. Introduction..... | 20 |
| 2.2. Methods | |
| - 2.2.1. Transformation..... | 22 |
| - 2.2.2. pCold construct growth and induction..... | 22 |
| - 2.2.3. pCold construct peptide extraction and purification- Cell lysis, centrifugation, Ni IMAC, dialysis and TEV cleavage, SEC and SDS PAGE gels..... | 23 |
| - 2.2.4 New construct Growth and induction..... | 25 |
| - 2.2.5. New construct purification- Guanidine purification, Ni IMAC, dialysis, peptide cleavage and RP HPLC..... | 26 |
| 2.3 Results | |
| - 2.3.1. Introduction..... | 28 |
| - 2.3.2. GFP DP construct- Ni IMAC column..... | 31 |
| - 2.3.3. GFP DP construct- TEV cleavage..... | 32 |
| - 2.3.4. GFP DP construct- SEC elutions..... | 33 |
| - 2.3.5. New construct- Expression tests..... | 34 |
| - 2.3.6. New construct- Ni IMAC columns..... | 35 |

| | |
|---|-----------|
| - 2.3.7. New construct- Chemical cleavage..... | 36 |
| - 2.3.8. New construct- RP HPLC..... | 37 |
| 2.4. Discussion..... | 40 |
| <u>Chapter 3- Delta Peptide structure</u> | |
| 3.1. Methods | |
| - 3.1.1. NMR..... | 43 |
| 3.1.1.1. Isotopically labelled growth..... | 43 |
| 3.1.1.2. Sample optimisation..... | 44 |
| 3.1.1.3 Experiment optimisation..... | 44 |
| 3.1.1.4. Lipid experiments..... | 45 |
| - 3.1.2. CD..... | 45 |
| 3.2. Results | |
| - 3.2.1. Expression and purification of ¹⁵ N labelled protein..... | 46 |
| - 3.2.2. NMR sample optimisation..... | 47 |
| - 3.2.3. NMR experiment optimisation..... | 50 |
| - 3.2.4. NMR lipids experiments..... | 53 |
| - 3.2.5. CD..... | 56 |
| 3.3. Discussion | |
| - 3.3.1. NMR sample optimisation..... | 59 |
| - 3.3.2. NMR experiment optimisation..... | 61 |
| - 3.3.3. NMR lipid experiments..... | 62 |
| - 3.3.4. CD..... | 64 |
| <u>Chapter 4- Delta peptide activity</u> | |
| 4.1. Introduction..... | 68 |
| 4.2. Methods | |
| - 4.2.1. UV membrane insertion assay..... | 70 |
| - 4.2.2. Dye leakage assay..... | 70 |
| 4.3. Results | |
| - 4.3.1. UV membrane insertion assay..... | 72 |
| - 4.3.2. Dye leakage assay..... | 73 |
| 4.4. Discussion..... | 78 |

Chapter 5 Conclusion

- 5.1. Structure.....83
- 5.2. Activity.....84
- 5.3. Future work.....86

Chapter 6- Bibliography.....87

I. List of figures

- Figure 1- Map of Ebola virus outbreaks and their spread.
- Figure 2- Diagram of proteins encoded by Ebola virus.
- Figure 3- Helical wheel predictions of DP's C-terminal portion and lytic peptide NSP4 of Rotavirus.
- Figure 4- Plasmid map of pCOLD GFP DP construct.
- Figure 5- Plasmid map of the new DP construct.
- Figure 6- GFP construct SDS PAGE gel of Ni IMAC gravity column fractions.
- Figure 7- GFP construct mass spectrometry analysis of the sample after TEV cleavage.
- Figure 8- GFP construct SDS PAGE gel of elutions from the largest absorbance peak of the SEC column.
- Figure 9- New construct SDS PAGE gels of protein expression tests.
- Figure 10- New construct SDS PAGE gel of Ni IMAC fractions.
- Figure 11- New construct SDS PAGE gels of cleavage tests.
- Figure 12- New construct RP HPLC elutions chromatogram.
- Figure 13- New construct SDS PAGE gel of RP HPLC elutions.
- Figure 14- New construct mass spectrometry analysis of the third elution from the RP HPLC.
- Figure 15- Overview of the optimised growth and purification of the new construct.
- Figure 16- SDS PAGE gel of Ni IMAC columns of ¹⁵N labelled peptide.
- Figure 17- HSQC NMR spectrum of DP dissolved in 30% acetic acid.
- Figure 18- HSQC NMR spectrum of DP LMNG detergent solubilisation test.
- Figure 19- BEST TROSY NMR spectrum of DP dissolved in 40% methanol D4.
- Figure 20- HMQC SOFAST NMR spectrum of DP dissolved in 40% methanol D4.
- Figure 21- HSQC NMR spectrum of DP dissolved in 40% methanol D4.
- Figure 22- BEST TROSY NMR spectrum of DP dissolved in 40% methanol D4

- Figure 23- BEST TROSY NMR spectrum of DP dissolved in 40% methanol D4 overlaid with DP sample with LMNG asolectin bicelles.
- Figure 24- BEST TROSY NMR spectrum of DP dissolved in 40% methanol D4 overlaid with DP sample with asolectin vesicles.
- Figure 25- BEST TROSY NMR spectrum of DP dissolved in 40% methanol D4 with asolectin vesicles overlaid with DP sample with asolectin vesicles and LMNG.
- Figure 26- FarUV CD plots of oxidised and reduced DP in 40% methanol.
- Figure 27- FarUV CD plots of reduced DP in 40% methanol with and without asolectin vesicles.
- Figure 28- FarUV CD plots of oxidised DP in 40% methanol with and without asolectin vesicles.
- Figure 29- Standard curves of protein secondary structures.
- Figure 30- UV microscopy insertion assay images of asolectin GUVs with labelled DP.
- Figure 31- Fluorescence intensity of dye leakage assays of full-length reduced DP over a range of concentrations.
- Figure 32- Fluorescence intensity of dye leakage assays of full-length oxidised DP over a range of concentrations.
- Figure 33- Percentage membrane permeability caused by reduced and oxidised full-length DP.
- Figure 34- Percentage membrane permeability caused by reduced and oxidised short DP fragment and full-length DP.

II. List of tables

- Table 1- K2D3 database predictions of secondary structure composition of DP in 40% methanol.
- Table 2- Optimised NMR conditions and settings for DP NMR.
- Table 3- Percentage membrane permeabilization caused by 50 μ M of each peptide sample

III. Abbreviations

- DP- Delta Peptide
- NMR- Nuclear magnetic resonance
- CD- Circular dichroism
- sGP- small glycoprotein

- ssGP- small soluble glycoprotein
- NSP4- Non-structural protein 4
- RP HPLC- Reversed phase high pressure liquid chromatography
- IPTG- Isopropyl β -D-1-thiogalactopyranoside
- TM- Transmembrane
- LB- Luria Bertani media
- Rpm- Revolutions per minute
- DTT- Dithiothreitol
- Ni IMAC- Nickel Immobilized metal affinity chromatography
- CV- Column volumes
- SEC- Size exclusion chromatography
- SDS PAGE- Sodium dodecyl sulphate-polyacrylamide gel electrophoresis
- GFP- Green fluorescent protein
- TFA- trifluoroacetic acid
- HFIP- 1,1,1,3,3,3 Hexafluoro-2-propanol
- TEV- Tobacco Etch Virus nuclear-inclusion-a endopeptidase
- HCl- Hydrochloric acid
- MW- molecular weight
- DSS- Sodium trimethylsilylpropanesulfonate
- GUVs- giant unilamellar vesicles
- HMQC SOFAST- Heteronuclear Multiple Quantum Coherence Band-Selective Optimized Flip Angle Short Transient
- HSQC- Heteronuclear Single Quantum Coherence
- BEST TROSY- Best Transverse relaxation-optimised Spectroscopy⁷
- ER- Endoplasmic reticulum
- LMNG- Lauryl maltose neopentyl glycol
- DHPC- Dihexanoylphosphatidylcholine
- TFE- Tetrafluoroethylene
- Rf- resonance frequency

IV. Abstract

The Ebola virus is a highly pathogenic virus that emerged in 1976 and remains a pressing research target due to its rapid transmission and potential to cause widespread, fatal pandemics. The Ebola virus encodes seven proteins produced following infection that aid with its replication and infection of further cells. One of these proteins is a small peptide called Delta Peptide (DP) which is produced as a result of the cleavage of a glycoprotein following RNA editing. DP is one of the few Ebola proteins whose structure remains unsolved and its function is widely unknown. It is predicted that DP behaves as a Viroporin. The aim of this project was to investigate the activity of DP and how this may relate to or be dependent on its structure. DP activity was investigated through the use of dye leakage assays and a UV microscopy membrane insertion assay. These confirm predictions that DP inserts into asolectin lipid membranes and forms pores to permeabilize the membrane. DP has also been predicted to have a mainly α -helical structure using circular dichroism (CD) and nuclear magnetic resonance (NMR). The NMR experiments also demonstrate protein-lipid interactions occurring when DP was added to asolectin vesicles and suggest a structural change occurred. This project concluded that DP is likely an α -helical peptide able to insert into asolectin membranes causing Viroporin like permeabilization. It also indicates that this membrane permeabilization is possible when DP is in its oxidised or reduced state and in the absence of its C-terminal portion and Trp25.

1. Introduction

1.1 Ebola virus background and history

Ebola virus is a highly pathogenic species of the Filoviridae Ebolaviruses family that causes systemic infections leading to hemorrhagic fever in humans and non-human primates.(1) Its contagious nature facilitates a rapid spread that frequently leads to outbreaks emerging across the equatorial belt of Africa. Ebola virus is a pressing research target due to its high fatality rate and potential for global consequences.

Ebolaviruses first emerged in 1976 in two areas of northern Zaire (now the Democratic Republic of Congo) and Sudan in central Africa and was identified as a new viral hemorrhagic fever.(2) The two outbreaks were thought to be the same event spread between separate locations through human travel. However, the outbreaks later transpired to have been caused by two genetically different Ebola

viruses. These were named the Zaire Ebola virus and the Sudan Ebola virus. They were discovered to have originated from two separate reservoirs but moved into human infection due to an unknown common factor. In the years following, fieldwork has identified that the Ebola virus may spread through sylvatic ecosystems - mainly through certain species of fruit bats.(3)(4) Fruit bats act as a reservoir species but it is not ultimately known exactly where the virus moves into humans from. There are now six known subtypes of the Ebolaviruses each named after the region in which they were discovered: Zaire, Sudan, Bundibugyo, Tai Forest (formerly Côte d'Ivoire), Reston and Bombali. Reston can cause human infection but is the only subtype that isn't pathogenic to humans and doesn't cause disease. However, it does cause disease in non-human primates such as apes and macaques. Since the first two outbreaks of Ebola virus, there have been 23 further outbreaks, 14 of which were caused by the Zaire Ebola virus. Zaire is, therefore, an important species to investigate further and will be investigated experimentally in this report.

The largest outbreak in the history of Ebola virus was the 2013-2015 West African epidemic. It is also widely considered the most severe Ebola virus outbreak to date as it's been the most fatal, longest lasting, and farthest spreading. It was labelled an international public health challenge with cases spreading as far as the USA, UK, Italy, Spain, Nigeria, Mali, and Senegal.(5) WHO reported a suspected total of 11,323 deaths occurred in this epidemic. Previous outbreaks hadn't exhibited a geographical impact this widespread and had remained more isolated and local to the initial cases of human infection.(5)(6)

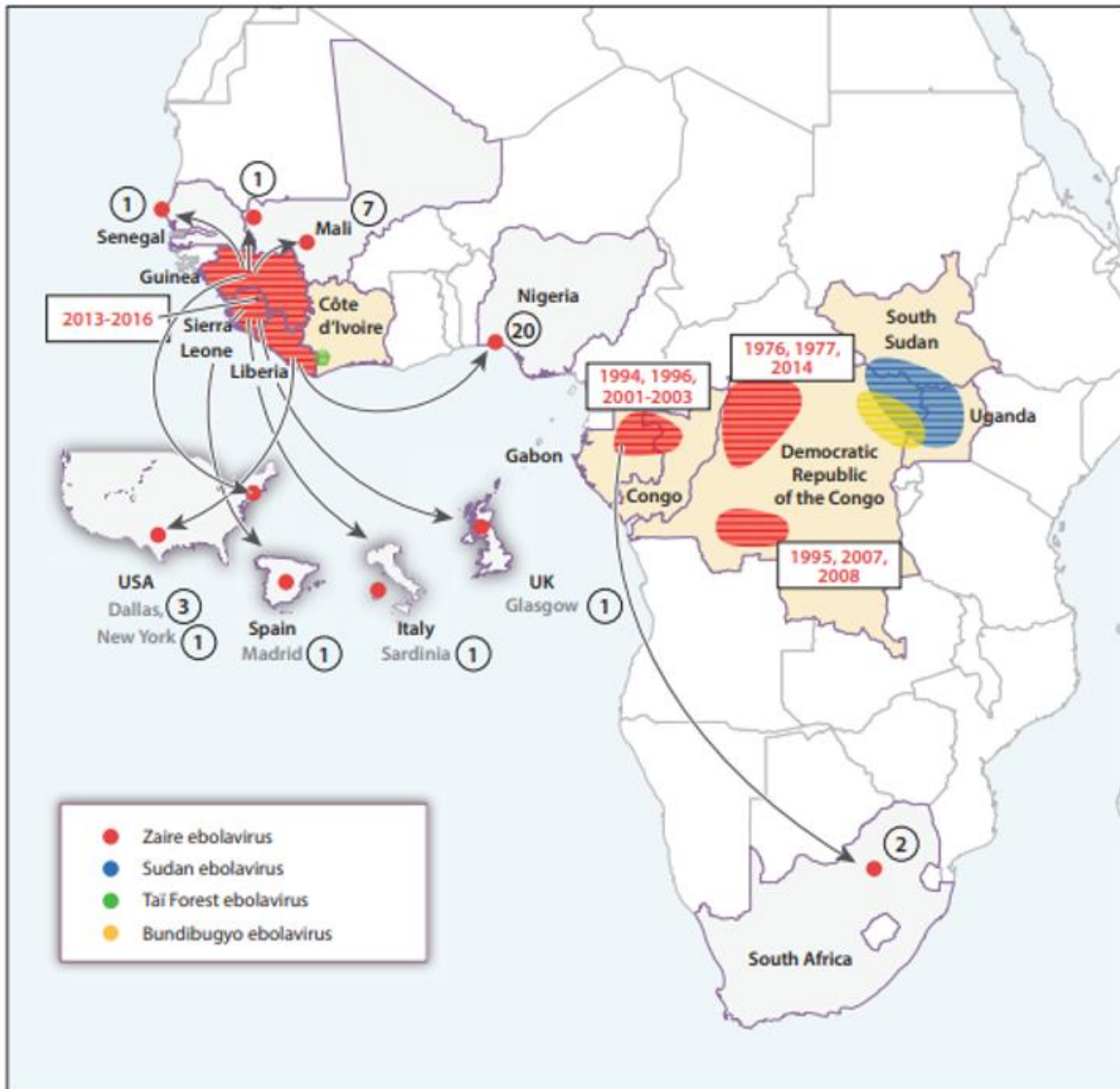


Figure 1- Map of location of Ebola virus outbreaks and their spread illustrating how widespread and damaging the 2013-2016 outbreak was. Figure by Baseler et. al. (5)

1.2 Ebola virus transmission

The exact mode of transmission from the initial reservoir of the Ebola virus to humans is not known, yet its human-to-human transmission is well understood. Human infection is assumed to occur through handling and consuming contaminated bush meat from animals, such as some species of fruit bat, already infected with the Ebola virus. Once the virus has moved into human infection, human-to-human transmission occurs very easily through contamination of mucosal membranes, viral entry into the bloodstream, or contact of nonintact skin with infected fluids or tissues. Efficient transmission makes

the spread of the virus difficult to control, particularly in caregiving environments where healthcare professionals or family members are in regular close contact with infected individuals.(7) One of the fastest modes of transmission in African countries seems to be their handling of the dead and unsafe burial practices such as body washing. These practices expose members of the deceased's family or community to infectious bodily fluids leading to them becoming infected and continuing the spread of the virus.(8) The 1976 Zaire outbreak is thought to have been primarily transmitted through contaminated needles and syringes used in hospitals. Blood from an infected patient (who may be in the symptomless incubation stage so feels well but is infectious) was transferred to other healthy individuals infecting them with the virus too.(3)(9)

1.3 Clinical presentation of disease

During the first week following infection with the Ebola virus, patients are symptom-free and capable of continuing their lives as usual. Despite a lack of symptoms, patients are able to transmit the virus to others via their bodily fluids at this stage as there are viral particles present in their blood and infected cells. Following this asymptomatic incubation period, nonspecific symptoms of the disease begin to develop. These include but are not limited to fatigue, muscle weakness, and fever. The peak of the illness occurs within the first week of symptom onset and renders patients incapacitated - asthenia develops and becomes worsened by vomiting, nausea, and diarrhoea lasting up to two weeks. Fluid losses occur due to fever (e.g. sweating), diarrhoea, rapid breathing, intra to extravascular volume shifts, and capillary endothelial leakage. Without supportive care, these can result in severe dehydration and hypovolemic shock. Without fluid and electrolyte replacement and supportive treatment, this will result in organ failure and death.(10)(11) With a 25-90% fatality rate, an average of 1 in 2 patients infected with the Ebola virus won't survive.(6)

For those who survive the peak of the disease once virus levels in the blood drop, approximately four weeks post symptom onset, tissue repair can begin to recover some organ damage and tissue injury. In some cases, the live virus can persist in immune-privileged sites causing the late onset of other conditions caused by Ebola virus infection. In 20% of Ebola virus survivors, uveitis develops causing some vision loss, light sensitivity, eye pain and watering, blurred vision, and a burning sensation in the eyes.(12) Other longer-term conditions found to remain or develop post Ebola virus recovery include fatigue, cognitive difficulties, hearing loss, tinnitus, weakness, and muscle pain. These can continue for over a year in some cases. A case of clinical meningitis, with live Ebola virus still present in the

cerebrospinal fluid, has even been reported to have occurred nine months after the patient's initial recovery.(13)

Along with its rapid spread, one of the main factors contributing to Ebola virus's high fatality rates is the lack of an effective specific treatment. Antiviral compounds have been trialled and have shown therapeutic promise during in vitro and animal studies. However, none have been proven effective in humans or granted regulatory approval for use. As a result, the primary treatment for the Ebola virus is supportive care. Supportive care has been able to cause a reduction in the case-fatality ratio seen in previous outbreaks. Supportive care involves close, continuous monitoring of patients through the least invasive means possible e.g. indwelling venous catheters for frequent blood sampling, bedside ultrasounds to assess cardiac function, etc. Alongside supportive care, drugs can help manage disease symptoms: antidiarrheal medications, analgesics, antibiotics, sedatives, enteral or parenteral nutrition, and antiemetics. Breathing difficulties and hypoxia may be eased using supplemental oxygen – however, if a respiratory failure occurs mechanical intervention is necessary. The correct use of effective supportive care can result in tissue repair and recovery of organ function in patients treated early enough in their illness. Problems are encountered delivering this level of care in the crucial early stages of disease in rural locations and less economically developed countries where hospitals are not easily accessed. For example, in the Equatorial African countries in which the Ebola virus outbreaks have historically originated.(5)

As a result of this lack of treatment and difficulties receiving supportive care, the best possible 'treatment' for the Ebola virus is prevention and containing outbreaks. Areas of high risk have been identified throughout the countries of equatorial Africa. High vigilance, public education, and continuous monitoring are employed here to enable fast identification and containment of cases.(14) Stopping transmission is the best way to prevent geographical spread and epidemics in the future. For this to be effective rapid communication between communities and countries is essential. With prompt diagnosis, isolation, contact monitoring, and minimal exposure of healthy individuals to infected patients, we can hope to keep infection transmission to an absolute minimum and avoid future widespread outbreaks, epidemics or pandemics. Many Ebola virus vaccines have been designed and undergone clinical testing, but none are licensed yet. Until such a time that an effective vaccine is developed and approved, education and case-control is the best defence we have against the Ebola virus.(5)

1.4 Proteins of the Ebola virus

Ebola virus is a filamentous lipid-enveloped virus with a negative-strand single-stranded RNA genome that contains seven genes.(15) These code for: nucleoproteins NP and VP43, matrix protein VP40, glycoprotein (GP), accessory proteins VP24 and VP30, and a large multifunctional viral polymerase (L).(16) While the genome only contains these seven genes, it encodes for many more proteins. This is possible due to RNA processing of the glycoprotein. The glycoprotein gene gets transcribed into two or three messenger RNAs which code for different versions of GP. RNA editing adds additional nucleic acid, adenine, to a site of 6 uridines in the GP mRNA. Adenine addition shifts the reading frame resulting in the production of a different amino acid sequence at the C-terminal end of each GP. The change in nucleic acid sequence and resulting amino acid sequence is dependent on the number of adenines added and results in the production of slightly different GP products. The addition of two non-templated adenines results in the production of a truncated GP called small soluble GP (ssGP). Adding one adenine results in Viron associated GP which is glycosylated in the endoplasmic reticulum (ER) and delivered to the membrane where its C-terminal TM domain anchors it to the membrane. Unedited RNA transcript produces soluble GP (sGP) which doesn't contain this anchoring TM domain and remains in the cytoplasm. Soluble GP is cleaved at a furin-like protease-sensitive site releasing dimeric sGP for secretion and a 40 residue C-terminal fragment that remains in the cell- this is DP.(1)(15)(17)

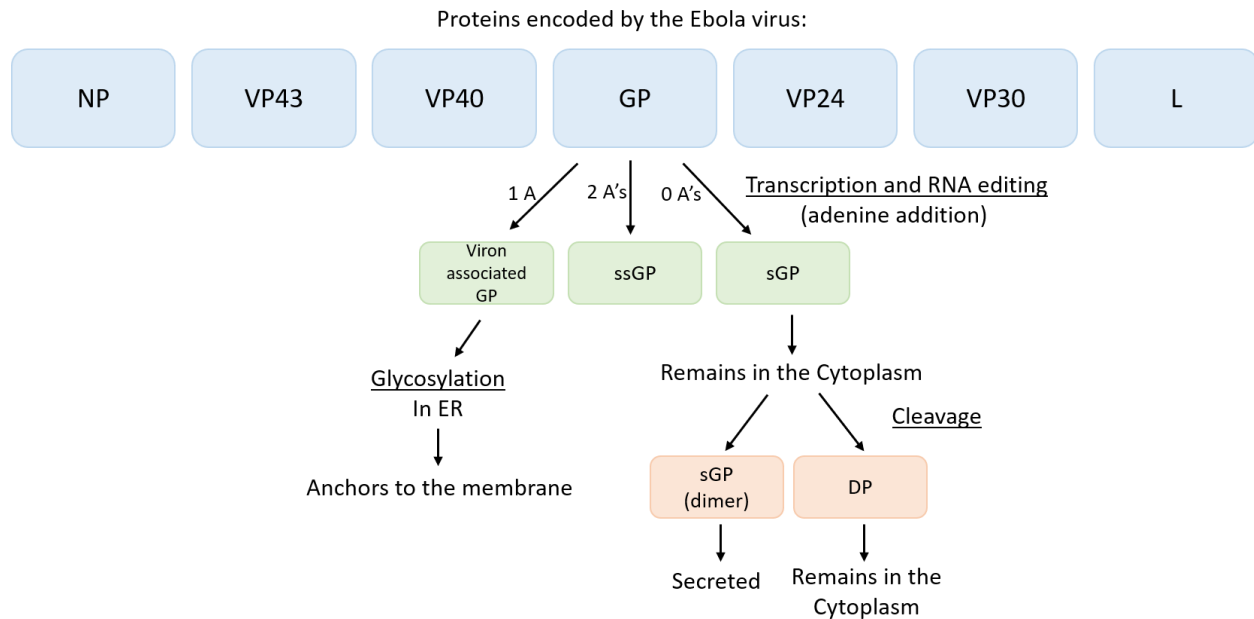


Figure 2- Diagram of the proteins encoded for by the Ebola virus RNA genome and the following processes resulting in modification and production of DP.

1.5 Viroporins

DP is a small partially conserved hydrophobic peptide initially thought to be non-structural. DP is one of only two remaining proteins of the Ebola virus whose structure hasn't been solved but it's predicted to behave as a Viroporin.

Viroporins are small hydrophobic proteins, usually 60-120 residues long, encoded by a number of viruses whose main function is to increase membrane permeability. Many viral glycoproteins act as Viroporins and oligomerize in membranes to form a pore. Pore formation permeabilises the membrane and can cause complete cell lysis. This permeabilization functions on two levels - short-term and long-term effects on cells. In the short term, membrane permeabilization disrupts the function of the cell which can aid viral infection and pathology. For example, when the influenza virus enters cells, the low endosomal pH activates a protein in the virus called M2. M2 forms a pore in the membrane that allows protons to enter the virion. Proton entry causes a pH change which weakens interactions between the viral matrix protein and the ribonucleoprotein complex leading to virus uncoating. M2 has also been linked to budding and egress as its membrane oligomerisation dissipates cell membrane potentials. This depolarisation of the membrane allows the negatively charged inner membranes to merge and budding to occur.(18) Oligomerisation of peptides in cell membranes also disrupts the organisation of the lipid-

bilayer disrupting its function and destabilising the cell further. Continuous permeabilization of the membrane and long-term disruption of membrane essential processes, concentrations, and gradients required for effective cellular functioning leads to cell death.(17)(19)

The majority of Viroporins can be categorised into two classes according to their structural features. Class I Viroporins have a single transmembrane (TM) helix - subclass IA have an intracellular C-terminus in the cell cytosol, IB on the other hand, have an intracellular N- terminus. Class II Viroporins have multiple TM helices in a helix-turn-helix structure. Subclass IIA Viroporins have extracellular termini and, IIB Viroporins have both their termini in the cell cytosol.(20)

1.6 DP structure

DP is a small peptide of 40 amino acids with a MW of 4815.78 Da. DP has a variable N-terminal region and a better conserved 23 residue C-terminus of 23-31 residues containing a high proportion of aromatic and basic residues and two cysteine residues (Cys29 and Cys38) conserved in DP of all five Ebola species.(15) There is limited knowledge available about the structure of DP, as membrane proteins are difficult to structurally investigate. Membrane proteins only exhibit their native structure, folding, activity, and stability when in a lipid bilayer. This makes x-ray crystallography and NMR very difficult. For this reason, only 2% of all known protein structures in the Protein Data Bank are solved membrane protein structures.(21)

When analysing DP's amino acid sequence Gallaher et al. found a high frequency of E, Q, A, L, W, F, and K residues which have a known tendency to form α -helices. They also produced molecular models of DP and observed a 3/4/7 repeating pattern of positively charged amino acids (Lysine and Arginine) opposite a similar repeating pattern of hydrophobic residues. This pattern is characteristic of an amphipathic helix and has been identified in Viroporins of other viruses such as lytic peptide non-structural protein 4 (NSP4) from the Rotavirus (illustrated in figure 3). Amphipathic helices have hydrophobic residues along one side and hydrophilic residues down the other side of their helical turn. This forms polar and non-polar faces that allow the protein to interact with membranes and other proteins. Amphipathic helices allow oligomerisation of DP in the membrane following insertion to facilitate pore formation. The hydrocarbon chains of the phospholipids making up the membrane are hydrophobic so, when DP forms pores, it must oligomerise with the hydrophobic faces of the TM helices facing out into the membrane. The hydrophilic side of the amphipathic α -helices face inwards, forming a hydrophilic pore.(22)(16) The 3/4/7 pattern is observed in a range of lytic Viroporins suggesting DP will also behave as a Viroporin.

1.7 DP Function

There is minimal understanding of the activity and function of DP. However, sequence analysis using various bioinformatic techniques suggests it behaves as a Viroporin.(17) Viroporins are small hydrophobic proteins produced by many viruses. Following production, they oligomerise in host cell membranes forming TM amphipathic pores. These pores remove the function of the membrane by dissipating membrane potentials, removing selectivity, disrupting concentration gradients, and many other mechanisms essential for cell survival. As a result, DP is considered one of the key peptides involved in the pathogenicity of the Ebola virus. This suspected pathogenicity has led to Viroporins becoming novel drug targets in recent years. Despite the strong case provided suggesting DP is a Viroporin, its molecular mechanism and mode of action are not yet understood.(15)

Since Gallaher et al. made their bioinformatic and molecular modelling-based predictions about DP, experimental techniques have been employed to try and better understand its activity and investigate if it functions as a lytic Viroporin. He et al. used different sized synthetic DP fragments to conduct permeabilization experiments and investigate pore-forming behaviour in DP. They tested the hypothesis that DP is able to permeabilise animal cell plasma membranes, internal cell membranes, and the viral envelope. They also investigated if the C-terminal portion, Cys29-Cys38 disulphide bond and Trp25 were essential for membrane permeabilization. These experiments confirmed DP had membrane permeabilising activity in its oxidised state with the disulphide bond present between Cys29 and Cys38. Reduced DP fragments were inactive, suggesting the disulphide cross-link is essential for DP's membrane permeabilising activity. Through their use of different sized DP fragments, they identified the C-terminal portion and Trp25 to also be essential for DP membrane insertion as fragments without them had no membrane insertion activity. The effects of DP membrane permeabilization were long-lasting, indicating its activity isn't a transient effect and so could lead to cell lysis.(17)

The pores DP forms are suspected to be small and selective. This selectivity has been analysed using synthetic membranes in a dye leakage assay which concluded that DP forms small ion-permeable pores. Permeabilization of mammalian plasma membranes by DP altered the permeation of ionic compounds and small molecules across the membrane. The same behaviour has been observed in known Viroporins e.g. NSP4. NSP4 is a transmembrane glycoprotein of the rotavirus that inserts in the ER membrane and causes an increase in cytoplasmic Ca^{2+} levels altering the membrane homeostasis of the cell. NSP4 activity is possible due to an amphipathic α -helical region (the TM region) and a conserved lysine cluster

(directs integral membrane insertion). The Ca^{2+} increase is needed for virus replication and morphogenesis and so aids viral infection and spread.(17)(25)

The oligomerisation of DP in cell membranes was recently investigated by Pokhrel et al. using all-atom molecular dynamic simulations. Pokhrel et al. hypothesised that DP functions as a Viroporin and aids virus particle release from infected host cells. Oligomeric models of DP as a tetramer, pentamer, and hexamer in an explicit membrane environment were produced. These models were used to investigate their pore-forming mechanisms and the optimum oligomeric state. The series of basic residues at DP's C-terminus were modelled facing into the centre of the channel - this provided selectivity for chloride ions. In contrast, the hydrophobic residues faced outwards into the hydrophobic centre of the membrane to enable peptide insertion and stabilise the pore. The tetrameric pore was unstable which indicates the homo-oligomeric pores DP forms are comprised of more than four DP monomers. The pentameric and hexameric simulations both formed stable ion-permeable pores. These selectively allowed water and chloride ions to move across the membrane but prevented the passage of sodium ions or macromolecules. Tighter packing of helices was seen in the pentameric pore strengthening the Van der Waals forces and the two hydrogen bonds stabilising the pore. As a result, the pentameric pore was the most stable oligomeric state. The pentamer is therefore the most likely conformation occurring naturally in the membrane. The conserved disulphide bond at the C-terminus of the peptide was found to be essential for ion flux and stabilising the pore. Without the disulphide bond, the C-terminus of the peptide flipped out of the membrane and the pore structure became disrupted. This destabilisation was most severe in the hexameric pore which became distorted in the absence of the disulphide bond. Consistent with experimental suggestions, the destabilisation of the pores led to a reduced pore radius, decreased chloride ion density, and flux.(15)

1.8 Project outline

This project aims to shed light on the structure and function of DP. The structure of DP is yet to be solved and most research conducted since its discovery in 1999 has centred around its function and activity. A likely amphipathic helix structure has been predicted from bioinformatic investigations and modelling. This proposal suggests DP has a Viroporin like structure with possible lytic activity. Experiments using synthetic peptide proved DP to be active when in its oxidised state with the full C-terminal portion, including Trp25 present. Finally, through molecular dynamics analysis, it has been hypothesised that DP can form hexameric pores highly selective to chloride ions.

It is the intention of this project to determine the structure of DP. Solving DP's structure has proved difficult so has been somewhat neglected in recent years. DP structure will be investigated through the use of solution NMR and CD secondary structure analysis. A UV microscopy membrane insertion assay will also be used to assess the function of DP and investigate membrane interactions. Dye leakage assays will observe the activity of DP and identify if the pore-forming predictions made through computational methods can be demonstrated experimentally. The aim being to identify if DP does indeed permeabilise membranes by forming pores and if its activity is dependent on its oxidation state and the presence of its C-terminus. In short, the objective is to gain a clearer image of DP's structure and to confirm if it does indeed act as a Viroporin.

2. Delta peptide growth and purification optimisation

2.1 Introduction

Protein expression can be achieved through a range of systems. Cell based systems are most widely used and involve using an expression vector containing cloned DNA of the target protein gene that is transfected into a host cell which then produces the protein during its own protein expression processes.

Baculovirus-insect cell systems can be used to express recombinant proteins. These systems are mainly used for soluble, toxic or TM proteins and are capable of large-scale protein production. Baculovirus is used as the vector for the target protein gene to infect insect cells or larvae which then produce the target protein. This system successfully produces active protein but the culture conditions are demanding.(26)

Yeast and mammalian cells can all also be used, they are both eukaryotic systems so produce fully folded proteins with all the post-translational modifications they require. The cloned target gene is transfected into the mammalian cells via a vector, protein production and post translational modifications are then performed as usual in the cell. The target protein can then be purified. Proteins produced in this way are as close as possible to the native protein and are fully folded and modified. Whilst mammalian cell expression produces proteins as close as possible to native proteins due to their ability to perform the whole expression process, they produce low protein yields. The culture conditions required are also time consuming and demanding due to short cell cycles. This would therefore not be a suitable option for this project as high protein yields are required for structural determinations and NMR experiments.(27)(28)

Yeast cell systems work in a similar way to mammalian expression but are able to produce higher protein yields and are far quicker and cheaper. A frequently used example is *pichia pastorius* capable of large-scale recombinant protein production as it is single-celled and easy to culture so large-scale fermentation production can be used to produce high concentrations of protein. This system would potentially work well for DP production as its commonly used for proteins with low molecular weights (MWs) as DP is a very small peptide.(29)

Bacterial cells are able to easily produce lots of protein. *E. coli* cells are the most commonly used bacterial expression host with plasmid vectors used to insert the target protein gene into the cells for expression and production. *E. coli* have a short life cycle so reproduce quickly and can achieve large scale

fermentation and produce lots of protein relatively quickly. Bacterial cell systems tend to be used for smaller proteins as they struggle to express high MW proteins which suits this project well as DP has a low MW of just 4.8135kDa. *E.coli* cells were chosen to express both DP variants due to their relatively simple transformation process, quick and efficient protein expression and their short lifecycle.(30)

In vitro protein expression is also an option, this technique involves using translation and transcription machinery extracted from cells to express DNA or mRNA of the target protein. The cellular machinery needed for transcription and translation can be from a range of cells including human, rabbit or *E. coli* cells and cell cultures are not required. However, only a small amount of protein is produced so this would not be an effective technique to use in this project.(31)

Following expression proteins must be purified, once the cell contents have been extracted the proteins can be separated through a range of techniques. SEC is often used to separate proteins of a known MW as proteins are separated based on their size. An elution of the target protein can be collected based on when it elutes from the separation column. Similarly, proteins can be separated based on their hydrophobicity using ion exchange, hydrophobic interaction chromatography or reversed phase high pressure liquid chromatography (RP HPLC). These techniques rely on proteins binding to the columns based on their surface hydrophobicity and ionic charge respectively which the target protein then being eluted from the column and collected by changing the conditions (buffer) in the column. Affinity chromatography can also be used in various forms, this involves the protein of interest binding to the column stationary phase e.g. specific resins, immobilised antibodies or antigen tags to allow other proteins to flow past and leave the column before an eluting agent is added and the purified target protein can be collected from the column. Processes based on hydrophobic separation and size would likely work well for DP purification as it is a very small peptide so will be easy to identify eluting from a size exclusion column and is very hydrophobic.(32)(33)

2.2 Methods

2.2.1. Transformation

To reduce the risk of bacterial contamination aseptic techniques were used for all experiments involving bacteria. These included using a flame to create a sterile field, cleaning glassware with Chemgene disinfectant, and autoclaving all equipment and media involved.

Competent C43 *E. coli* cells were used as these were found to grow most successfully and gave the highest yields of peptide following induction with Isopropyl β -D-1-thiogalactopyranoside (IPTG).

10 μ L C43 cells were transfected with 1 μ L DP DNA using the heat shock transformation method. DNA and cells were pipette mixed together then incubated on ice for 15 minutes. This was then heat shocked at 42°C for 45 seconds and left for a further 15 minutes on ice. The cells were incubated in 500 μ L antibiotic-free Luria Bertani media (LB) (10g tryptone, 5g yeast extract and 10g sodium chloride per litre of dH₂O) for 1 hour at 37°C 200 revolutions per minute (rpm). 250 μ L of this was streaked on an LB agar plate (LB with 15g agar per litre of dH₂O) containing ampicillin to select for successfully transfected cells.

2.2.2. pCold construct growth and induction

The following day, individual colonies were selected from the agar plates and transferred on a clean, autoclaved pipette tip into conical flasks containing 50mL LB media. These were left to grow overnight at 37°C and 200rpm. Each of these starter cultures was then added to a 2L conical flask containing 1L of LB media to accelerate the growth process. The OD₆₀₀ of each flask was measured every 30 minutes using WPA colourwave CO7500 Colorimeter until they reached 0.7. An OD₆₀₀ of 0.7 indicates the cells are in the optimum growth phase, their exponential growth phase, to be induced and produce the maximum possible protein yield. Upon reaching OD₆₀₀ 0.7 cell cultures were immediately cooled in ice water and left to stand for 30 minutes. IPTG was added to each flask to a final concentration of 1mM to induce protein expression by the cells. These were left for 24 hours at 15°C 200rpm.

2.2.3 pCold construct peptide extraction and purification

Cell lysis

Following growth, the cells were harvested by centrifuging at 4000rpm for 20 minutes in a high-speed centrifuge to remove the LB media and then resuspended in lysis buffer (50mM Tris, 150mM NaCl, and 6M Guanidine at pH8). A protease inhibitor was added to prevent proteases breaking down the peptide once the cells were lysed. Sonication was used to lyse the cells. The cells were sonicated for 30 seconds at a time with 30-second breaks to prevent overheating for a total of 10 minutes. Cells were on ice during sonication and kept on ice for all following purification steps.

Centrifugation

Cell lysate was spun down following lysis using an ultracentrifuge at 40,000 rpm, 4°C for 45 minutes to separate the soluble portion of the cell lysate from the cell membranes. This soluble portion appeared green indicating the DP was present in the supernatant. This was then purified using an Ni IMAC column.

Nickel Immobilized metal affinity chromatography (Ni IMAC)

The pCold DP construct has a His-tag on its C-terminus comprised of 6 histidine residues. Histidine residues have a high affinity to nickel atoms allowing DP to be separated from other proteins present using an IMAC column. The IMAC column has a chelating sepharose resin stationary phase charged with Ni²⁺ ions to bind to the His-tag. The column was first washed by allowing 10CV (column volumes) of water to flow through the bead bed and then equilibrated with 10CV of lysis buffer. The supernatant from the final ultra-centrifugation was mixed and incubated with the resin for 30 minutes on a rocker at room temperature. This incubation time allowed the His-tags on the DPs to bind to the nickel ions. The incubated resin was returned to the column and the flow-through was collected as the beads settled. The column now contained the bead bed with His-tagged peptides attached to the beads through the histidine imidazole ring. Any proteins that didn't bind, so didn't contain have a His-tag, left the column in the flow-through.(34) 10CV of lysis buffer was added and allowed to drip through the column as a wash step. The wash removed any non-specific electrostatically bound peptides which didn't contain a His-tag. The bound DP peptide was eluted using an elution buffer containing lysis buffer with imidazole (50mM Tris, 150mM NaCl, 6M Guanidine, and 500mM Imidazole at pH8) and the elution collected for dialysis. The flow-through was run back through the column twice more to ensure all the available DP was exposed to the beads and had the opportunity to bind during the incubation periods. Repeating the

column ensured the maximum amount of peptide could be extracted without overloading the maximum binding capacity of the column.

Dialysis and TEV cleavage

The elutions from the three Ni affinity column runs were dialysed into buffer containing 50mM Tris HCl and 1mM EDTA at pH8. The elutions were pipetted into SnakeSkin dialysis tubing with a MW cut off of 3500Da and floated in 5L of buffer. This was left for 24 hours to allow the buffer exchange to occur.

In order to remove the His-tag and green florescent protein (GFP) from the peptide, Tobacco Etch Virus nuclear-inclusion-a endopeptidase (TEV) protease was used to cleave the DP after the GFP tag. TEV protease is a sequence-specific cysteine protease that cleaves at -E-x-L-Y-y-Q-z- (where x could be any residue, y is any large or medium hydrophobic residues and z is a small hydrophobic or polar residue).(35) The sequence -E-N-L-Y-F-Q-G was present in the plasmid sequence after the GFP and His-tag before the DP sequence for TEV to cleave between the Q and G residues.

The contents of the dialysis membranes were transferred into a falcon tube and TEV protease and 1mM Dithiothreitol (DTT) were added. This was left rocking for 6 hours at 25°C to allow the cleavage to take place.

Size exclusion chromatography (SEC)

The cleavage mixture was concentrated using spin concentrators with a cut off of 1kDa at 4000rpm at 4°C for 10 minutes at a time until it reached a final volume of 500µL as only 500µL of the sample can be injected into the SEC.

The cleaved DP was separated from the components remaining post TEV cleavage (TEV protease, cleaved His-tag, etc.) using SEC. A Superdex 200 column was equilibrated with degassed HEPES buffer (20mM HEPES and 50mM NaCl) and used to separate the proteins in the mixture.

SEC separates proteins based on their size as large proteins can move quickly through the column as they pass around the beads and elute out. Small proteins, however, will pass through the beads which takes much longer so they elute at the end of the method. DP is a very small peptide of only 4815.78Da so it's easily purified and identified based on its size. The chromatogram recording fluorescence intensity of proteins leaving the column was used to predict which elutions contain the DP. These elutions were run on a sodium dodecyl sulphate-polyacrylamide gel electrophoresis (SDS PAGE) gel to confirm the

peptide present is DP and identify exactly which elutions contained the most peptide. These elutions were then combined to give a high concentration sample.

SDS PAGE gel

Sodium dodecyl sulphate-polyacrylamide gel electrophoresis was used to separate proteins based on their size so components of a mixture can be seen. Separation is achieved on the basis of charge, sample buffer containing: 10% w/v SDS, 10mM DTT, 20% w/v Glycerol, 0.2M Tris HCl pH8, and 0.05% w/v Bromophenol blue, was added to the samples. The sample buffer denatures and negatively charges the proteins. The gel was run in a running buffer containing 30g/L Tris, 140g/L glycine, and 10g/L SDS.

When an electric current (200mV) is applied the proteins move towards the positively charged anode at the bottom of the gel. Smaller proteins can move faster down the gel as they can move through the pores of the gel matrix more quickly. As a result, when the current is stopped, just before the front reaches the bottom of the gel, smaller proteins will have travelled further down the gel and large proteins remain near the top. Gels were stained using a Coomassie quick stain method - the gel was microwaved in 50mL of solution 1 for 25 seconds (50% ethanol, 10% acetic acid, and 40% water). Then allowed to cool for 10 minutes and microwaved again in 50mL solution 2 (5% ethanol, 7.5% acetic acid, and 87.5% water) with 400µL Coomassie stock solution (0.75g Coomassie R-250, 400mL methanol, and 100mL acetic acid) for 35 seconds. The distances the protein bands had travelled down the gel were compared to a protein standard ladder also run on the gel to estimate MW of the proteins.

When running SDS gels 20µL samples were mixed with 5µL sample buffer and 10µL of this was added to the cassette wells to run on the gel. Any samples containing cells were first treated with 8M urea to lyse the cells and denature the proteins.

All SDS PAGE gels in this report were run using these conditions.

2.2.4. New construct Growth and induction

To grow the new construct *E. coli* cells were transformed using the heat shock method in the same way as for the GFP labelled construct.

Expression tests were conducted to determine the best conditions for maximum possible peptide production. For these, both C43 and BL21 cells were transformed with the new DP construct plasmid.

Growths were set up at 20°C, 30°C, and 37°C. Samples were taken before induction with 1mM IPTG, 3 hours post-induction, and 24 hours post-induction. 20µL of each sample was mixed with 8M urea and sample buffer to lyse the cells and prepare the proteins. An SDS PAGE gel was run to separate the proteins and identify which conditions lead to the production of the most peptide.

Cell cultures were prepared and grown in the same way as the GFP construct until they reached OD₆₀₀ 0.7 at which point 1mM IPTG was added to each flask. These were then incubated at 30°C 200rpm for 24 hours with samples collected after 3 hours and 24 hours.

2.2.5 New construct purification

Guanidine purification

Cells were spun down to remove the LB media and sonicated to lyse them in the same way as they were for the GFP labelled construct growth. The purification process from this point onwards was slightly different however.

The peptide was purified using a denaturing guanidine purification method. The sonicated cells were spun at 11000g for 20 minutes at 4C to pellet them. This spin was to collect the lysed cells, their inclusion bodies and the cell debris as a pellet in the bottom of the tube. This supernatant was removed and the pellets resuspended in lysis buffer containing 1% triton X11 for 1 hour at room temperature. This was centrifuged in the same way again and the supernatant containing all solubilised components of the cell, including proteins, were collected and the insoluble pellets removed. The supernatant was kept on ice ready for further purification steps.

Ni IMAC

An IMAC Nickel gravity column was again used to separate the peptide from other peptides present in the sample. The same method as detailed in the pCold GFP construct method in 2.2.3 was used.

Dialysis

Elutions were dialysed in a membrane with a MW cut off of 3500Da in 5L Milli-Q water for 24 hours to dilute out the guanidine buffer. Dialysis works on the basis of concentration gradients- the guanidine in the elutions diffused out of the membrane into the water down its concentration gradient. The guanidine and other buffer components were able to move out of the membrane but, the DP was too

large to pass through the pores as it has a MW of 4815.78Da and so remains inside the membrane. Guanidine could only leave the membrane when diffusing down its concentration gradient, to maintain this gradient, the water was changed 3 times at intervals of at least 6 hours to ensure the guanidine became as dilute as possible. Dialysis caused the peptide to crash out of the solution and remained in the membrane as a white powder. The contents of the dialysis membrane were transferred into a falcon tube and centrifuged at 4000rpm for 5 minutes at 4°C and the liquid pipetted off to leave just crashed out peptide powder.

Cleavage of the peptide

The chemical cleavage site in the new construct was designed to be cleaved with hydrochloric acid (HCl) or formic acid so, three different conditions were trialled. 0.1M HCl was added to 1/3 of the dialysis powder, 0.2M HCl to another, and 70% Formic acid to the last, 1mM DTT was present in all cleavage reactions. These were incubated overnight at 60°C in 1.5mL Eppendorf tubes in a heat block then samples were run on SDS PAGE gels to identify if cleavage was successful and which conditions were best.

Reversed phase HPLC

DP was neutralised with Sodium hydroxide and lyophilised overnight to freeze-dry the peptide. Following this it was dissolved in 500µL 1,1,1,3,3,3 Hexafluoro-2-propanol (HFIP), 400µL Milli-Q water, and 50µL 10% trifluoroacetic acid (TFA) and purified using a Delta-Pak C4 column 300Å C4 column. The C4 column has a hydrophobic stationary phase (silica with alkyl chains four carbons in length covalently bound to the surface to make it non-polar) and a polar mobile phase and separates proteins based on their hydrophobicity. The polar mobile phase contains an organic solvent mixed with water to keep the polarity low enough for the solute to dissolve into the mobile phase but still allow target solutes to bind to the hydrophobic stationary phase. Hydrophobic solutes bind to the stationary phase via hydrophobic interactions and get retained in the column. Any polar components remain in the mobile phase. Thus, these components move quickly through the bead bed and elute from the column before non-polar components do. Hydrophobic, bound components are removed from the column using a buffer containing a higher concentration of organic solvent. The organic solvent increases the hydrophobicity factor of the mobile phase. When this hydrophobicity factor reaches that of a bound protein it's no longer energetically favourable for it to remain bound to the stationary phase. The protein will instead move into the mobile phase and elute from the column.

In this experiment, the organic solvent used was acetonitrile. 95% buffer A (95% water, 5% acetonitrile, and 0.1% TFA) and 5% buffer B (60% acetonitrile, 40% water, and 0.1% TFA) were used to equilibrate the column. The peptide sample was injected and a gradient elution method was used to gradually increase the amount of buffer B in the column and slowly increase the acetonitrile concentration. The UV trace detected at the bottom of the column was used to determine when elutions needed to be collected. Peaks in absorbance intensity at 280nm indicated peptide was leaving the column. DP typically eluted between 22 and 26 minutes.

2.3. Results

2.3.1 Introduction

Initially a pCold DP DNA construct with a GFP incorporated was grown and purified, however this was unsuccessful as there were problems cleaving the peptide from the tags. A new construct was then designed which included a chemical cleavage site to remove the His-tag and KSI during the protein purification. The growth conditions, purification, cleavage method and RP HPLC separation were all altered and optimised to achieve maximum possible peptide expression and purification.

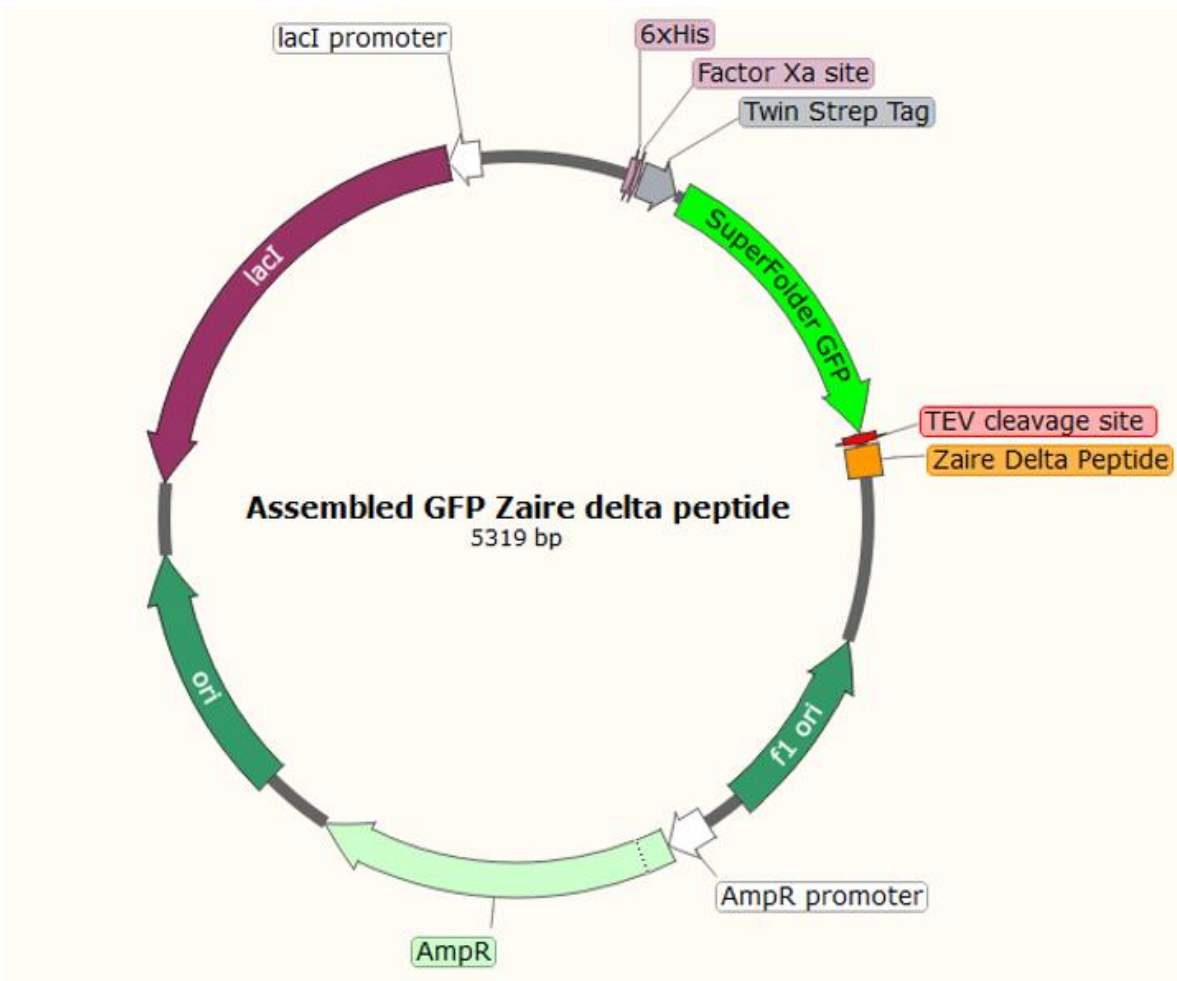


Figure 4- PCOLD DP construct containing superfolder GFP, twin Strep-tag, 6x His-tag and ampicillin resistance gene

Plasmid design

A new construct was designed to include a chemical cleavage site, the plasmid map for this can be seen in figure 5. This plasmid also included an ampicillin resistance gene to allow successfully transformed cell colonies to be selected. Only bacteria that have successfully taken up the plasmid will have ampicillin resistance and be able to grow on agar plates containing ampicillin. It also contains the gene encoding KSI, an expression tag used in the production and purification of small peptides. KSI causes the recombinant protein to accumulate into insoluble inclusion bodies. The inclusion bodies can then be isolated by centrifugation after cell lysis and the peptide can then be purified.

There is also a His-tag on the C-terminal end of the DP gene comprised of 6 histidine residues. The His-tag binds to Nickel affinity columns and to allow for separation of DP from other peptides produced

during the first stage of purification. A chemical cleavage site was included on either side of the DP sequence to allow the His-tag and KSI protein to be removed during the peptide purification process. The cleavage site used is an Aspartate-Proline sequence motif which can be cleaved using 0.1M HCl, 6M guanidine, or 70% formic acid at temperatures over 40°C.

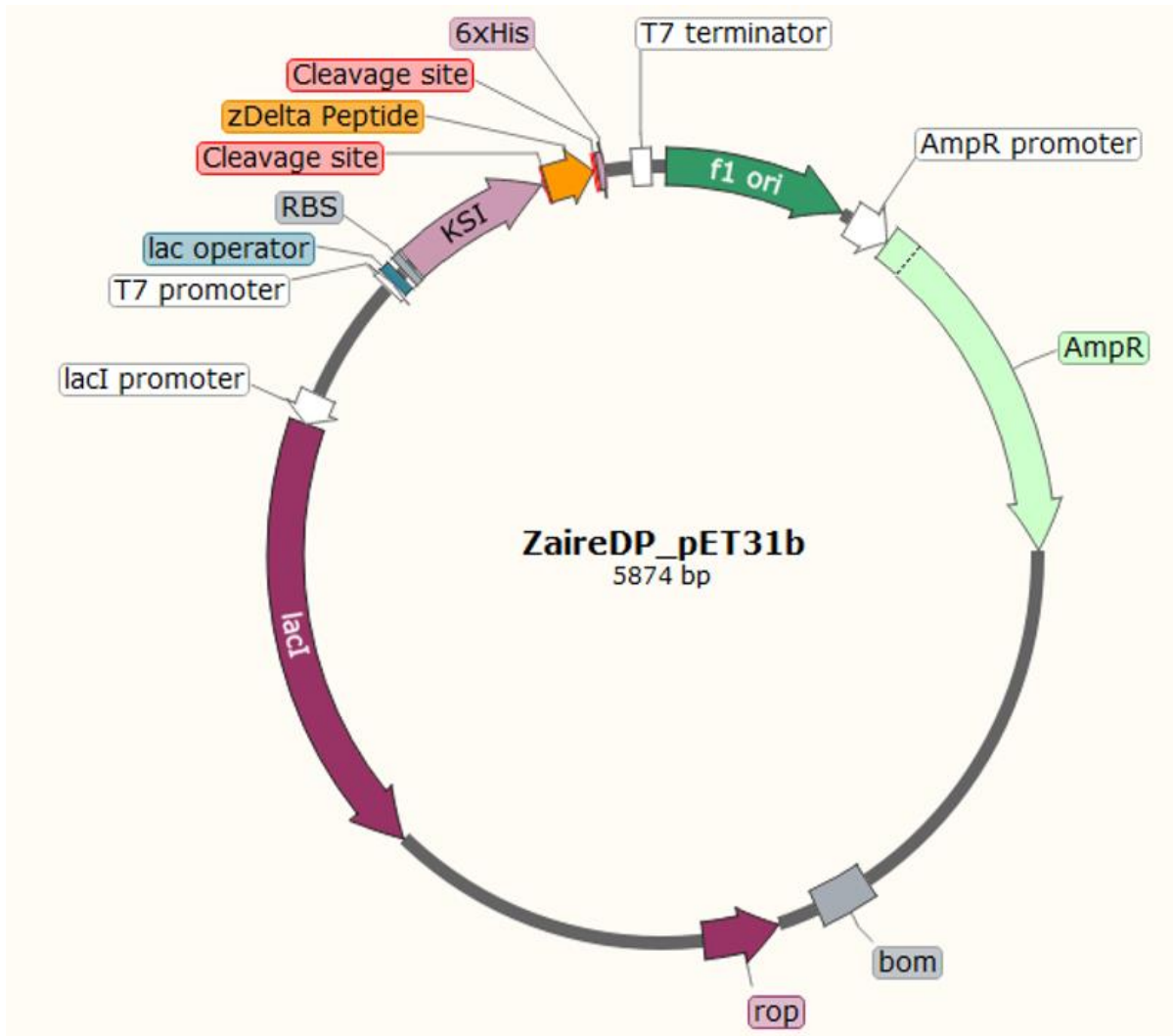


Figure 5- Plasmid map of the new construct DP DNA designed with the new inserted aspartate- proline cleavage sites highlighted in red.

2.3.2. GFP DP construct IMAC Ni gravity column

Running the flow-through, wash, and elution from the Ni IMAC column on an SDS PAGE gel generated a large smear of proteins in the flow-through lane. This was expected as the flow-through contains all the proteins in the cell lysate with no His-tag. The wash contained comparatively few proteins and the elution even fewer. There is a dark band present in the elution lane just below the 100kDa marker band of the protein standard ladder, this is DP with the GFP and His-tag attached as uncleaved DP has a MW of 55kDa.

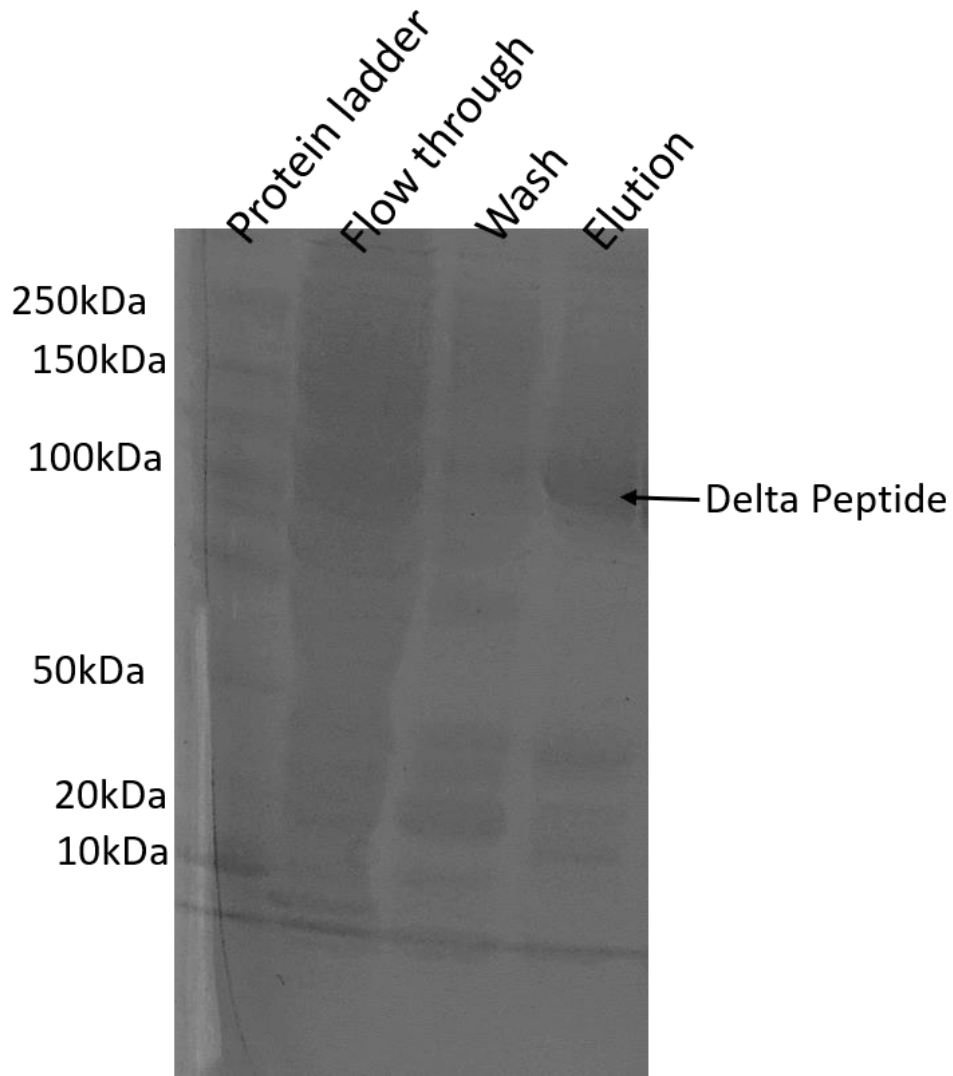


Figure 6- SDS PAGE gel of the flow-through, wash, and elutions from the Nickel gravity column. The column successfully separated DP from the cell lysate following sonication and centrifugation. SDS Page gel was run at 200mV for 45 minutes to achieve separation.

2.3.3. GFP DP construct- TEV cleavage

An Electrospray mass spectrum of the powder produced following TEV cleavage dissolved in 30% acetic acid was recorded on a Bruker micrOTOF-Q II mass spectrometer. An aliquot of 200 picomoles was desalted on-line by RP HPLC- A Phenomenex Jupiter C4 column running on an Agilent 1100 HPLC system using a short water, acetonitrile, 0.05% TFA gradient. The eluent was monitored at 280nm and then directed into the electrospray source operating in positive ion mode at 4.5kV to record mass spectra from 500-300m/z. The data was analysed and deconvoluted to give uncharged protein masses with Bruker's Compass Data Analysis software. A UV trace plotted at 214nm shows the mass-to-charge envelope produced from the peptide. The envelope indicates TEV cleavage has not been successful as the peptide peak at 55064.2 has the same MW (55.064kDa) as would be expected of DP with the His-tag and GFP fused (55kDa). If cleavage had been successful the peptide would have a MW of 4.8kDa.

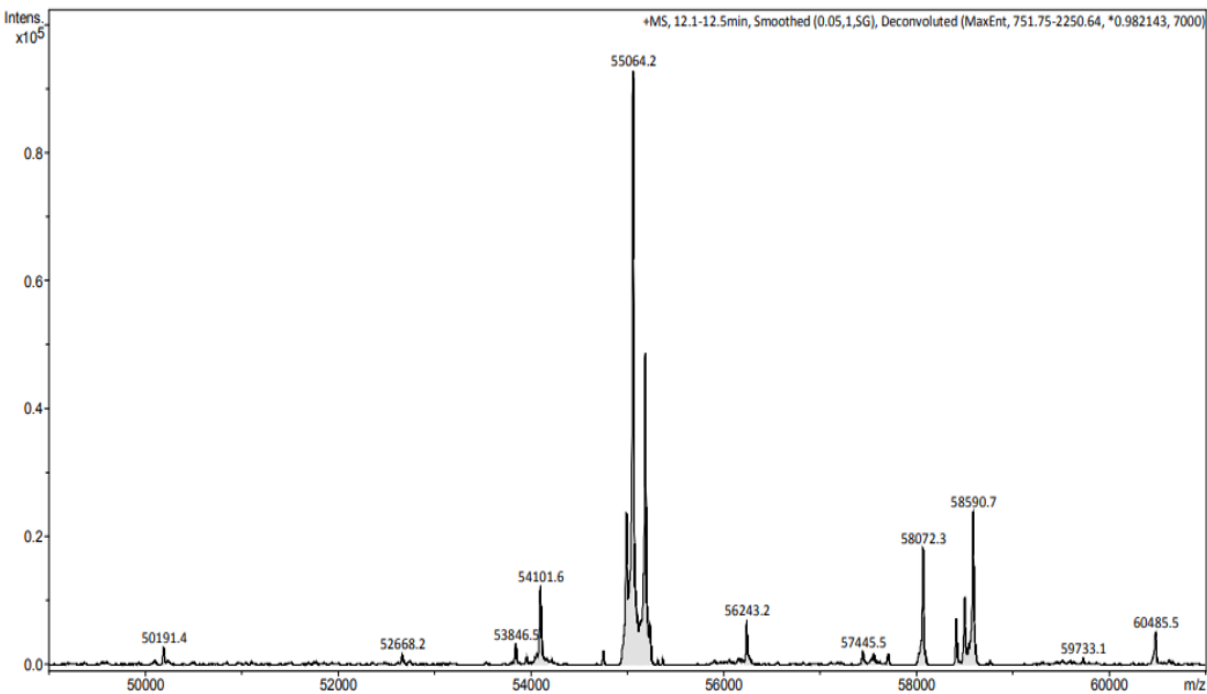


Figure 7- Mass spectrometry electrospray analysis of GFP- fused DP post TEV

2.3.4. GFP-DP construct- SEC elutions

Following the SEC column, the largest peak in absorbance at 280nm was identified from the chromatogram recorded as the column was run. Elution fractions collected from this peak were run on an SDS PAGE gel to check for DP presence and confirm exactly which elutions contained the majority of the peptide. Elutions 2-5 contained the most peptide and so were combined to give a concentrated sample.

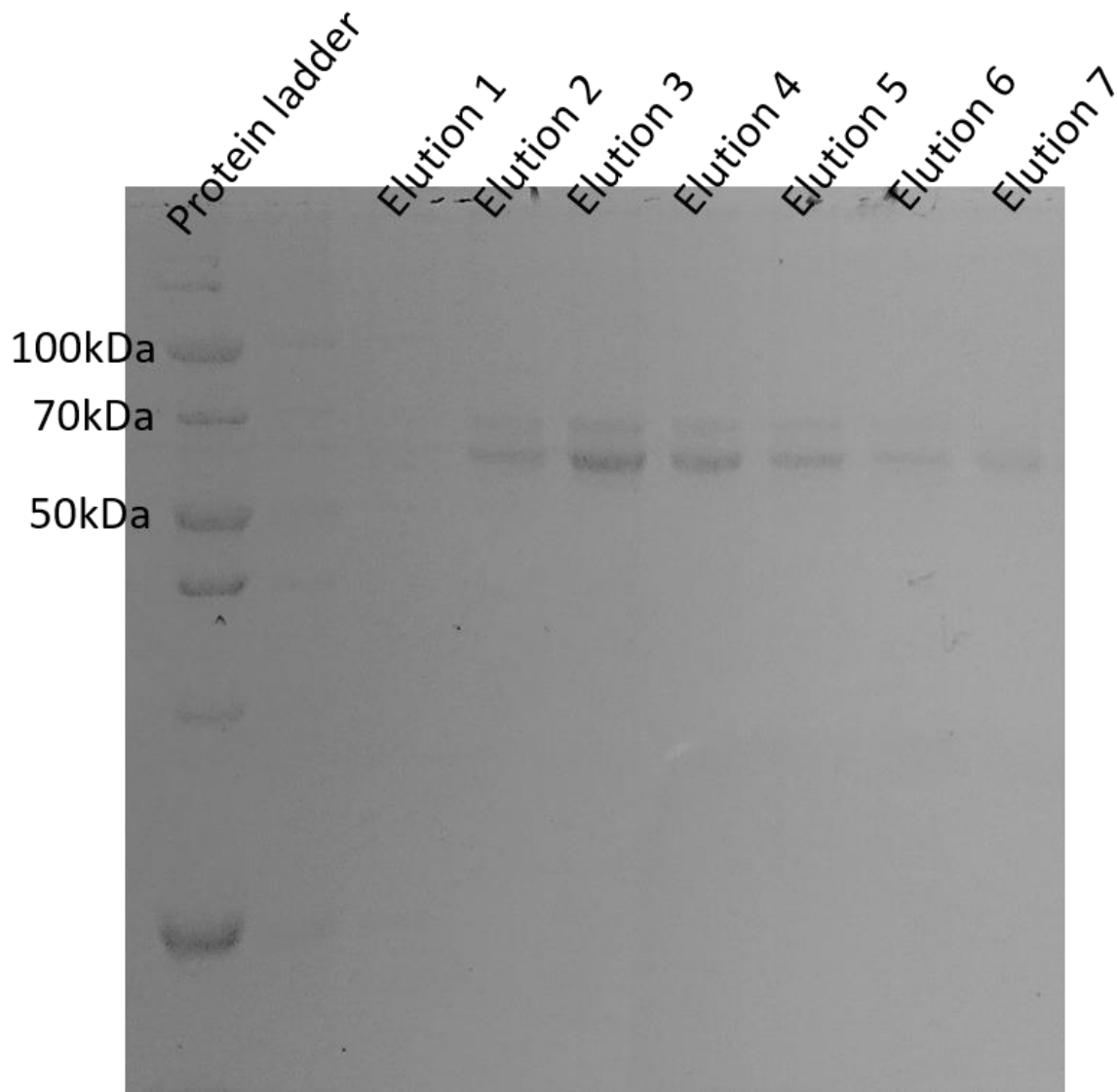


Figure 8- SDS PAGE gel of elution fractions from the largest absorbance peak at 280nm separated using a size exclusion Superdex 200 column to confirm DP purification.

2.3.5. New construct- Expression tests

Expression tests indicated that BL21 cells didn't produce any DP despite being transformed successfully. The C43 cells, on the other hand, did produce DP. Cells grown at 20°C produced a small amount of DP, yet those at 30°C and 37°C successfully produced a much greater yield of DP. The best conditions for maximum DP expression were C43 cells grown at 37°C for 24 hours.

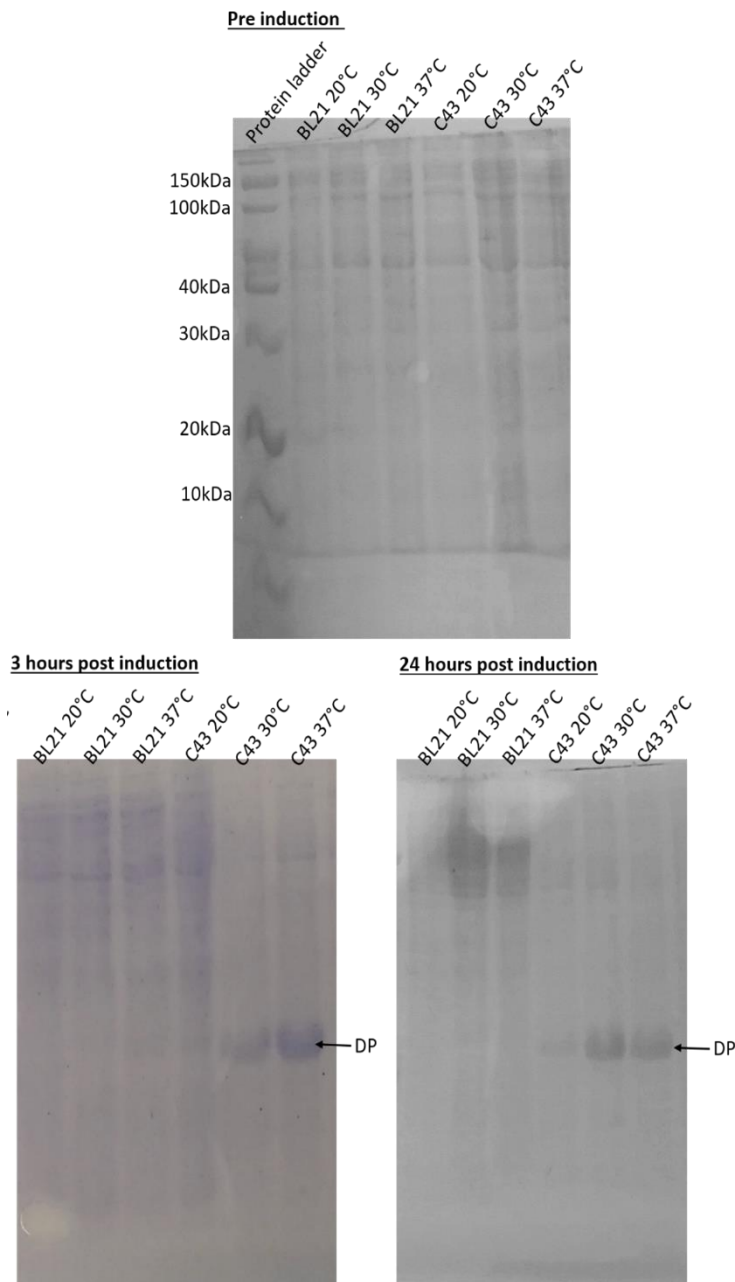


Figure 9- Expression test of C43 and BL21 cells transformed with Zaire DP new construct DNA, grown at 20°C, 30°C and 37°C. Samples taken pre induction, 3 hours post induction and 24hours post induction run on an SDS PAGE gel.

2.3.6. New construct- Ni IMAC gravity column elutions

Uncleaved DP, with the His-tag and KSI intact, has a MW of 20kDa. This MW matches the band in both elution lanes of the SDS PAGE gel of the Ni gravity column products. There is a large dark band in the elution from both columns- these peptide bands indicate DP extraction with Ni IMAC was successful. It also highlighted that multiple runs of the Ni IMAC column allow more DP to be collected. For all future purifications, three Ni gravity columns separated proteins of the cell lysate to purify maximum yields of DP.

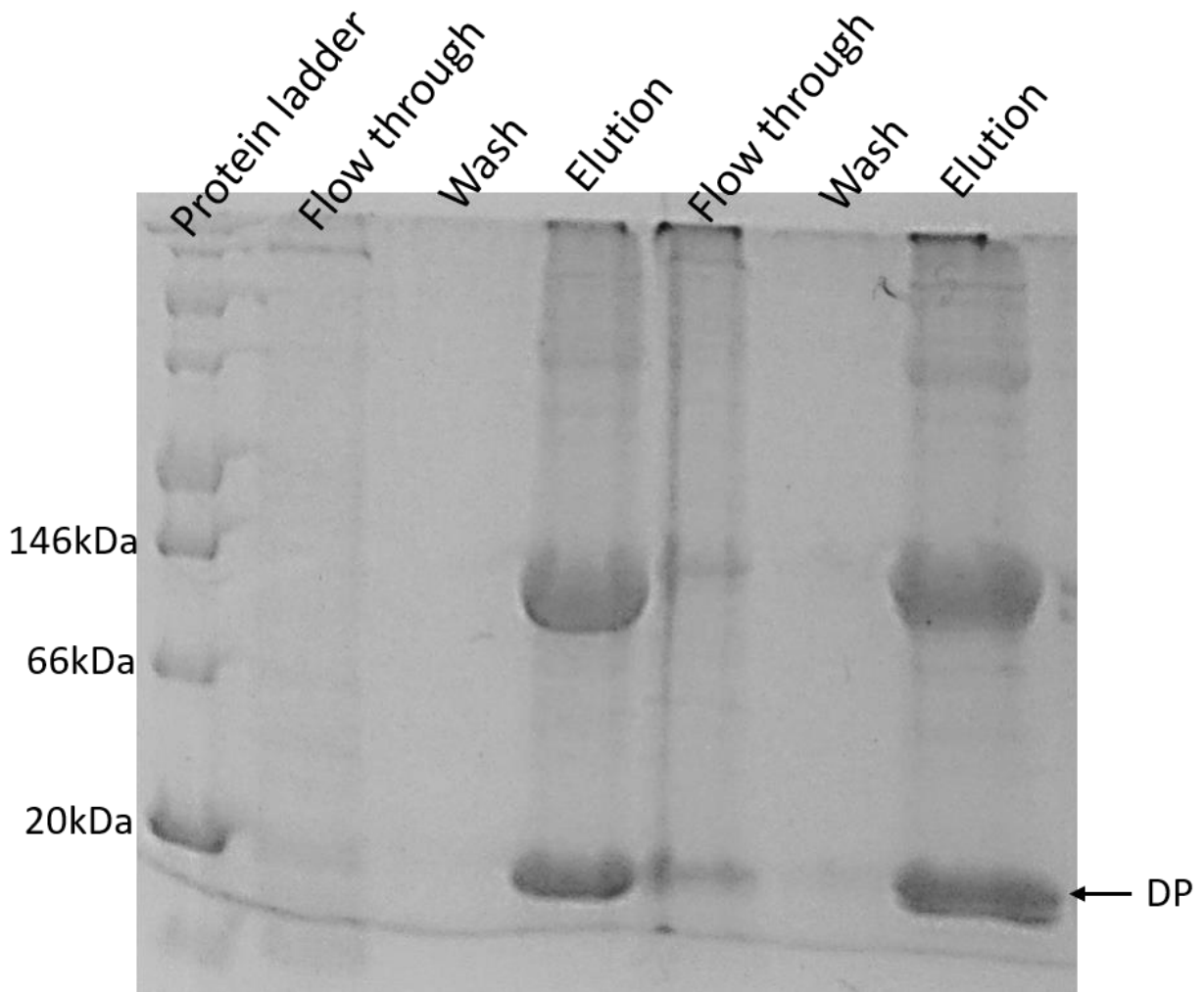


Figure 10- SDS PAGE gel of flow through, wash and elutions collected from the Ni IMAC gravity columns used to separate the cleaved peptide from other proteins in the cell lysate.

2.3.7. New construct- Chemical cleavage

Both 0.1M and 0.2M HCl caused cleavage of the DP as seen by the band at the very bottom of the SDS PAGE gels. Cleaved DP is very small with a MW of just 4.815kDa so appears as a band at the very bottom of SDS PAGE gels. The most effective cleavage and safest conditions were 0.1M HCl for 24 hours at 60°C as stronger HCl solutions are corrosive. All future DP grown from the new construct was cleaved using these conditions.

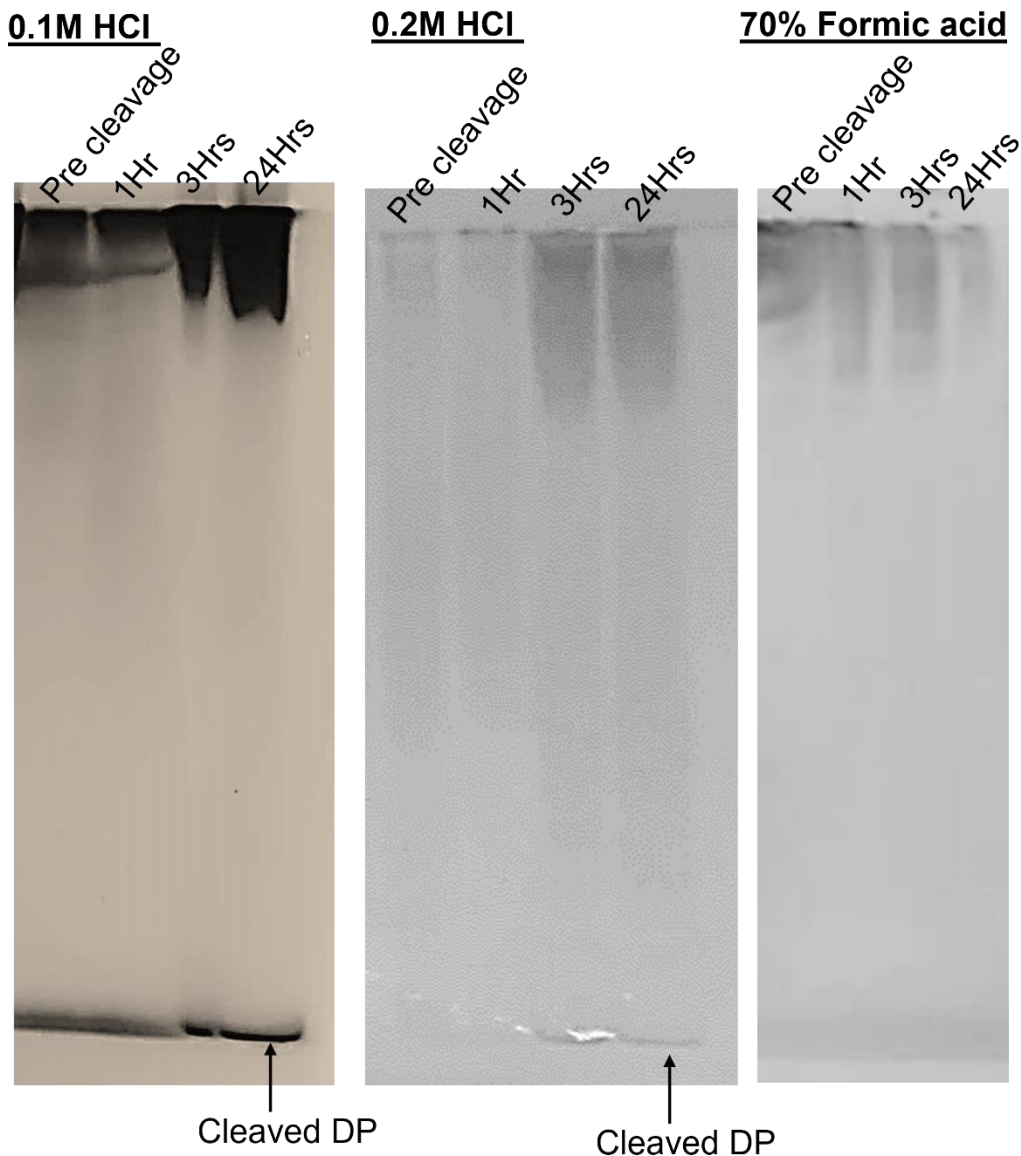


Figure 11 - Samples from chemical cleavage tests of DP with 0.1M HCl, 0.2M HCl and 70% Formic acid with 1mM DTT before cleavage, after 1 hour incubating at 60°C, after 3 hours and after 24 hours.

2.3.8. New construct- RP HPLC

The chromatogram from the RP HPLC shows three peaks. The first of these is a large, sharp peak at four minutes caused by sample injection into the column.

The second peak, between 16 and 18 minutes, is likely KSI cleaved from the DP by the HCl cleavage step. KSI elutes before DP as they have different hydrophobic points giving them separate retention times.

The final peak is DP eluting between 22 and 17 minutes.

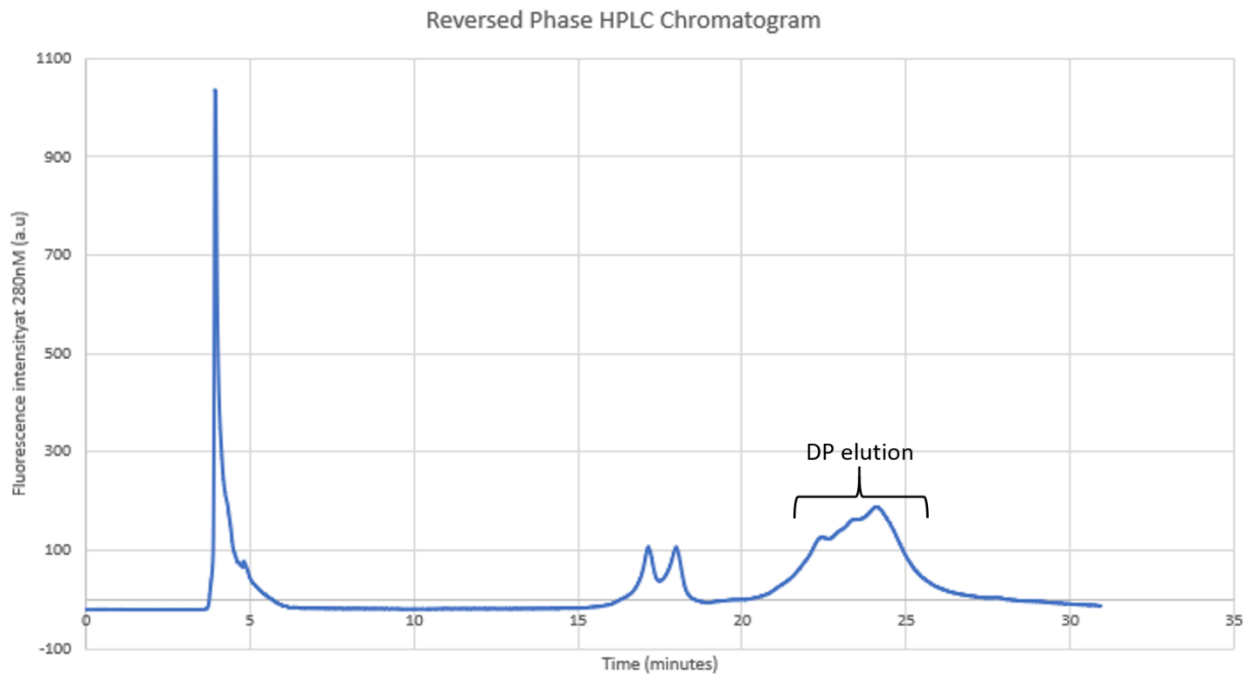


Figure 12- RP HPLC chromatograph of proteins eluting from the C4 delta pak column measured as peaks in fluorescence intensity detected at 280nm.

The RP HPLC elutions were run on an SDS PAGE gel to confirm that the final elution is DP. The gel produced didn't run well and has large smears at the top however, bands can be seen at the bottom of the last 2 lanes. This indicates that peptide is present in the elution collected during the third peak on the HPLC chromatogram. The peptide band is DP as it's at the bottom of the gel and has travelled the same distance down the gel as the 5kDa marker band of the protein ladder as would be expected as cleaved DP has a MW of 4.8157kDa.

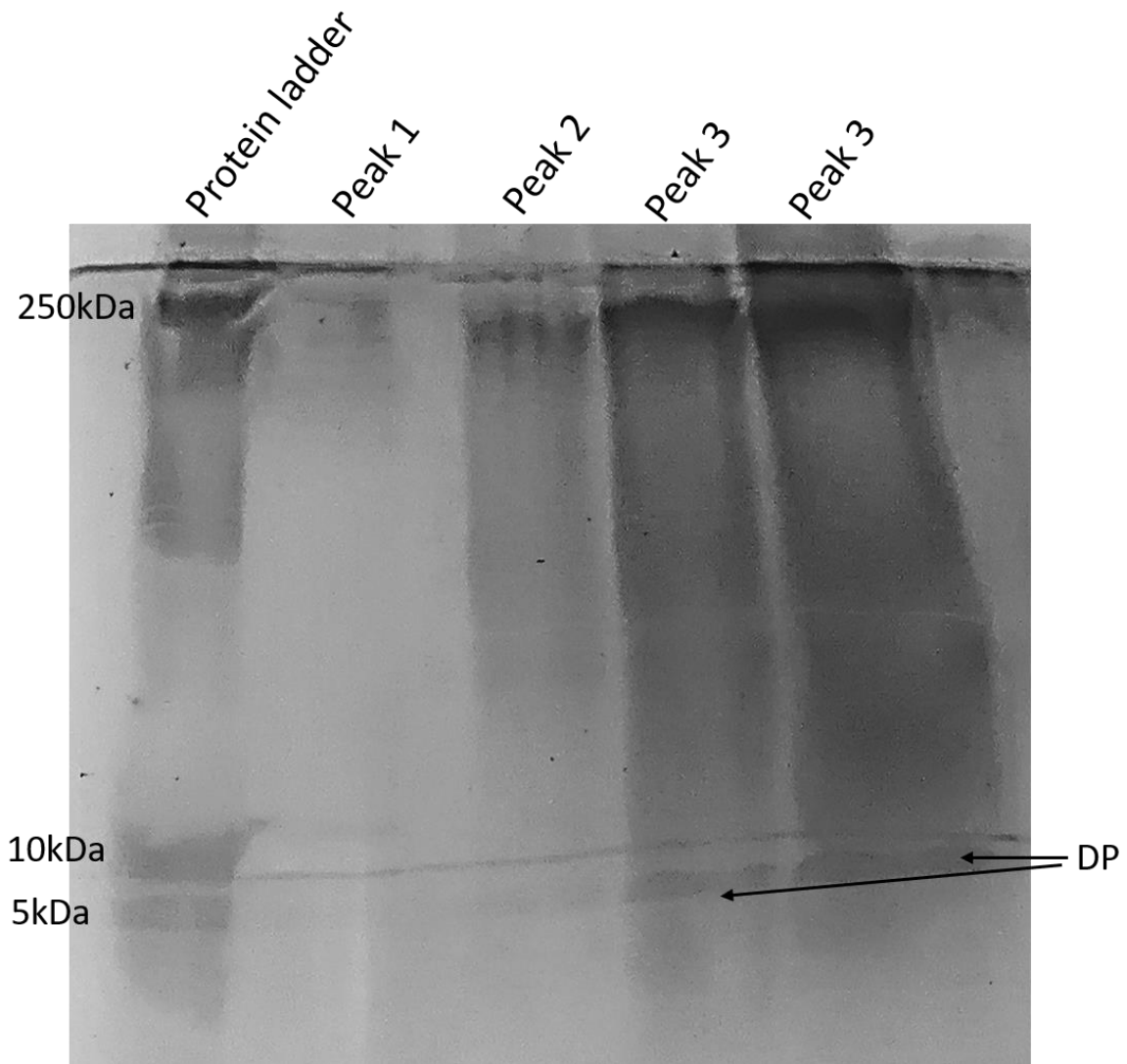


Figure 13- RP HPLC elutions run on an SDS PAGE gel to identify which elution DP is in. Peak 3 took a long time to elute so was collected in 2 aliquots. DP is present in both the first and second half of peak 3 indicating it's the final peptide to elute from the column.

An Electrospray mass spectrum of elution three recorded in the same way as the mass spectrum of the TEV cleavage sample was collected. Cleaved DP has an expected MW of 4.8157kDa. The large peptide peak on the mass spectrometry graph is 4.023kDa which corresponds to the weight of DP minus its last 7 residues. There is also a smaller peak at 2000.1 which is the MW of DP with the His-tag and KSI still attached showing a very small amount of peptide wasn't cleaved. This also shows that the DP has been purified well as there are few other peaks present and those which are present are very small.

The elution contains a high concentration of DP - this is confirmed by the large amount of powder collected after the elution was lyophilised overnight.

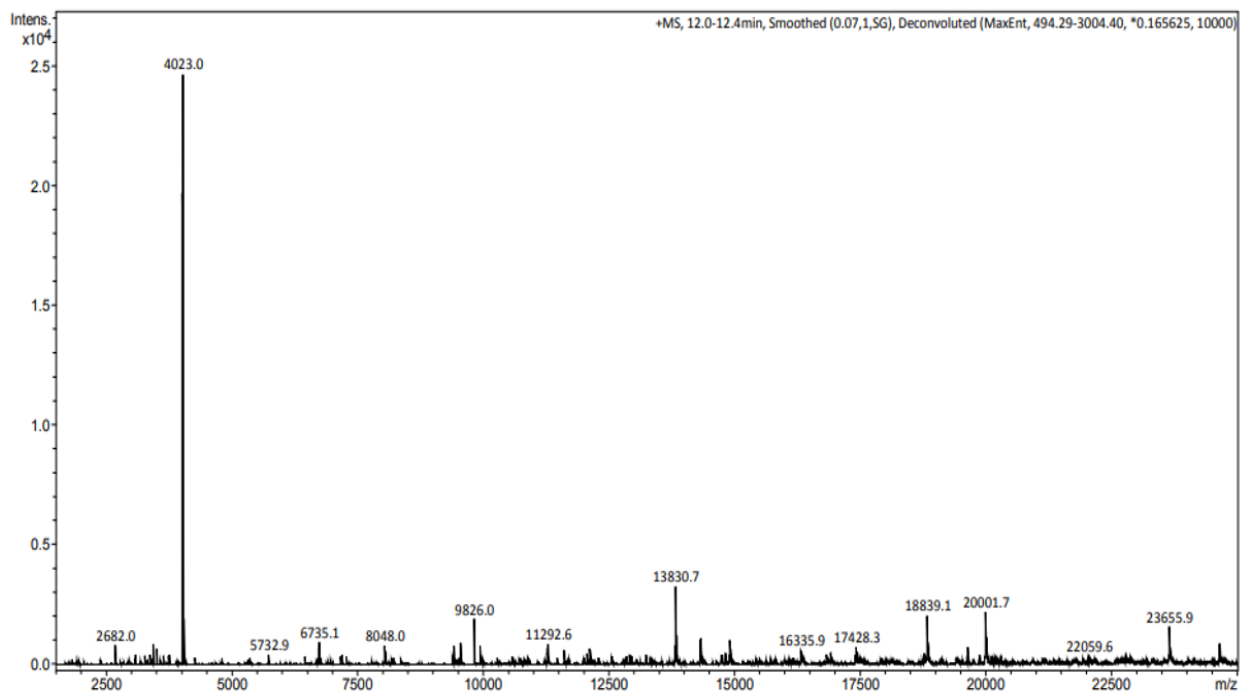


Figure 14- Mass spectrometry electro spray analysis of the final elution from RPHPLC showing DP is present in this elution and it's been successfully purified as there are no other proteins

2.4 Discussion

The pCOLD GFP construct transformed well into BL21 *E. coli* cells producing a full agar plate of individual colonies. The starters and growths from these colonies also grew well. DP expression was evident as the growth cultures appeared slightly green due to the presence of the GFP tag on the DP. The SDS PAGE gel confirmed DP production with a band of 55kDa in the elution from the Ni IMAC gravity column.

The TEV cleavage for cleavage of DP from the rest of the construct was unsuccessful. Failed TEV cleavage is apparent from the electrospray mass spectrometry graph as DP with the His-tag and KSI still attached has a MW of 55kDa, cleaved DP however has a MW of just 4.8157kDa. The large peptide peak present on the mass spectrometry graph has a MW of 55.064kDa representing uncleaved DP and indicating cleavage hasn't occurred and the GFP and His-tag are still present on the DP. Tagged DP can't be used for future experiments as GFP is large and would interfere with DPs activity and structure.

As TEV cleavage was unsuccessful, a new construct was needed. This new construct design allowed chemical cleavage methods to be employed. The chemical cleavage site, Asp-Pro was chosen based on Hwang et al.s investigations into chemical cleavage of fusions peptide bonds. This was the safest and most economical method discovered that would work effectively for this type of peptide. The Asp-Pro cleavage motif was inserted either side of the DP DNA sequence of the new construct. This arrangement was designed for KSI and His-tag removal from DP following its expression to acquire purified DP with no tags for further investigations.(36)

The expression tests of the new construct allowed the best conditions for successful growth and maximum peptide production to be determined. Both the BL21 and C43 *E. coli* cells transformed and grew well on LB agar plates containing ampicillin. This growth indicates the construct worked and successfully transformed into *E. coli* cells. Cultures from these transformations also grew successfully. However, samples run on an SDS PAGE gel indicated that only the C43s expressed DP - there was no DP expression in BL21 cells. Expressed DP is seen on the SDS PAGE gels as a band at 20kDa as this is the MW of DP with the His-tag and KSI still attached. The most effective conditions to grow the C43 cells were to incubate cultures at 37°C until IPTG induction then leave them at 30°C overnight to express. These conditions produced more DP than when cultures were grown at 20°C or 30°C pre-induction which is apparent from the darker peptide bands seen in the final column of the expression test SDS PAGE gels. Growths of the new construct using these optimised conditions were very successful. Clear bands of DP were visible in the elution lanes at 20kDa on the SDS PAGE gel run following Ni IMAC gravity columns.

Following overnight water dialysis, the peptide crashed out as a white precipitate visibly showing a good amount of peptide was produced and extracted from the cell lysate using the Ni IMAC gravity columns.

HCl achieved effective cleavage of the DP at both 0.1M and 0.2M however formic acid was not able to cleave DP from the KSI and His-tag. 0.1M HCL was used for future purifications as using lower concentration HCl conserves stocks, is cheaper and safer to work with. The optimum cleavage conditions for 0.1M HCl cleavage of DP were to leave the reaction for 24 hours at 60°C. Although some cleavage had occurred after 3 hours it was considered better to leave the reaction longer to ensure as much peptide was cleaved as possible. The cleavage reaction was carried out in a 1.5mL Eppendorf tube in a heatblock to maintain the 60°C temperature needed. Using a heatblock was the best way to ensure a constant temperature - performing the cleavage reaction in a 20mL universal flask on a hot plate was unsuccessful as the temperature wasn't consistent enough.

The final step to obtain purified, cleaved DP was separation using RP HPLC to remove the other cleavage products and proteins following HCl cleavage. The final product - pure DP can be seen on the SDS PAGE gel and mass spectrometer analysis of the last RP HPLC elution. These optimisation processes gave the final growth and purification method shown in figure 15.

New construct growth and purification overview

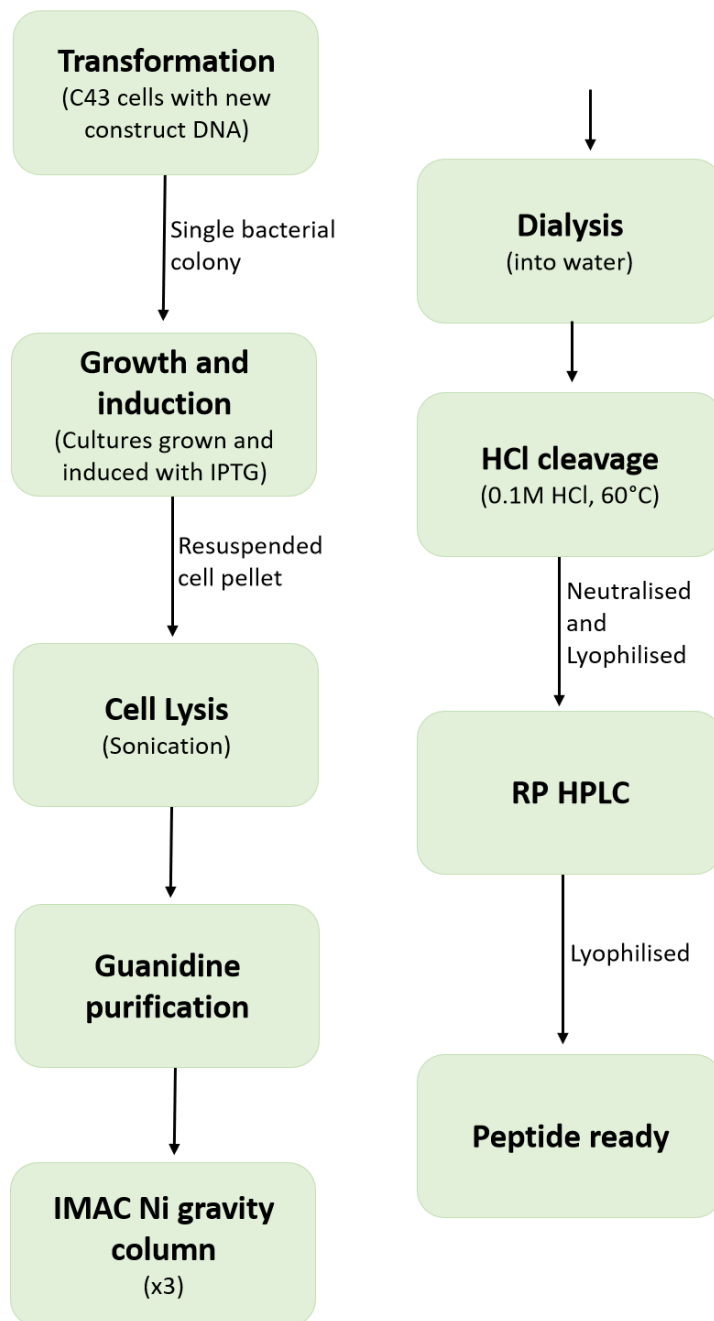


Figure 15- Overview of the optimised protocol for the growth and purification of the new Zaire DP construct.

3. Delta peptide structure

3.1 Methods

3.1.1 NMR

3.1.1.1. Isotopically labelled growth:

Nuclei can only be detected on NMR experiments if they possess spin $\frac{1}{2}$. To have spin $\frac{1}{2}$ nuclei must have an uneven number of neutrons or protons to give them an odd mass number. Neither nitrogen nor carbon have odd mass numbers so their isotopes, ^{13}C and ^{15}N , have to be incorporated into the peptide for 2D or 3D experiments. 2D experiments were performed in this study so, only ^{15}N labelling was necessary. Hydrogen atoms only contain one neutron and already have spin $\frac{1}{2}$ - no isotope labelling is required to see them. A minimal media growth protocol incorporated ^{15}N into the DP used for NMR experiments.

The initial growth was the same as a normal unlabelled growth - transformations, starter cultures, and cell growths were performed in exactly the same way. Once the cells reached OD_{600} 0.7, they were spun down at 4000rpm for 20 minutes at 4°C to remove the LB media they were grown in. The pellets were kept on ice and gently resuspended in reconstituted minimal M9 media. This minimal media consisted of:

- 100mL 10x M9 salts (2.15M Sodium phosphate dibasic, 4.19M Potassium phosphate monobasic, and 10.23M Sodium chloride at pH 7.4)
- 1mM Magnesium sulphate
- 0.1mM Calcium chloride
- 1mM Thiamine HCl
- 22.2mM D-Glucose
- 53.49M ^{15}N Ammonium chloride
- 0.29 μM Ampicillin
- 821ml Milli-Q water to give 1L total volume.

All components of the minimal media excluding, ampicillin, glucose, and ammonium chloride, were autoclaved to avoid bacterial contamination of the cells. The cells resuspended in 1L minimal media per 4L of initial growth culture were incubated, at 30°C , 200rpm for 45 minutes. 1mM IPTG was added to

induce protein expression overnight at 30°C, 200rpm. The peptide purification process was then performed in the same way as for unlabelled growths detailed in 2.3.5.

3.1.1.2. Sample optimisation:

DP does not dissolve in water as it is hydrophobic. Thus, to dissolve the DP a range of solvents were used to aid its solubilisation. The first solvent tried was acetic acid, 30µL of 30% deuterated acetic acid was added to the lyophilised DP powder with 1% chemical shift standard trimethylsilylpropanesulfonateas (DSS), 5% D₂O and 2mM DTT. The sample was loaded in a clean Shigemi NMR tube and spun to remove bubbles and a Heteronuclear Single Quantum Coherence (HSQC) was collected.

The 30% acetic acid didn't dissolve the DP well enough and some precipitate was present so lipid screening tests were used to identify if lipid addition would aid the solubilisation of DP. DP was dissolved in 400µL chloroform and mixed with lipids and trials of both 2mM Lauryl maltose neopentyl glycol (LMNG) and 1mM Dihexanoylphosphatidylcholine (DHPC) were performed. After drying the mixture into a thin film, it was dissolved in phosphate buffer (20mM Sodium phosphate, 20mM Sodium chloride pH 7.4). Samples were prepared in the same way as before and HSQCs collected. The LMNG sample dissolved fully and an HSQC NMR spectrum was collected from it. However, the DHPC sample was too insoluble to collect a spectrum from.

Another sample was dissolved successfully in 40% methanol D₄ and all the DP solubilised well. Again, 2mM DTT, 1% DSS, and 5% D₂O were added and the sample was measured in a Shigemi tube.

3.1.1.3 Experiment optimisation

From the sample dissolved in 40% methanol D₄, three different 2D experiments – a HSQC, a Heteronuclear Multiple Quantum Coherence Band-Selective Optimized Flip Angle Short Transient (HMQC SOFAST) and a Best Transverse relaxation-optimised Spectroscopy (BEST TROSY) were collected to identify which yielded the best quality spectrum. 1024 points in the ¹H dimension and 128 increments in the ¹⁵N dimension were collected at 298K. The spectrum width was ¹H 14ppm by ¹⁵N 40ppm and 32 scans were performed using a Bruker 600MHz spectrometer. All future experiments were collected using these parameters unless stated otherwise.

3.1.1.4. Lipid experiments

Lipid experiments looked for changes in the DP structure occurring due to membrane interactions or insertion. The first of these was to add asolectin and LMNG bicelles, bicelles are micelles comprised of lipid and detergent. The long-chain lipids form the planar length of the bicelle with shorter chain detergent molecules forming the high curvature regions at either end of the disk-shaped bicelle. In this case, the asolectin lipids formed the long planar side regions and LMNG the curved ends. Because bicelles are smaller than vesicles any residues interacting with them will still be able to be seen using solution NMR. The LMNG asolectin bicelles were made to a q-ratio of 0.4 (40mM lipid/100mM detergent). 40mM asolectin was dissolved in 1mL chloroform and dried into a thin film. 6µL of bicelle stock was added to an NMR sample of ¹⁵N DP dissolved in 40% methanol D4 with 2mM DTT, 1% DSS and 5% D₂O then a BEST TROSY was collected.

The effects of lipids on DP structure were also investigated by adding asolectin vesicles to a ¹⁵N DP sample prepared in the same way. 50µM asolectin vesicles in phosphate buffer were added to the peptide sample and a BEST TROSY was collected using the same parameters previously optimised (3.1.1.3.). 64 scans were collected instead of 32 to achieve a better signal-to-noise ratio.

LMNG was then added to this sample to see if adding detergent caused any further changes. 1% LMNG dissolved in water was added to the NMR sample containing DP and asolectin vesicles. However, the DP crashed out upon addition and the resulting signal from the sample was too low to collect a spectrum.

3.1.2. Circular Dichroism

Information about the secondary structure of DP was also obtained using FarUV CD. Four samples were run: oxidised DP, oxidised DP with asolectin, reduced DP and a reduced DP sample with asolectin. All DP samples contained 20µM DP with reduced also containing 1mM DTT and oxidised 5mM H₂O₂. The samples with asolectin added contained 150µM asolectin vesicles in phosphate buffer to look for changes in peptide structure due to membrane insertion.

Data was collected using a Jasco J-710 CD Spectropolarimeter and 8 scans of each sample were accumulated at 20°C. The reduced DP samples were measured over a wavelength range of 200- 260nm. However the oxidised DP samples saturated the detector too early so could only be measured between 204- 260nm.(37)

3.2 Results

3.2.1 Expression and purification of ^{15}N labelled protein

An SDS PAGE gel of the flowthrough, wash, and elution from the Ni gravity column of the ^{15}N growth was run. A protein band at the bottom of the gel can be seen - this is DP as it has a MW of 4.815kDa apparent as it has travelled the same distance down the gel as the 5kDa protein marker band. This shows that labelled DP was successfully expressed and harvested from the minimal media growth.

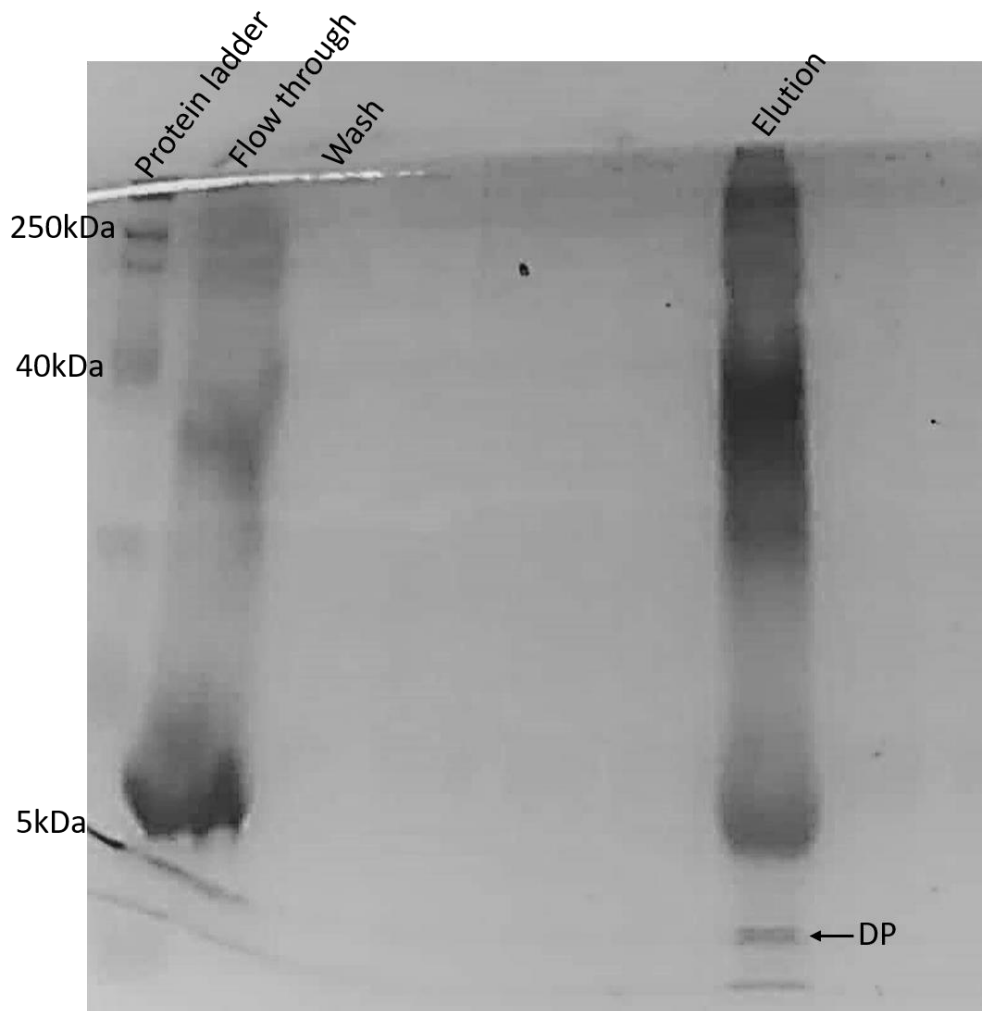


Figure 156- SDS PAGE gel of flow through, was and elution from the first Ni gravity column performed on the cell lysate from the ^{15}N labelled minimal media growth.

3.2.2. NMR Sample optimisation

The sample dissolved in 30% acetic acid failed to dissolve fully, some DP went into solution but there was white precipitate present in the sample. As a result of this, the HSQC spectrum collected had a weak signal and it was difficult to distinguish the residue peaks from background noise. This spectrum is shown in figure 17. Reducing the pH to aid solubilisation of the peptide helped it transition into solution more completely. However, the low pH made it impossible to get a stable lock on the NMR spectrometer so the sample couldn't be used.

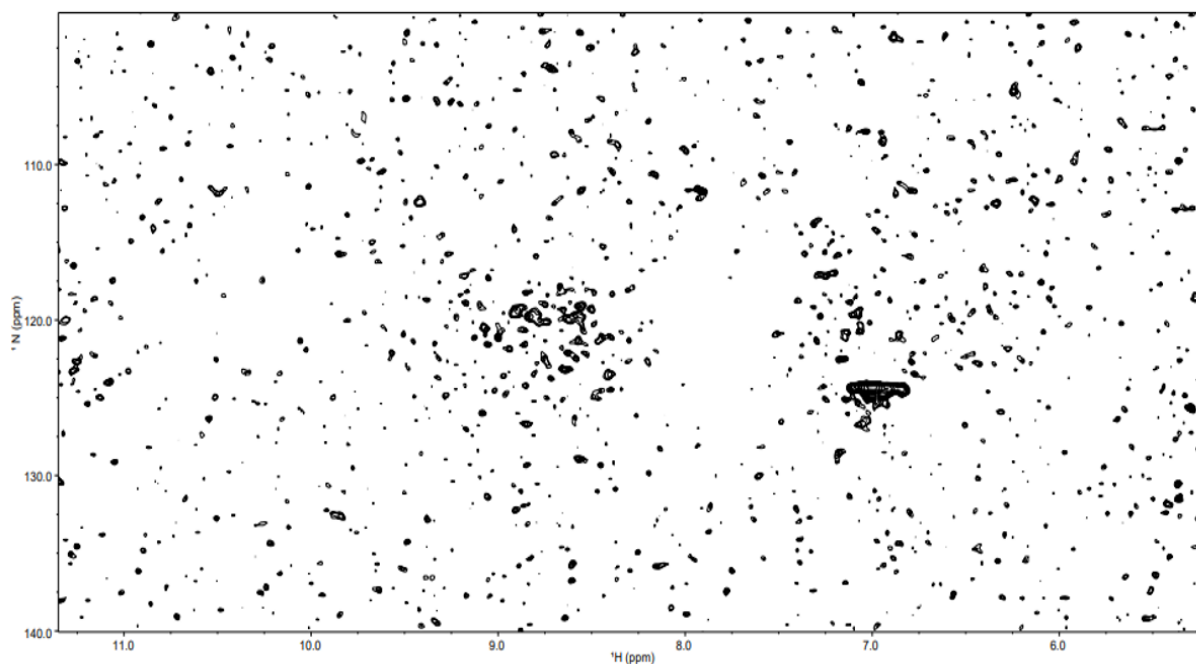


Figure 167- HSQC NMR spectrum of DP dissolved in 30% Acetic acid.

The DHPC lipid test was unsuccessful in dissolving the DP and a spectrum couldn't be collected from the sample. LMNG on the other hand, did help the DP dissolve more effectively than 30% deuterated acetic acid and an HSQC was collected. The spectrum collected (figure 18) has a poor signal-to-noise ratio but peptide peaks are visible.

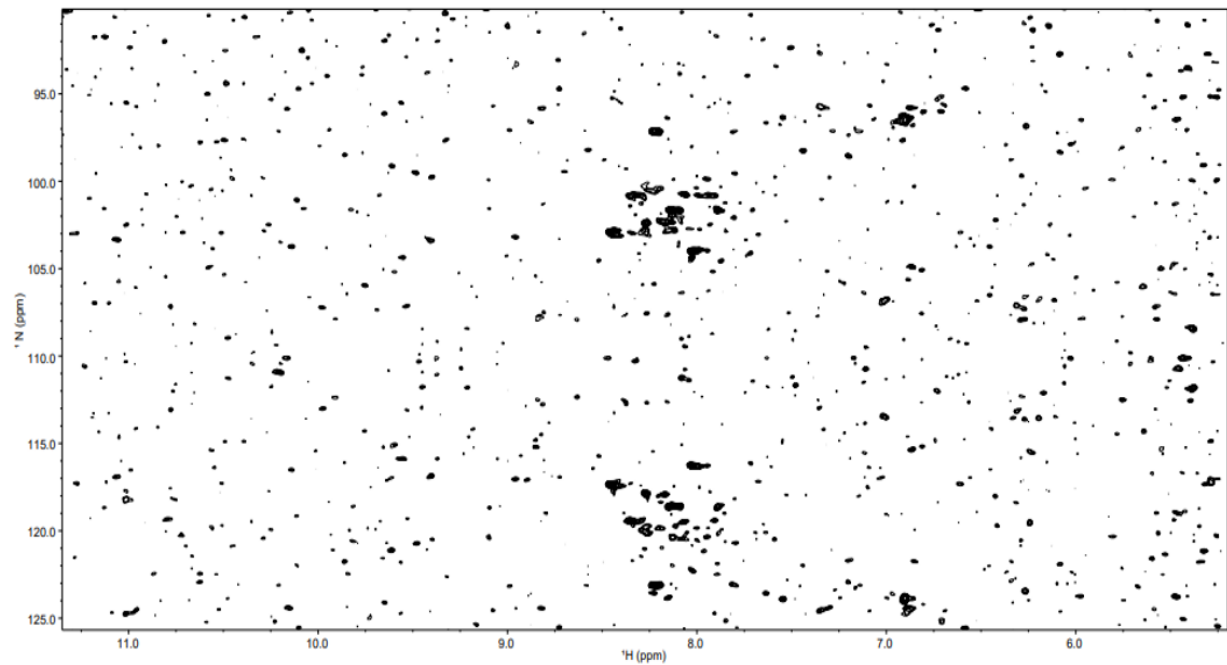


Figure 178- HSQC NMR spectrum of LMNG detergent solubilisation test

DP almost completely dissolved in 30% methanol D4 and when increased to 40% methanol D4 it fully dissolved. Plenty of signal was seen resulting in a high signal-to-noise ratio indicating the BEST TROSY spectrum collected is good. The spectrum shows clear peaks each of which represents a residue of the peptide. Although there was a crowded region in the centre of the spectrum individual peaks were still identifiable when the intensity of the spectrum was altered. A total of 36 peaks would be expected on this spectrum. This is because a peak should be visible for each residue apart from Prolines and the Glutamate on the N-terminus as they don't have amino groups. Despite the lower resolution region in the centre a total of 34 peaks can be identified on this spectrum. This spectrum is far clearer than the one collected from the sample in 30% deuterated acetic acid.

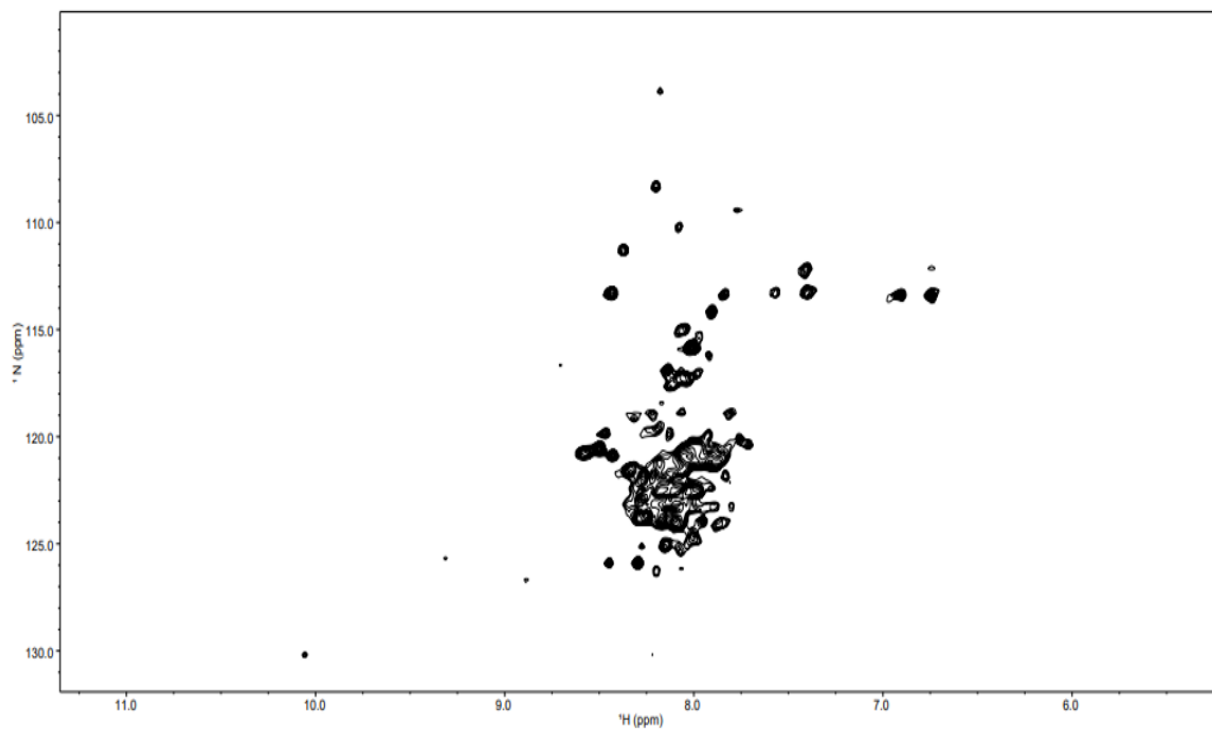


Figure 189- BEST TROSY NMR spectrum of DP dissolved in 40% methanol D4.

3.2.3. NMR experiment optimisation

A HMQC SOFAST experiment was tried first which produced an unclear spectrum. There were some distinguishable individual peaks but a large region of broad, messy peaks in the centre and some broad unclear peaks in the top right of the spectrum. Only 19 of the 36 peaks which should be distinguishable can be identified on this spectrum.

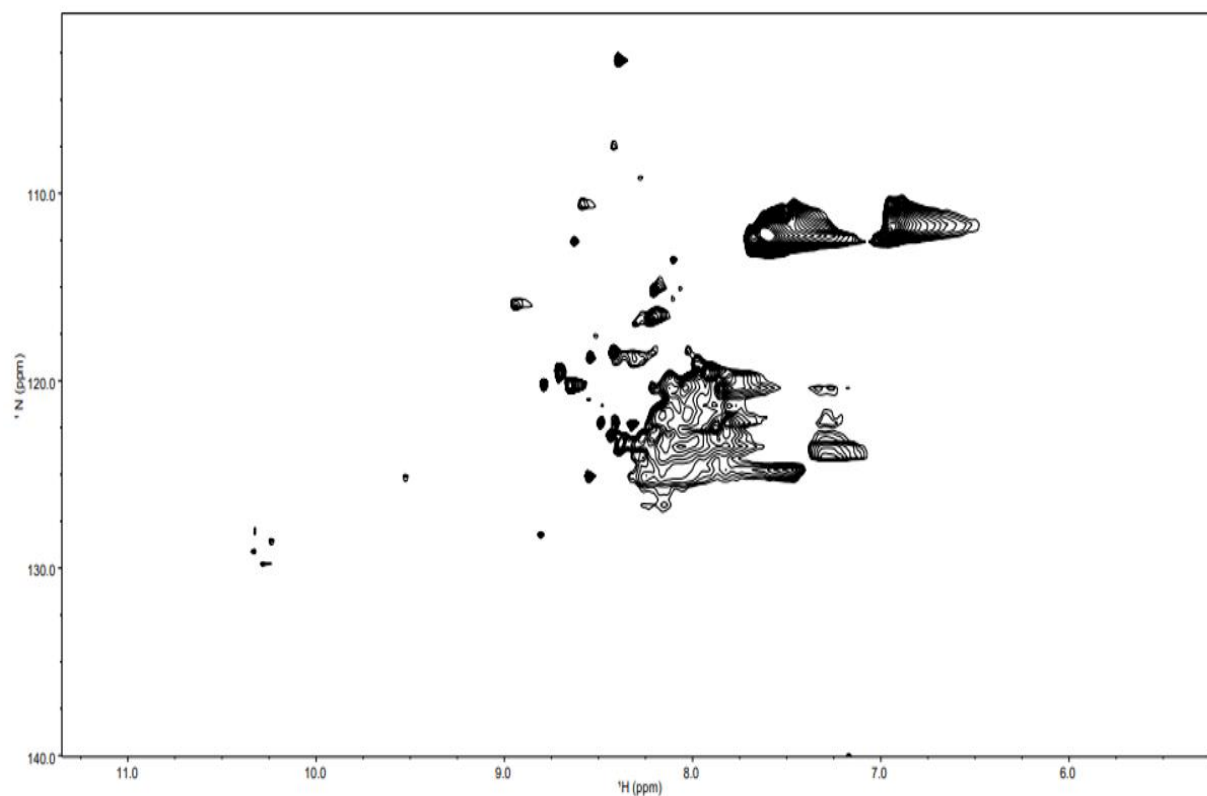


Figure 20- HMQC SOFAST NMR spectrum of DP dissolved in 40% methanol D4.

The HSQC produced a clearer spectrum, but many peaks were still broad and it's difficult to identify individual peaks in the overlapped region in the centre. This spectrum was more successful than the HMQC SOFAST with 25 peaks identified.

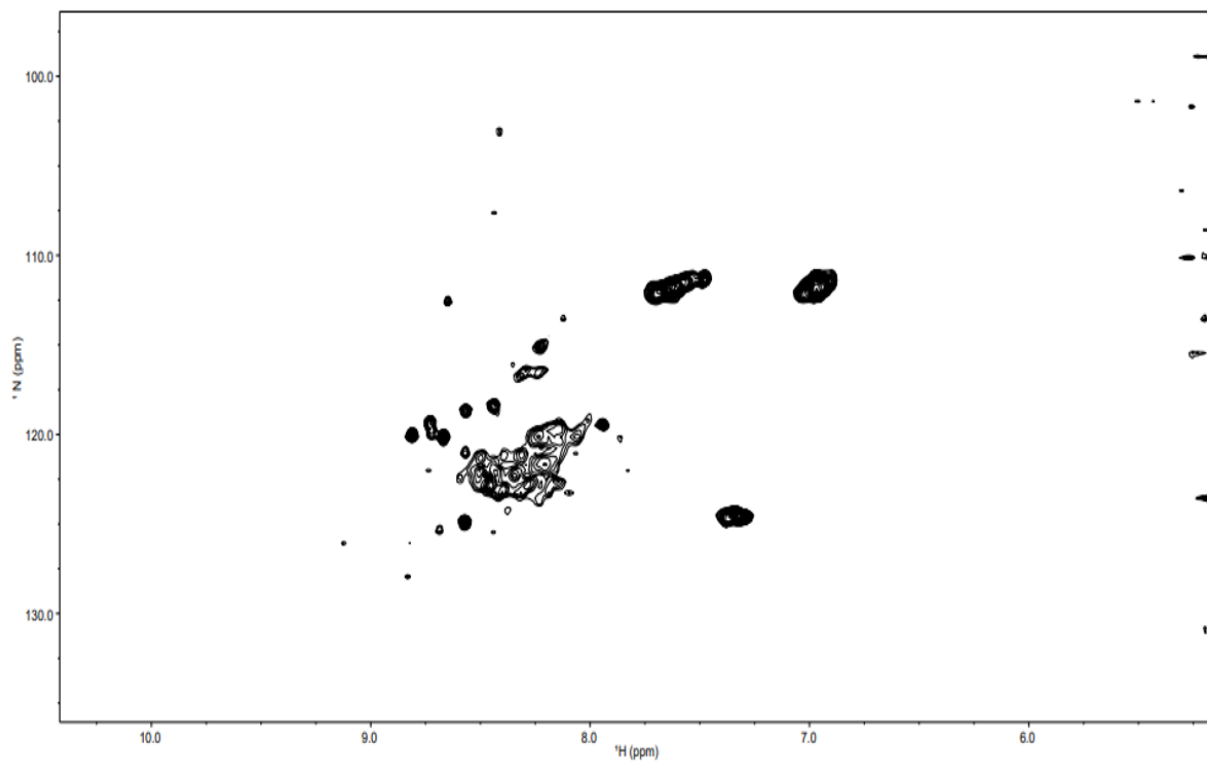


Figure 191- HSQC NMR spectrum of DP dissolved in 40% methanol D4.

Finally, a BEST TROSY was collected, this gave the best spectrum. The overlapped area in the centre of the spectrum, although still rather messy, was far clearer making identification of individual peaks possible when the spectrum was viewed at very low intensities. The best peak definition of the three experiments was seen on this spectrum with 34 resolved peaks visible – more than both the HSQC and the HMQC SOFAST collected previously. The signal-to-noise ratio is also good yielding a clear spectrum.

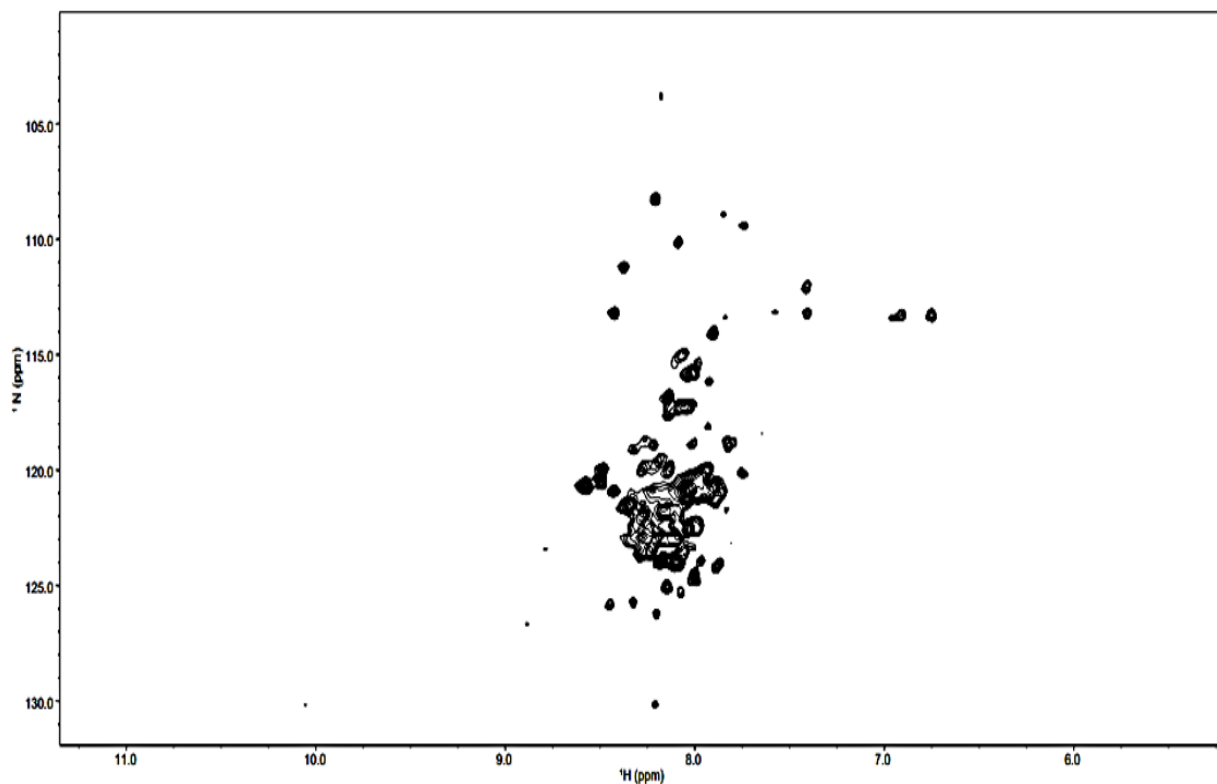


Figure 202- BEST TROSY NMR spectrum of DP dissolved in 40% methanol D4 for experiment optimisation.

3.2.4. Lipids experiments

Adding asolectin LMNG bicelles to the sample caused DP to crash out of solution forming a white precipitate. Spinning the DP sample down allowed the powder to be removed and a BEST TROSY was collected. However, the signal was weak resulting in a poor spectrum with broad peaks. The spectrum (red) was overlaid onto the BEST TROSY collected before the bicelles were added (black) and a shift can be seen in the location of some peaks but due to the poor quality of the spectrum this is not a clear result.

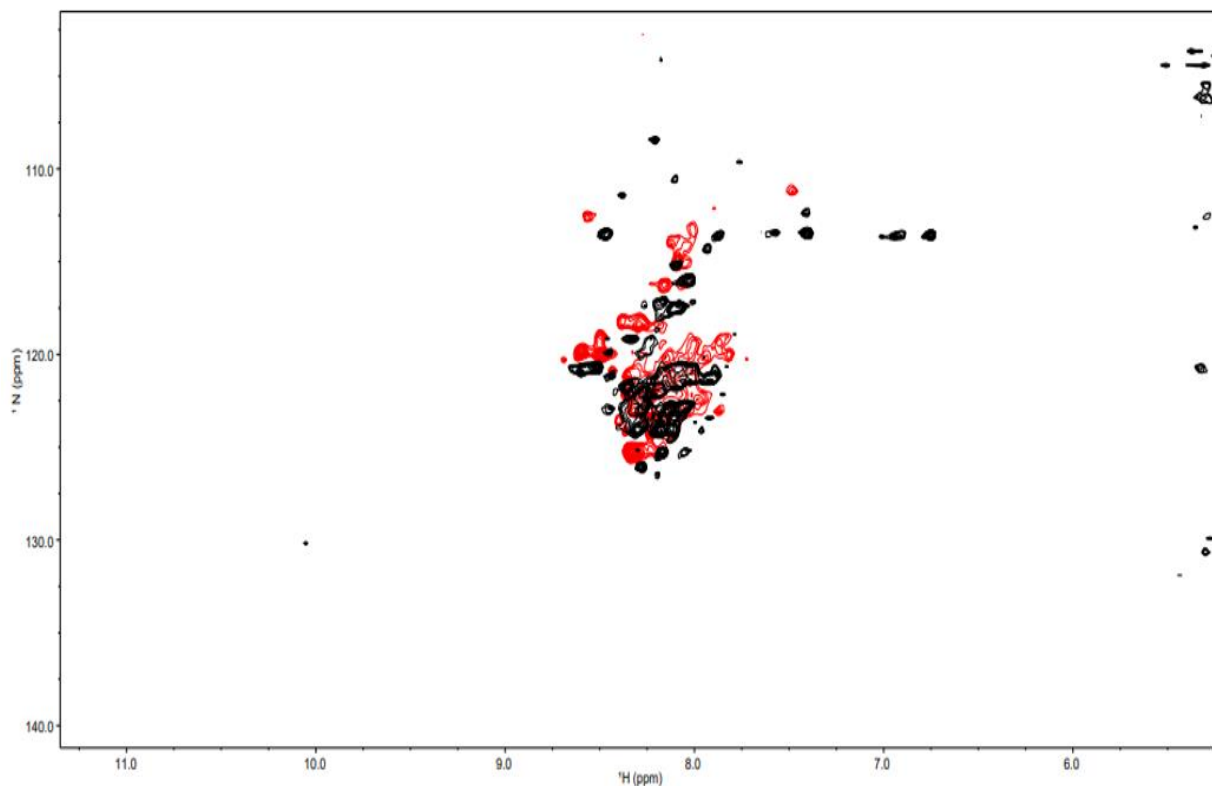


Figure 213- BEST TROSY spectrum of DP dissolved in 40% methanol D4 shown in black with BEST TROSY spectrum of DP in 40% methanol D4 with LMNG asolectin bicelles added overlaid in red.

Adding asolectin vesicles to the peptide sample in 40% methanol D4 caused a shift in the BEST TROSY peaks collected from 17 residues. Peak shifts occur when the local environment around a residue changes. These changes occurred due to secondary structure alterations caused by DP membrane insertion. Residue peaks that shifted were therefore involved in or very close to regions of DP which underwent a structural change. 8 peaks also disappeared when asolectin vesicles were added, this is significant as it indicates these residues were interacting with the lipids in the membrane, which makes them too big to be detected by solution NMR.

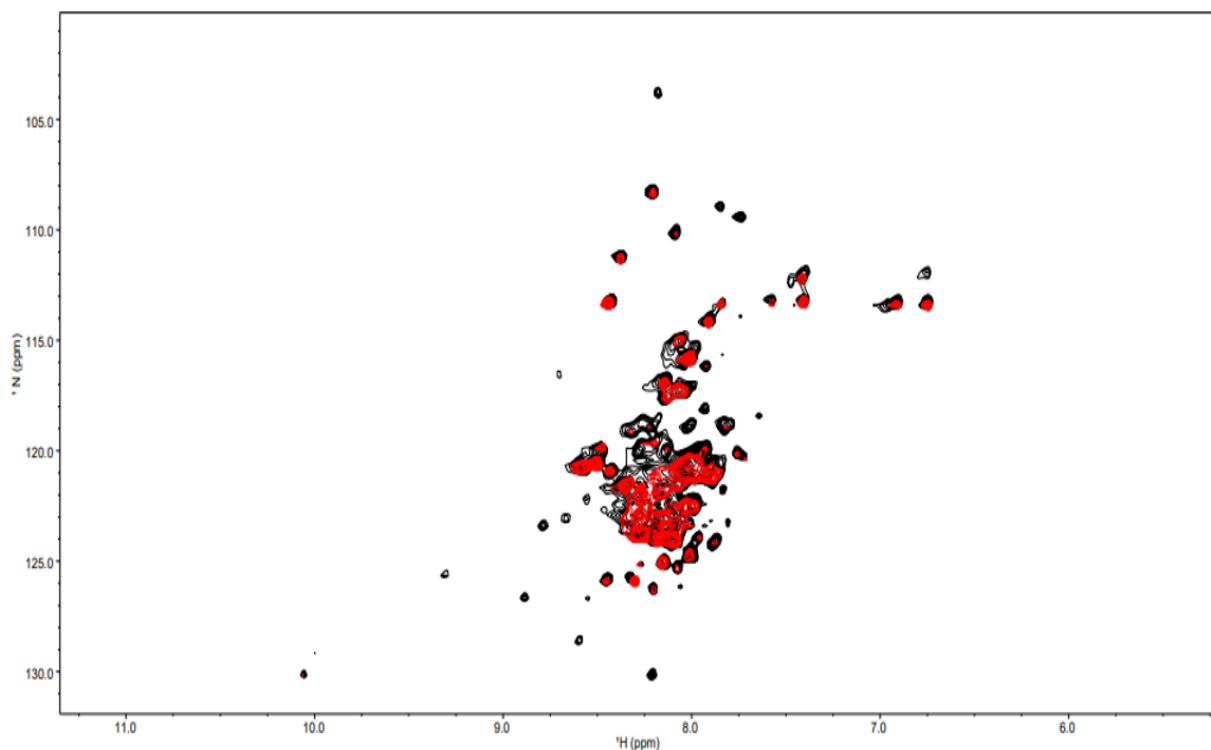


Figure 224- BEST TROSY NMR spectrum of DP dissolved in 40% methanol D4 (black) with BEST TROSY NMR spectrum of DP dissolved in methanol D4 with asolectin vesicles added overlaid on top (red).

Adding LMNG to the sample containing asolectin vesicles caused some insolubility, the sample didn't produce a good spectrum as this made the signal weak. A BEST TROSY was still collected and can be seen below (red) overlaid with the BEST TROSY collected before LMNG addition (black).

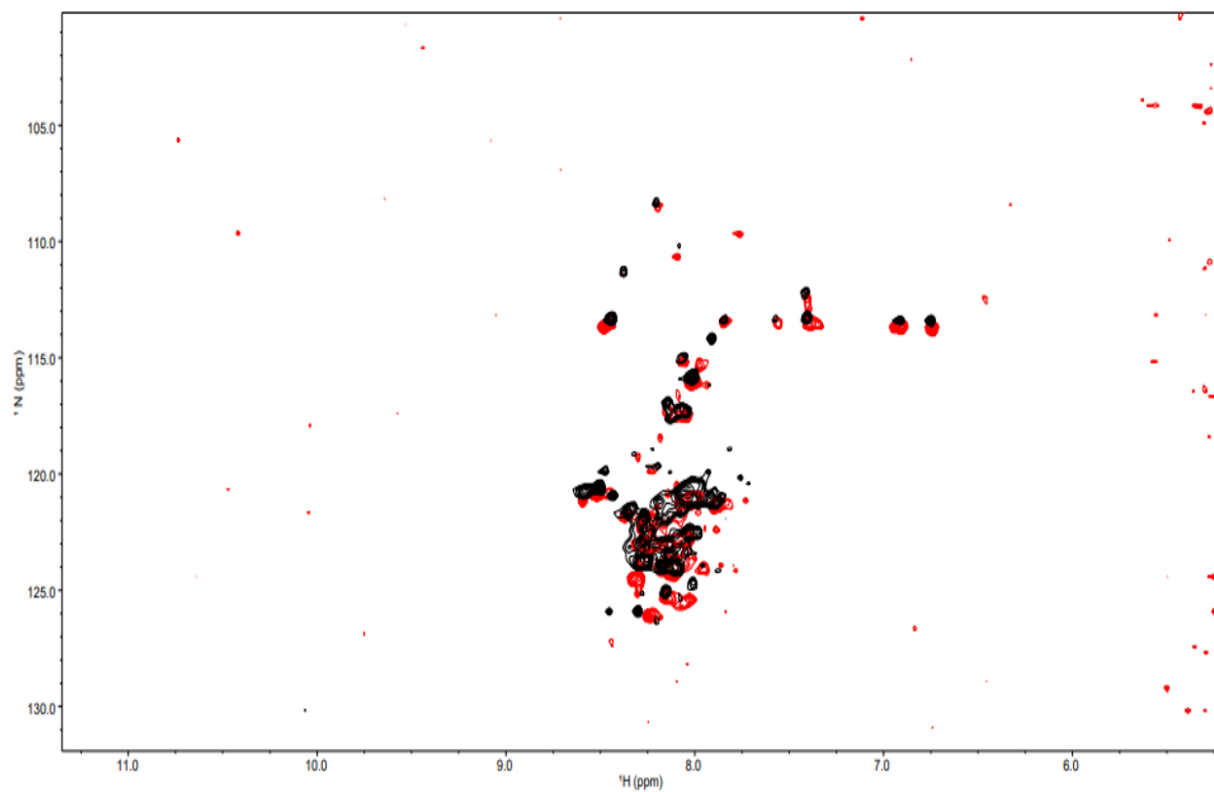


Figure 235- BEST TROSY NMR spectrum DP with asolectin vesicles (black) with BEST TROSY of DP with asolectin vesicles following LMNG addition (red).

3.2.5. CD

The CD plots of DP, in its reduced and oxidised states, were overlaid. The overlaid graph highlights the differences in DPs structure due to its oxidation state. The different states have similarly shaped graph plots but slightly different CD (mdeg) intensities indicating that the two samples contain DP with a mildly different secondary structure. The difference is however very small.

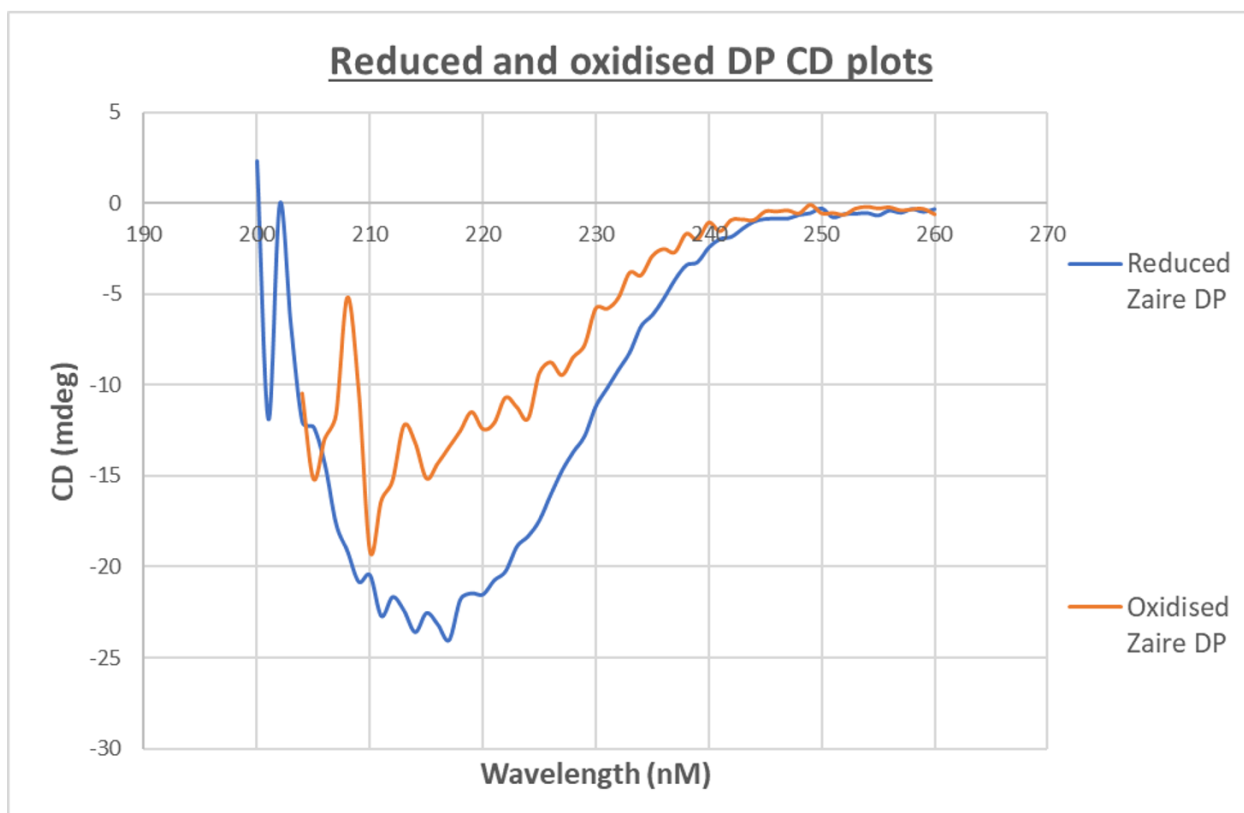


Figure 246- FarUV CD plots of oxidised and reduced DP in 40% methanol measured between 200-260nm.

Overlaying the plots produced from DP samples with asolectin present over those with no DP made changes occurring due to membrane insertion apparent. A greater difference was observed when asolectin was present in the reduced DP sample than the oxidised DP sample. The differences are very minimal however and likely due to experimental error as the plots before and after asolectin addition are the same shape and trend. Only the intensity varies. This intensity difference is particularly small for the oxidised samples with the two plots collected almost superimposable (figure 28). The CD therefore shows that no secondary structure changes occurred when asolectin vesicles were added to either the reduced or oxidised samples and the variation seen is due to experimental error.

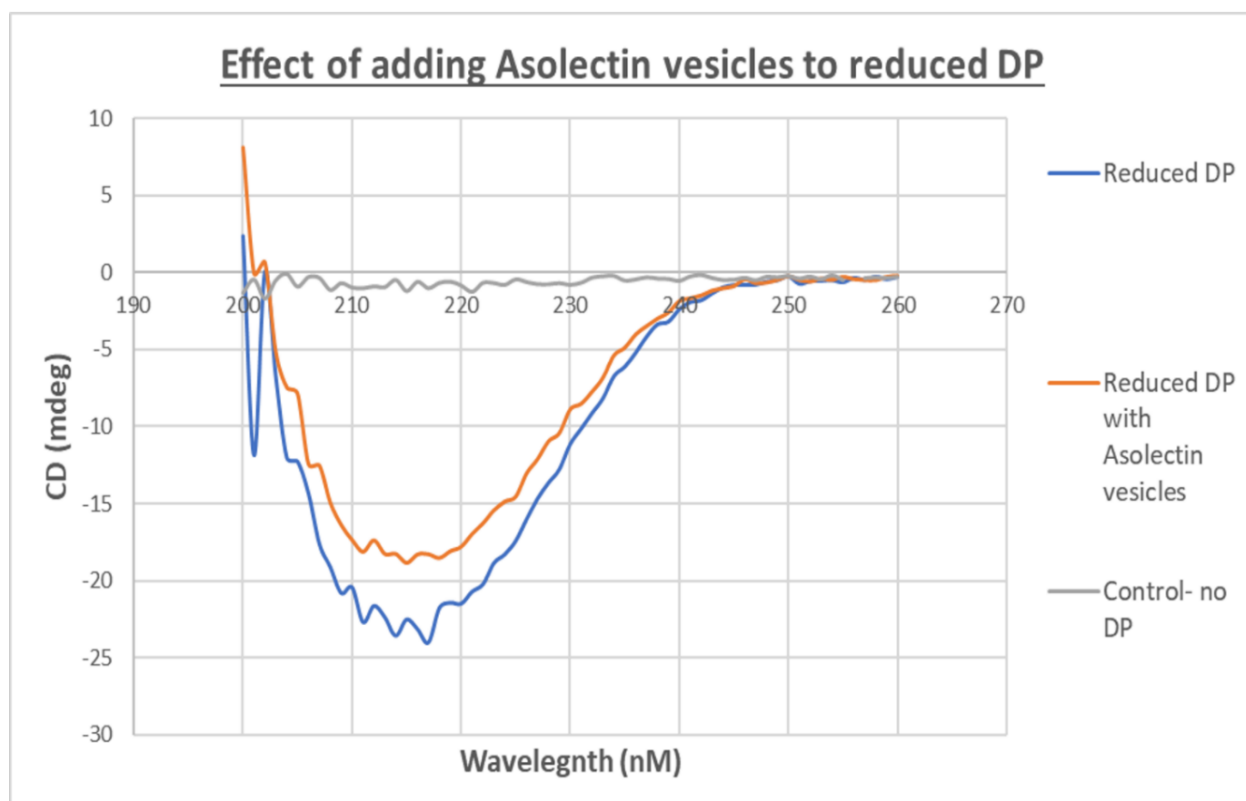


Figure 257- FarUV CD plots of reduced DP dissolved in 40% methanol before and after the addition of 150 μ M asolectin vesicles measured between 200-260nm.

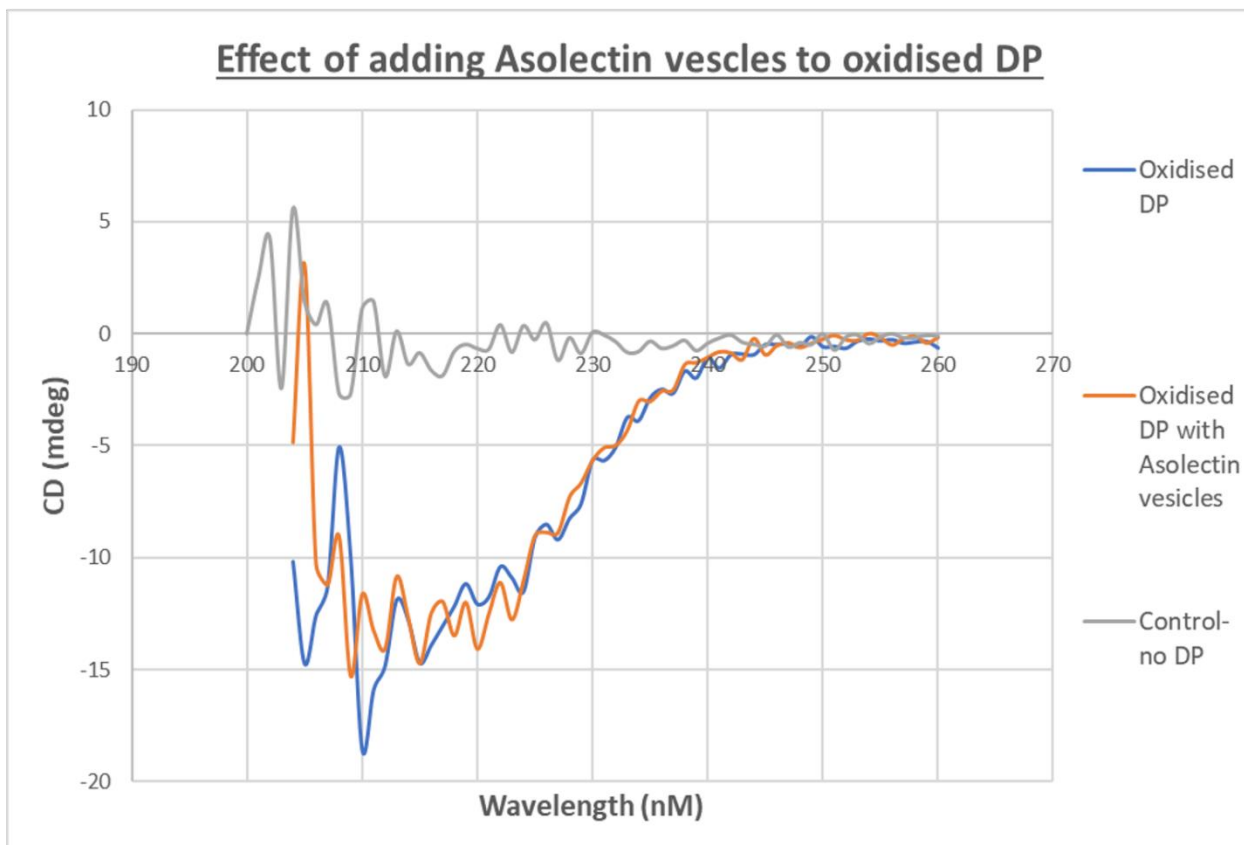


Figure 28- FarUV CD plots of oxidised DP dissolved in 40% methanol before and after the addition of 150 μ M asolectin vesicles measured between 204-260nm.

The oxidised DP CD data was only collected between 204-260nm rather than 200-260nm like the reduced DP data as the detector became saturated too early due to the higher intensity so 200nm couldn't be reached safely.

The data sets obtained from the CD experiments were also analysed using K2D3 to predict the secondary structures present in DP. This prediction tool provided percentage composition predictions of the secondary structures present in the samples. K2D3 predicted that from the CD data collected DP in both its oxidation states is almost entirely α -helical with little to no change occurring due to asolectin vesicle addition.

Table 1- K2D3 database secondary structure predictions indicating the percentage of α -helix and β -sheet regions present in the 20 μ M reduced and oxidised peptides both in the presence of 150 μ M asolectin vesicles and without from the CD spectra collected in 40% methanol.

| Peptide sample | α -Helix (%) | β -Sheet (%) |
|-------------------------|---------------------|--------------------|
| Reduced | 94.83 | 0.01 |
| Oxidised | 94.34 | 0.03 |
| Reduced with asolectin | 94.93 | 0.01 |
| Oxidised with asolectin | 94.34 | 0.03 |

3.3 Discussion

3.3.1 NMR sample optimisation

Optimising sample preparation was the first important step in performing NMR experiments as the peptide must be fully dissolved in order to carry out solution NMR experiments. Solution NMR requires the sample to be consistent to ensure the magnetic field is homogenous throughout the sample tube. The magnetic field will get distorted if there are particulates or precipitation in the sample. This distortion results in indistinct spectra. Poor quality spectra are generated from partially dissolved samples as only the peptide in solution can be seen. Incomplete solubilisation results in a lower relative concentration as not all of the DP is visible to the NMR - spectra collected will reflect this. NMR sensitivity is highly dependent on sample concentration meaning low concentrations result in poor quality spectra.(38)

Dissolving the peptide in 30% deuterated acetic acid was unsuccessful as it wouldn't fully dissolve resulting in a low concentration. An HSQC was collected but, the spectrum is poor due to the low peptide concentration. Low concentration causes poor signal-to-noise so the peaks merge into the background noise detected and the peptide spectrum isn't clear. To dissolve DP more fully the pH had to be reduced to pH 1 through the gradual addition of small increments of 2% HCl. Although more DP dissolved, the pH then proved too low to achieve a stable lock on the NMR spectrometer. As a result, a spectrum couldn't be collected from this sample. 30% deuterated acetic acid is therefore not a suitable solvent for DP solution NMR.

Detergents can aid the transition of membrane proteins into solution because they mimic the natural lipid bilayer environment that membrane proteins usually exist in. Detergents are amphipathic molecules with a very similar structure to lipids, they have a hydrophilic polar head group and a hydrophobic hydrocarbon chain. This structural similarity means that detergents behave using the same principles as lipids when exposed to aqueous environments. Lipids tend to have two hydrocarbon chains giving them a generally cylindrical shape so they form bilayers. Most detergents on the other hand have a single hydrocarbon chain which makes them more of a cone-like shape. This shape difference means they form spherical micelles rather than flat bilayers.(39)(40) Solubilisation with the aid of detergents was trialled for DP using LMNG and DHPC.

LMNG is a non-ionic detergent with two linked hydrophobic hydrocarbon chains and two hydrophilic maltoside head groups. Non-ionic detergents have uncharged polar head groups. LMNG mimics the environment of membrane proteins well resulting in effective solubilisation without denaturing the protein. The protein remains in its native state as LMNG doesn't break any protein-protein interactions. Preventing denaturing ensures the proteins retain their native function, structure and stability. In contrast, DHPC is a zwitterionic detergent. DHPCs hydrophilic head group carries both a negative and positive charge resulting in no overall net charge. DHPC is a harsher detergent than LMNG so it may have caused inactivation or structural changes to the protein.(41) DP dissolved with DHPC didn't solubilise well enough and the sample couldn't be used. The LMNG test was more successful with DP partially dissolving. However, the HSQC spectrum collected from this sample has a poor signal-to-noise ratio because the peptide concentration is too low as not all of the DP dissolved.

Solubilization of DP was ultimately achieved using 40% methanol D4. Initially, 30% methanol D4 was tried but DP didn't dissolve fully so the concentration was increased. In 40% methanol D4, DP dissolved well and no precipitate remained. The spectrum collected from this sample was of much better quality than those collected from the LMNG lipid test and the 30% acetic acid samples. The spectrum has better signal-to-noise making it far clearer and the peptide peaks are more defined.

3.3.2. NMR experiment optimisation

Using the optimised sample in 40% methanol a D4 BEST TROSY NMR spectrum was established as the best experiment to collect from DP.

The first NMR spectrum collected from solubilised DP was a HSQC. A HSQC is a 2D NMR experiment that produces a 'fingerprint' of the protein. One peak is seen for each residue present except for proline because it is a secondary amino acid and doesn't have an amino group. The proline side-chain bonds to the amino nitrogen in the residue backbone. This bond forms a pyrrolidine loop between the α -carbon and the amino nitrogen. HSQC experiments correlate the nitrogen chemical shift from the nitrogen of each residue with the chemical shift of its amide protons to produce a single peak. As proline doesn't have two amide protons it doesn't produce a peak.⁽⁴²⁾ Similarly no peak is seen for the N-terminal residue of the protein as this is also lacking the two amide protons required to produce a signal. An HSQC was collected as these can be used to base 3D assignment experiments on. The spectrum collected contains a number of very broad peaks, many of which are crowded together in the centre of the spectrum meaning they can't be separated in order to identify individual residues. This spectrum does however provide some information about the state of the peptide as unfolded proteins typically result in spectra with poorly dispersed signals and lots of peaks in a small area.⁽⁴³⁾ As this wasn't the case for DP the spectrum indicates that DP does contain some folding and isn't a completely disordered peptide.

Following the limited success of the HSQC experiment a HMQC SOFAST was measured. This is a HMQC type experiment which is very fast and sensitive. The data is acquired quickly using less resonance frequency (rf) pulses than an HSQC, this means there is less signal loss due to B1 inhomogeneity.⁽⁴⁴⁾ The resulting spectrum should therefore have better signal-to-noise than the HSQC. Although this spectrum was clearer than the HSQC there was still a region of very broad peaks in the centre of the spectrum with lots of overlap.

Finally, a BEST TROSY was collected. BEST TROSY experiments are typically used for large peptides. The BEST TROSY collected from DP had more defined peaks and better resolution than the HSQC and HMQC SOFAST. This improvement in the spectrum suggests DP is oligomerised as a BEST TROSY will only give a better spectrum than a HSQC and HMQC SOFAST if the protein is large. DP is a very small peptide and so wouldn't be expected to yield a good BEST TROSY spectrum. For this to be possible, the small DP monomers must have come together into a larger oligomeric state. This potential oligomerisation

supports the suggestions Pokhrel et al. put forward that DP forms an oligomer - most likely a pentamer comprised of 5 individual DP monomers.(15) It is also apparent from the BEST TROSY spectrum that DP isn't a non-structural peptide as was previously believed.(17) Non-structured peptides have far sharper peaks indicating that DP has secondary structure. The lack of spread on the spectrum also shows that DP is α -helical and doesn't contain any β -sheet structure.

It is, however, important to note that methanol D4 is a polar solvent and a 40% methanol solution is not representative of the physiological conditions in which DP would normally exist. Thus, the DP may not be in its native state and may have altered structure, activity and stability. Whilst this spectrum gives a good approximation of DP's structure, it may not be true of native active DP under physiological conditions.

Table 2 shows the optimal sample preparation and experimental conditions chosen based on these investigations. These were the conditions used for all further NMR experiments.

Table 2- Optimum NMR conditions for collecting spectra from DP in solution.

| | |
|-------------------------|---|
| Sample preparation | 40% Methanol D4 5% D ₂ O 1% DSS In 300 μ L Shigemi NMR tube |
| Experiment type | BEST TROSY |
| Temperature | 298K |
| No. of points collected | 1024 Proton 128 Nitrogen |
| Spectrum width | ¹ H 14ppm by ¹⁵ N 40ppm |
| No. of scans | 32 |

3.3.3. NMR Lipid Experiments

Once the successful BEST TROSY spectrum of the solubilised DP had been collected, the natural next step was to attempt to collect an NMR spectrum of DP in the presence of lipids. The WWIHS score, amino acid composition, sequence patterns, molecular model predictions and synthetic peptide experiments previously performed all suggest DP should insert into lipid membranes.(17)(16)

Considering these studies and the difficulties encountered solubilising DP, it was clear it is a partially hydrophobic peptide and likely inserts into lipid membranes. Lipid-based experiments were performed to look for structural changes in the peptide. Any changes in DP structure seen would be due to interactions with and possible insertion into lipid bilayers.

The first membrane experiment performed was to add bicelles of asolectin and LMNG to a sample of DP already dissolved in 40% methanol D4. Bicelles were used as they are smaller than vesicles and so if peptide interacts with them, it can still be seen using solution NMR. Vesicles on the other hand would be too large and so if DP interacted with them the residues involved would have disappeared as its too large to be seen. The bicelles caused DP to immediately crash out of solution, forming lots of white precipitate. Once the sample had been spun down and the powder removed to make the sample homogenous a BEST TROSY was collected. Due to the low peptide concentration, the spectrum has poor signal-to-noise and a weak signal. Decreasing the pH with HCl and the addition of more bicelles both failed to improve the solubilisation of the sample.

Due to the problems adding bicelles to the DP sample asolectin vesicles had to be used. The addition of asolectin vesicles to the DP sample was far more successful as the DP didn't crash out and the sample remained homogenous. There was a shift in the location of 17 of the peaks on the BEST TROSY spectrum and 8 peaks disappeared completely. The peak shifts indicate a structural change occurred due to asolectin addition as these residues' local chemical environments changed. This demonstrates that DP has inserted into the asolectin vesicle membranes. Residues whose peaks shifted are involved in a structural change of the DP. The 8 peaks which have disappeared represent residues which are interacting with the lipid membrane. When residues interact with vesicle membranes, they are no longer visible on the spectrum as they are too large to be detected by solution NMR.

These peak shifts and disappearances support the observations of He et al. that full-length, intact DP inserts into membranes to form small selective pores. It also agrees with the prediction Gallaher et al. made from the WWIHS that membrane interaction is favourable in terms of free energy.(16) However, this disagrees with He et al.s conclusions regarding DP's oxidation state. Experimental findings from He et al. indicated that DP only inserted into membranes when in its oxidised state. However, the sample used in these NMR experiments contained 2mM DTT meaning the peptide was in its reduced form when the asolectin vesicles were added. The shift and potential membrane insertion seen show that reduced DP is capable of membrane interaction and insertion. It is therefore clear from this NMR data that DP is active when in its reduced form and the Cys29-Cys38 disulphide bond isn't essential as He et al. and

Pokhrel et al. stated. (17)(16)(15) A double labelled DP sample would be required to identify which residues in the peptide these shifted peaks are. Double labelled growths produce proteins labelled with both ^{15}N and ^{13}C . This is achieved through a minimal media growth similar to the ^{15}N growths in this project but with ^{13}C glucose also present. From this sample, it would be possible to collect triple resonance spectra which could then be used to assign each peak to its corresponding residue. The assignment would show which residues are involved in membrane interactions and structural changes.

Following this, LMNG was added to the sample to observe if adding detergent caused any further effect. Detergents can extract proteins from membranes by inserting between the protein and flanking lipids in a wedge-like fashion. This insertion breaks lipid-protein interactions in the membrane causing the protein to transition from the lipid membrane into the detergent layer. Such peptide would appear on the NMR spectrum as another shift in the location of some peaks. Peak shifts would occur as leaving the asolectin vesicles will cause DPs structure to change again and the local environment of residues involved in this change and in membrane interactions would be altered. Upon the addition of LMNG to the asolectin sample some precipitation occurred. The resulting BEST TROSY spectrum collected does show some shift in the location of some peaks however, the spectrum is poor so this is not a certain correlation. Given more time for the project this experiment would be repeated to achieve a better-quality spectrum to properly assess the full effect of adding LMNG to the DP asolectin sample.

3.3.4. CD

The CD data collected provides information about DP's secondary structure. CD spectra were compared to standard spectra of pure α -helical, β -sheet and random coil structures (figure 29).(45) The reduced and oxidised plots both bear similarities to the α -helical and random coil protein spectra. These similarities indicate that when DP is solubilised in 40% methanol it is mainly α -helical. It's not apparent from CD data which regions of the peptide exist in which structure nor whether the helical portion exists as one long α -helix or multiple smaller helices throughout the peptide.

Reduced DP produced a plot with a deep trough between 200nm and 240nm, which then levelled off. This shape is similar to a characteristic α -helical protein plot. α -helical peptides have a low, broad trough with two small peaks at the bottom. A small peak is potentially visible at 218nm but, it is only small and may be noise. The oxidised plot is a similar shape but, slightly higher up the graph indicating that it is also mainly α -helical. The slight difference seen between the reduce and oxidised DP samples in figure

26 is very small and so likely due to experimental error. Such experimental errors could include but are not limited to: errors pipetting such small volumes, dust on the cuvette or margin of error of the equipment used. The difference between the curves isn't big enough to be experimentally significant and so indicates that no difference is seen between the two DP samples. As a result, it can be concluded that the oxidation state of DP doesn't affect its secondary structure when it's dissolved in 40% methanol.

With solution NMR experiments now also supporting the hypothesis that DP is capable of membrane insertion, it was important to observe this in CD experiments too. A change in the CD plot following the addition of asolectin vesicles would demonstrate what changes occur in DP's secondary structure when it inserts into a lipid membrane.

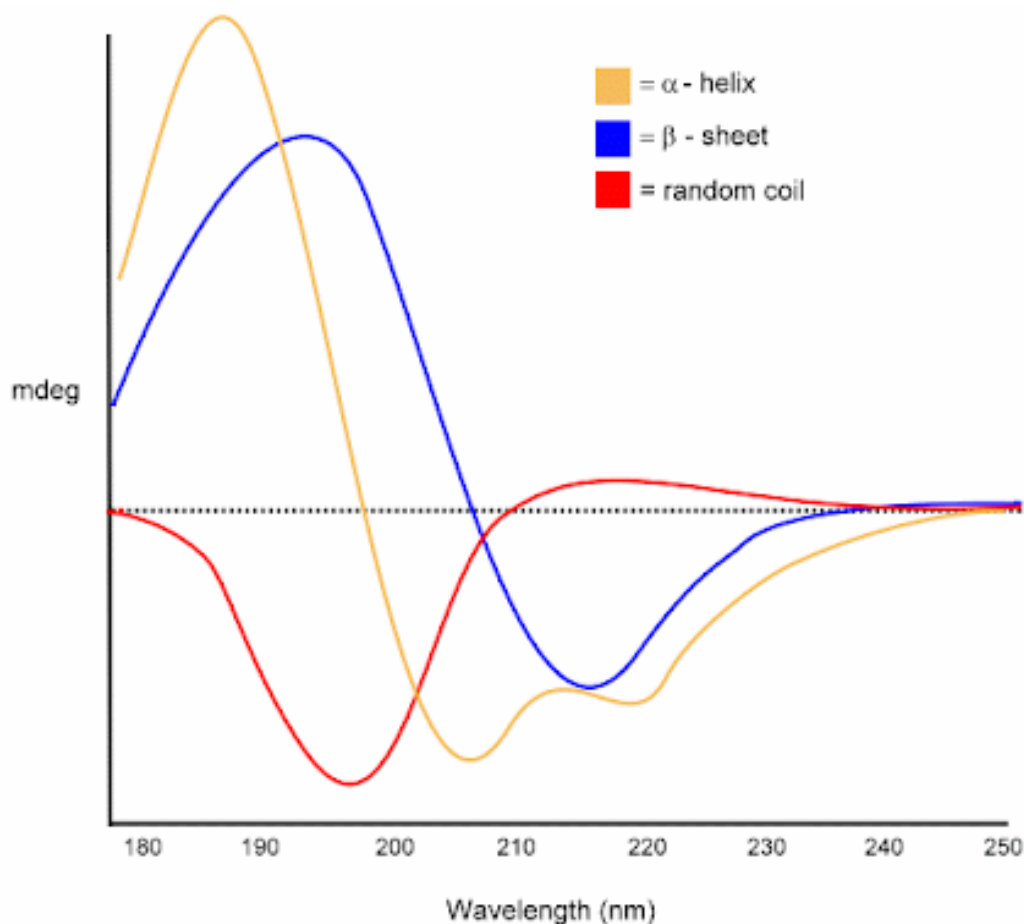


Figure 29- Standard 'pure' protein secondary structures using CD. Figure from Doderio et al.(44)

The addition of asolectin vesicles to the reduced DP sample produced an almost identically shaped curve on the CD plot. This indicates the DP has the same secondary structure before and after addition of the vesicles and so its structure hasn't changed due to membrane insertion. There is a slight difference in

the location of the pre and post asolectin addition curves on the graph indicating a difference in intensity. However, this is also likely due to experimental error as was found with the comparison of the oxidised and reduced DP samples in figure 26. The oxidised DP plots illustrate an even smaller difference upon asolectin addition with the two curves not only the same shape but almost superimposed on top of each other. This indicates that no structural change occurred when asolectin vesicles were added and DP exists as an α -helix in 40% methanol regardless of whether membranes are present.

Secondary structure predictions from the K2D3 tool indicate that both oxidation states of the peptide have an almost entirely α -helical secondary structure. Reduced DP was predicted to be 94.83% α -helical, this represents all 40 residues and shows the whole peptide is α -helical. Oxidised DP was predicted to be 94.34% α -helical which represents 38 residues of the peptide indicating only 2 residues are unstructured and remain as a random coil structure. When asolectin vesicles were added to reduced DP sample there was a 0.1% increase in the proportion of peptide predicted to be α -helical. This change is insignificant as the increase is trivial and it was already predicted that all residues of reduced DP were α -helical prior to asolectin addition. Asolectin vesicle addition to the oxidised DP sample resulted in no predicted structural change at all. This supports the observations made from the graphs of the CD data as K2D3 agrees that DP is mostly α -helical when in 40% methanol regardless of its oxidation state. It also confirms that this only changes insignificantly when asolectin vesicles are added - again supporting the conclusion that the difference on the graphs is likely due to an error in measurement as the difference is very small.

From this data it can be concluded that when dissolved in 40% methanol DP forms an α -helix both in the presence and the absence of membranes. As DP is predicted to form an α -helix when it inserts into membranes this means no change in secondary structure would be expected upon membrane insertion in this experiment. As the DP is already in an α -helix in the methanol solvent it is in the same structural conformation as when it inserts into the membrane. As CD detects protein secondary structure it therefore sees this as no change occurring to the peptide, hence the plot doesn't change.

Methanol has been found to aid secondary structure formation by strengthening interactions within peptide backbones. This indicates that DP may not be in its native soluble form when solubilised in 40% methanol. Methanol can also weaken hydrophobic interactions which may also alter the secondary structure of the DP and so the data collected during these CD experiments. The effect of methanol on protein structure has been simulated through molecular dynamics and investigated experimentally using NMR by Hwang et al. For these experiments a short model peptide called BBA5 was used. BBA5 has a

stable β -hairpin- α -helix structure when in aqueous solutions. However, Hwang et al. found that when in methanol the peptides hydrophobic core expanded due to weakened hydrophobic interactions and the polar backbone-backbone interactions were strengthened. These stronger backbone interactions occur as its less favourable for the backbone to hydrogen bond to methanol than to water so more protein-protein hydrogen bonds occur within the backbone instead. These hydrogen bonds cause a higher propensity for α -helix formation resulting more α -helical secondary structure being detected through the NMR experiments when BBA5 was in methanol than in water. This indicates that the methanol may be responsible for DP already existing as an α -helix prior to membrane addition in these investigations.(46)

Other alcohols have also been found to alter the secondary structure of peptides increasing the proportion of α -helix present. For example, when melittin, a protein found in honeybee venom, was investigated using CD and NMR it was observed as an unfolded protein when in an aqueous environment. After the addition of alcohol however, it had formed an α -helical structure. This was the case for a whole range of alcohols tested including Tetrafluoroethylene (TFE) and ethanol.(47) Molecular dynamics modelling has also demonstrated that TFE promotes secondary structure formation and stability in melittin as well as a β -sheet peptide called Betanova and the β -hairpin region of the B1 domain of protein G.(48) A secondary structure change may in fact occur when native solubilised DP in its usual physiological (aqueous) environment inserts into membranes, such as the plasma membrane of human cells during Ebola virus infection. However, no overall secondary structure change occurred in this experiment upon to addition of, and peptide insertion into, asolectin membranes as DP was already mainly α -helical when solubilised in 40% methanol.

These studies confirm that alcohols cause changes to proteins secondary structures increasing their α -helix content - likely also the case for DP when it's dissolved in methanol. This accounts for why no change in structure can be seen when membranes are present during the CD experiments yet peak shifts and disappearances were seen in the NMR experiments. The NMR lipid experiments indicates that membrane insertion is likely occurring and regions of DP are interacting with the membranes. However, the CD data with K2D3 predictions indicate that no change in secondary structure occurred. This is highly probable to be due to the use of methanol solvent and so further investigations were needed to illustrate membrane insertion. A UV microscopy insertion assay and dye leakage assay were used to investigate DP activity and membrane insertion further (chapter 4).

4. Delta peptide activity

4.1 Introduction

Having collected information about the structure of DP the next step was to investigate its activity. A number of investigations had previously been made into the activity of DP, mainly by He et al. using synthetic full-length DP and DP fragments. There was a general consensus that DP acts as a Viroporin. This was also predicted by Gallaher et al. through their bioinformatic analysis of the peptides sequence. This analysis identified a similarities with known cationic pore-forming peptides such as mellitin and a 3/4/7 residue repeat seen in many lytic Viroporins including, the enterotoxic Viroporin from Rotavirus, NSP4.(16)

He et al. investigated DP activity experimentally and reached the same conclusion - that DP behaves as a Viroporin. He et al. used synthetically produced full-length and short DP fragment in a range of assays. Fragments used were from the Makina variant of Ebola virus and were regions of the C-terminal portion of the peptide. The C-terminal portion was used as C-terminal fragments were stable in human serum when in their oxidised state. The N-terminal region on the other hand rapidly degraded. As a result, C-terminal fragments of 23, 17, 15 and 14 residues and full-length DP in both oxidised and reduced states were used for all the assays performed. The first assay to investigate permeabilization of cell membranes monitored entry of sytox green and efflux of calcein AM ester red range (CAMRO) from cells. All DP fragments and full-length DP were found to be inactive when reduced. When oxidised however, all apart from the 14-residue fragment were active and caused permeabilization of the cell membranes allowing sytox green to enter the cells and CAMRO to leave. This assay demonstrated that DP was only active when in its oxidised state and that the tryptophan 15 residues from the C-terminus (trp25) was essential for membrane permeabilization.(17)

A monolayer experiment was then also performed observing the effect of full length and 23 residue fragment DP on transendothelial electrical resistance across a confluent monolayer. As was the case with the plasma membrane assay, only the oxidised peptide was active. This led to the conclusion that membrane permeabilization activity of DP was dependent on the disulphide bond between the cysteine residues in its C-terminal portion (Cys29 and Cys38). He et al. was also able to prove that DPs activity is due to its physical chemistry and not sequence- specific interactions with other membrane components such as cell surface proteins or channels. This was achieved through 2 assays using synthetic lipid bilayers - the first of which monitored the movement of monovalent ions across the bilayer. The second

assay observed leakage of ANTS and DPX, a dye and quencher, from synthetic lipid vesicles to look for movement of small molecules (~350Da). These assays showed that DP formed small ion-permeable pores at low concentrations but at higher concentrations DP pores were able to release small molecules. He et al. concluded that DP permeabilises mammalian cell plasma membranes at micromolar concentrations allowing movement of ionic compounds and small molecules across the membrane. This activity has been seen in many Viroporins and so agrees with Gallaher et al.'s predictions that DP is a Viroporin.(17)

Pokhrel et al.'s bioinformatic investigations also found DP to behave as a Viroporin. They used all-atom molecular dynamics simulations of DP to demonstrate its ion activity and pore stability. Phyre2 software was used to predict DP's secondary structure which was built into tetramer, pentamer and hexamer pore models. A set of models without the disulphide bond (reduced pore models) were also produced to be used to investigate the importance of oxidation state on pore stability. The pores were placed in lipid bilayers using the CHARMM-GUI membrane builder and Molecular Dynamics simulations and Potential of Mean Force simulations performed. From these investigations it was concluded that the tetrameric assembly was not stable. The pentameric and hexameric assemblies of DP formed stable pores which selectively permeated water and Cl⁻ ions although the pentameric pore was slightly more stable. They also demonstrated that the disulphide bond was essential for this ion flux and for pore stability. When in its reduced state the C-terminal region (residues 32-40) of DP was found to sometimes flip out of the membrane. However, when the DP was oxidised this didn't happen. Additionally, the reduced peptide models exhibited a smaller (distorted) pore radius than the oxidised models indicating the pores were less stable without the oxidised disulphide bond. From this range of bioinformatic investigations Pokhrel concluded that, as Gallaher and He et al. also found, DP was highly likely to behave as a Viroporin with this activity dependent on its oxidation state.(15)

A UV microscopy membrane insertion assay and fluorescence dye leakage assay were used to investigate the activity of DP in this report. The aim being to confirm DP's ability to insert into lipid membranes and to investigate its suspected Viroporin activity. To confirm membrane insertion occurs, a UV microscopy insertion assay was performed. Following this, a dye leakage assay was used to monitor DP's pore-forming ability and see if it is indeed able to behave as a Viroporin and permeabilise lipid membranes. These experiments were performed using both the full-length peptide and a short, 23 residue construct of DP (Trp18-Ile40) with the C-terminal portion removed to observe the importance of the C-terminus and Trp25 on its activity. This 23-residue short DP fragment was designed to deliberately

exclude the C-terminus and Trp25 He et al. identified to be responsible for DPs membrane insertion activity. Similarly, all investigations were performed under both reducing and oxidising conditions to see the effect of DPs oxidation state and so presence of the Cys29 Cys38 disulphide bond on membrane permeabilization. A similar strategy was employed by Hyser et al. to investigate the activity of NSP4 an ER TM glycoprotein from the rotavirus that permeabilizes mammalian membranes causing altered cytosolic Ca^{2+} levels. They used truncated fragments of NSP4 with different regions deleted to determine which regions were necessary for membrane permeabilization.(25)

4.2 Methods

4.2.1. UV microscopy membrane insertion assay

To determine if DP inserts into asolectin membranes giant unilamellar vesicles (GUVs) of asolectin lipids were made. An electroformation method was used to prepare the GUVs - 26mg asolectin was dissolved in 1ml chloroform and dried into a thin film. This was then resuspended in 50mM HEPES buffer containing 1mM Nile-red dye to a final concentration of 50mg/ml. 10uL of this mixture was evaporated in a vacuum chamber overnight on the conductive sides of two indium-tin oxide coated coverslips. Once completely evaporated rubber O-rings were placed on the ITO coverslips and 70uL of 0.1M Sucrose and 1mM HEPES buffer were added in the well. The coverslips were attached to form a sealed chamber. Function generator leads were attached to the copper coated edges of the coverslip and 10Hz sine wave function at 1.5V used for 2 hours 30 minutes to form Nile-red stained GUVs. Two samples of FIT-C labelled DP, one oxidised and one reduced, were incubated with GUVs for 5 minutes. Following incubation, they were immediately viewed using a confocal microscope with a 594 laser and a x63 objective lens to see if the peptide inserted into the membrane. A control was also visualised which contained no DP just the Nile-red labelled GUVs. (Experiment performed by Diego Cantoni)

4.2.2- Dye leakage assay

Asolectin vesicles containing HEPES buffer with Sulforhodamine B dye in it were prepared. 22mM asolectin was dissolved in 1ml chloroform, dried into a thin film and resolubilised in 400uL HEPES buffer containing Sulforhodamine B (20mM HEPES, 100mM NaCl, 40mM Sulforhodamine B at pH 7.4). An extruder was used to push the vesicles through a membrane with 100nm pores. Extruding the vesicles

ensured they were all under 100nm and unilamellar. A PD-10 column was used to wash the dye-containing HEPES buffer from the outside of the vesicles. The column was equilibrated with 4CV dye-free HEPES buffer (20mM HEPES, 100mM NaCl at pH 7.4). The extruded vesicles were then added and allowed to enter the packed bead bed. HEPES buffer was used to elute them from the column. This washing removed any dye from the suspension the vesicles were in. The process yielded dye-containing vesicles in clean, dye-free HEPES buffer. As a result, any dye leakage from the vesicles would be detectable as an increase in fluorescence.

A kinetics assay was collected using a Varian Cary Eclipse fluorescence spectrophotometer. The sample in a 1cm cuvette was excited at 595nm and fluorescence emission was measured at 586nm. To perform the assay the fluorescence of 150 μ M of dye-containing asolectin vesicles was measured. After 2 minutes data acquisition was paused and 50 μ M DP in 40% methanol stock added. Fluorescence was measured for a further 8 minutes to observe the effect of DP on the vesicles. 10 μ L triton X-11 was added to rupture the vesicles. Vesicle rupture caused 100% membrane permeabilization and complete dye leakage. The reaction was then monitored until the fluorescence intensity levelled off.

The assay was repeated with 25 μ M, 12.5 μ M, 6.25 μ M, 3.125 μ M, 1.5625 μ M and 0.78125 μ M of DP under reducing and oxidising conditions. Reduced DP stock had 1mM DTT present and the oxidised stock contained 5mM H₂O₂.

The fluorescence dye leakage assay was also performed with the short 23 residue DP fragment to compare its activity to the full-length peptide. The assay was performed in the same way and results were collected from both oxidised and reduced peptide. (Short DP fragment experiments performed by Diego Cantoni)

4.3 Results

4.3.1. UV microscopy membrane insertion assay

Images of control reactions, in which only GUVs were present, and assays containing 20 μ M DP with GUVs were collected. The first image was captured using a Nile-red filter to image the membrane, the second used a FITC filter to see the DP. These images were overlaid to produce a merged image of the DP and asolectin GUVs together seen in the final column.

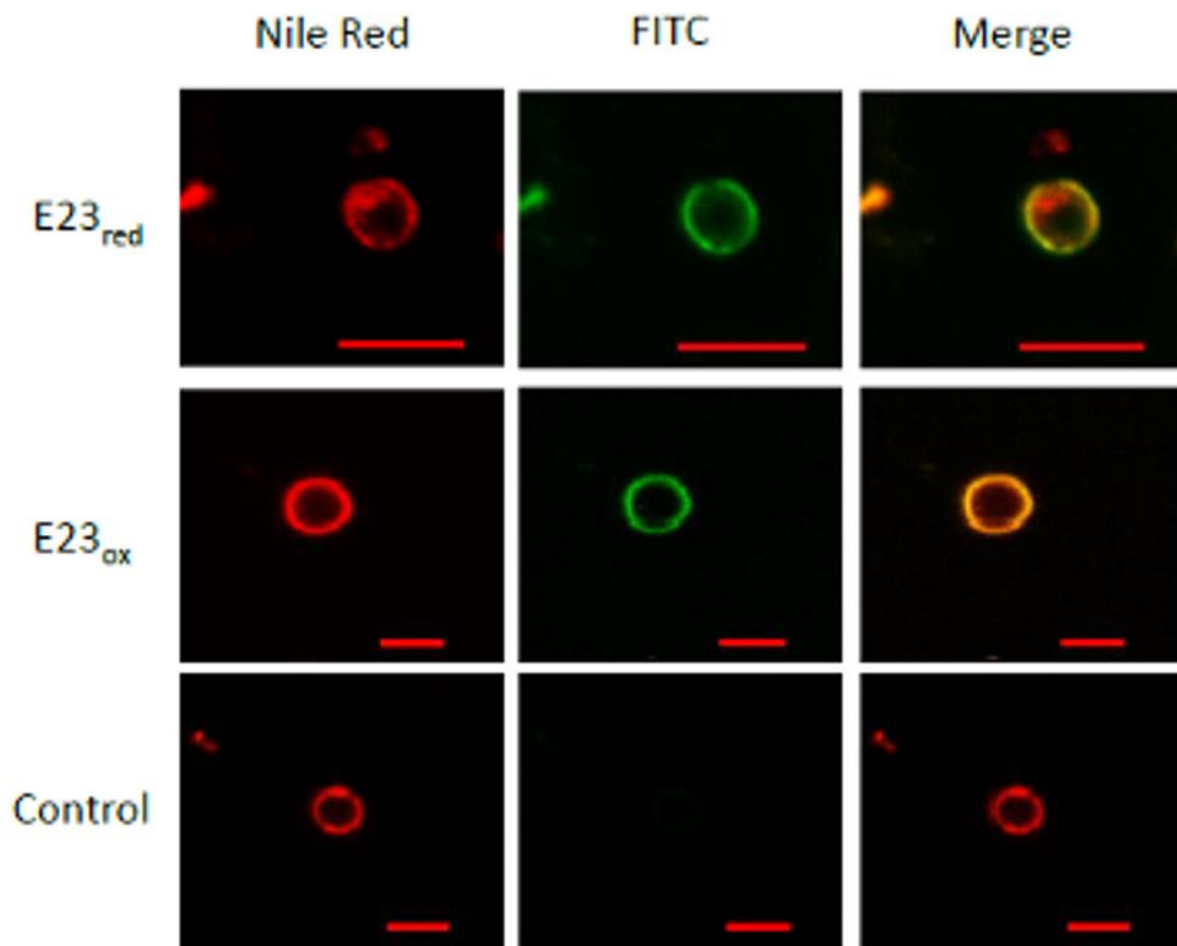


Figure 30- UV microscopy images of Nile-red- labelled asolectin GUVs showing FITC- labelled oxidised and reduced DP inserting. Images are taken using a confocal microscope with a Nile-red and then FITC filter. Scale bars represent 5 μ M. (Experiment by Diego Cantoni)

The FITC signal from both the oxidised and reduced DPs colocalises with the Nile-red fluorescence, confirming the association of DP with the membrane. No differences could be observed between the oxidised and reduced forms of DP.

4.3.2. Dye leakage assay

The fluorescence intensities measured for each concentration were overlaid, producing figures 31 and 32. These graphs show that DP caused an increase in the fluorescence emission at all seven concentrations measured indicating the Sulforhodamine B dye leaked from the vesicles. This fluorescence increase is consistent in both the reduced and oxidised assays showing membrane permeabilization was achieved by both samples. Sequential doubling of the concentration of DP resulted in increase in fluorescence increase.

Large peaks are visible at 2 and 10 minutes due to pipette mixing of the sample when DP and triton X11 were added respectively. This peak was not included when calculating % membrane permeabilization as it occurred purely due to disturbance of the sample through opening the spectrometer and sample mixing. The level at which the fluorescence settled following this was used as the true reading. The percentage of membrane permeabilization caused by DP was calculated from this reading.

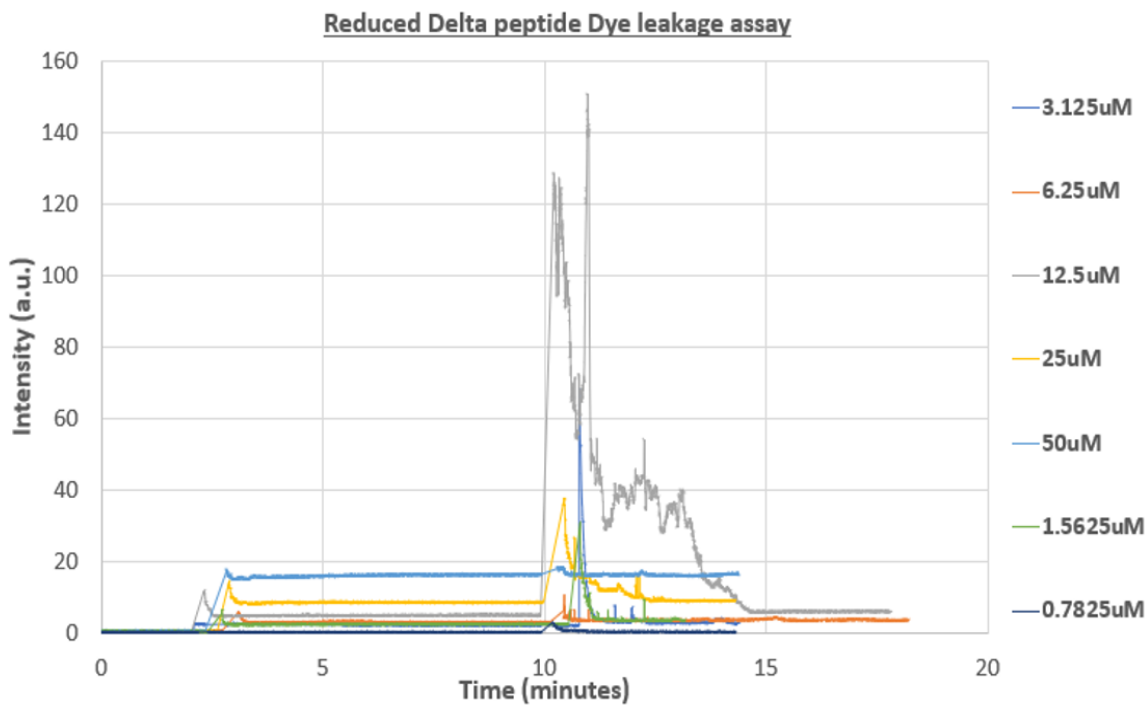


Figure 31- Fluorescence intensity when varied concentrations of reduced DP was added to 150µM asolectin vesicles to observe for fluorescence changes due to Sulforhodamine B from the vesicles caused by peptide induced membrane permeabilization.

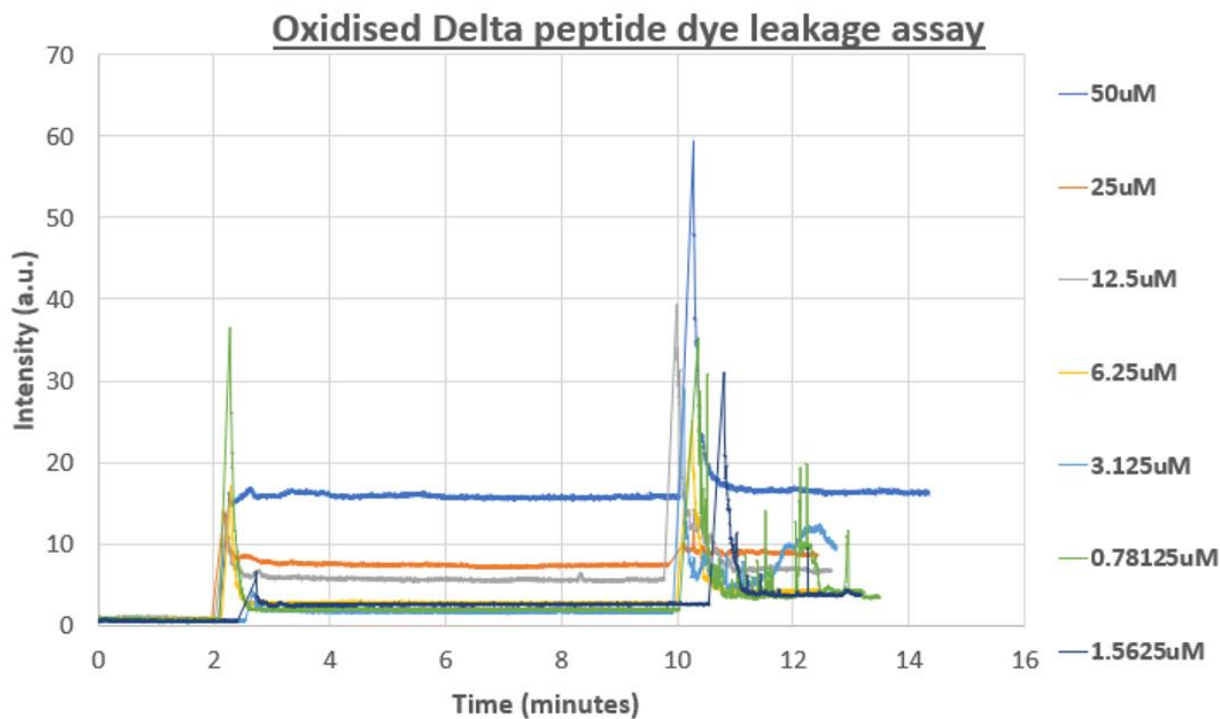


Figure 32- Fluorescence intensity when varied concentrations of oxidised DP was added to 150µM asolectin vesicles to observe for fluorescence changes due to Sulforhodamine B from the vesicles caused by peptide induced membrane permeabilization.

Rupturing the vesicles using triton X11 caused a large increase in fluorescence. The value the fluorescence settled at following mixing was taken as 100% dye leakage from the vesicles. From this 100% leakage, the % of leakage caused by DP addition was calculated. % Permeabilization was calculated for each concentration of reduced and oxidised DP added and plotted together in figure 33. From this, the effect of DP concentration on membrane permeabilization can be seen.

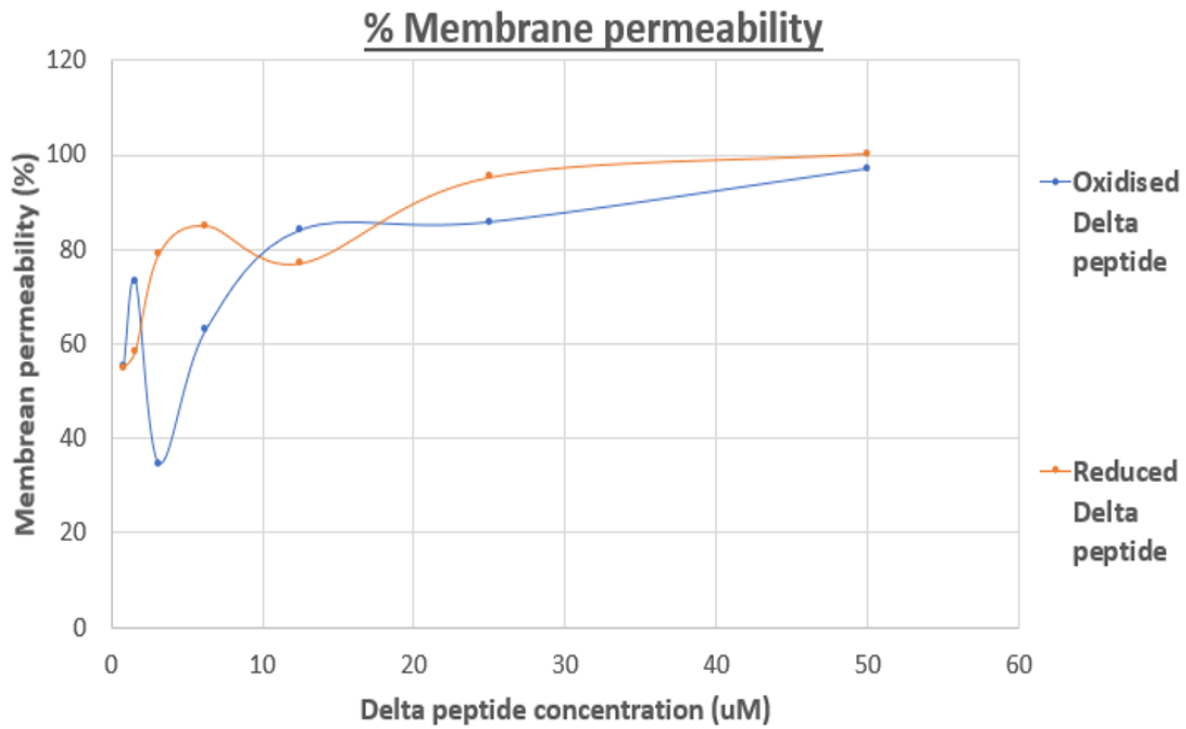


Figure 33- % of membrane permeabilization caused by addition of reduced and oxidised peptide compared to complete vesicle rupture and dye release when triton was added.

The trend in percentage membrane permeabilisation caused by DP is very similar when in its oxidised and reduced states. They both show an overall increase in the % of the membrane permeabilised as peptide concentration doubles. The steep increase at the start of both peptide curves show a large increase in the amount of membrane permeabilisation caused by increasing DP concentration occurs initially. This graph shows a few points which deviate from the expected curve and don't fit with the trend of the results. These are the points collected when 0.78125 μ M and 1.6525 μ M of oxidised and 12.5 μ M reduced DP were added - they likely occurred due to experimental error.

Both the reduced and oxidised DP % membrane permeabilisation curves plateau at concentrations above 12.5 μ M. This levelling off indicates smaller increases in membrane permeabilisation are being caused by the doubling of DP concentration. Adding 12.5 μ M of oxidised DP to the vesicles caused 84% membrane permeabilisation. Doubling the DP concentration to 25 μ M increased membrane permeabilisation by only 2% to 86%. Whereas doubling DP concentration between 0.78125 μ M and 1.6525 μ M caused an increase of 18% from 55% to 73%. This demonstrates 9x more membrane permeabilisation occurred as a result of doubling DP concentration at lower concentrations than at high concentrations. The same trend is seen in the reduced DP sample.

Membrane permeabilisation caused by both samples reaches high levels. The reduced DP achieved 100% membrane permeabilisation when 50 μ M was added. This indicates the vesicles membranes are completely permeabilised. The oxidised peptide reached membrane permeabilisation of 98% which is also almost complete permeabilisation.

A % membrane permeabilisation graph was produced in the same way for the 23 residue short DP fragment data. This was overlaid with the % membrane permeability data collected from the full-length peptide to compare the effect removing the C-terminus and Trp25 on DP activity. For this comparison the 3 outlier points identified in the full-length DP data were removed.

% Membrane permeability of Full-length DP and short DP fragment

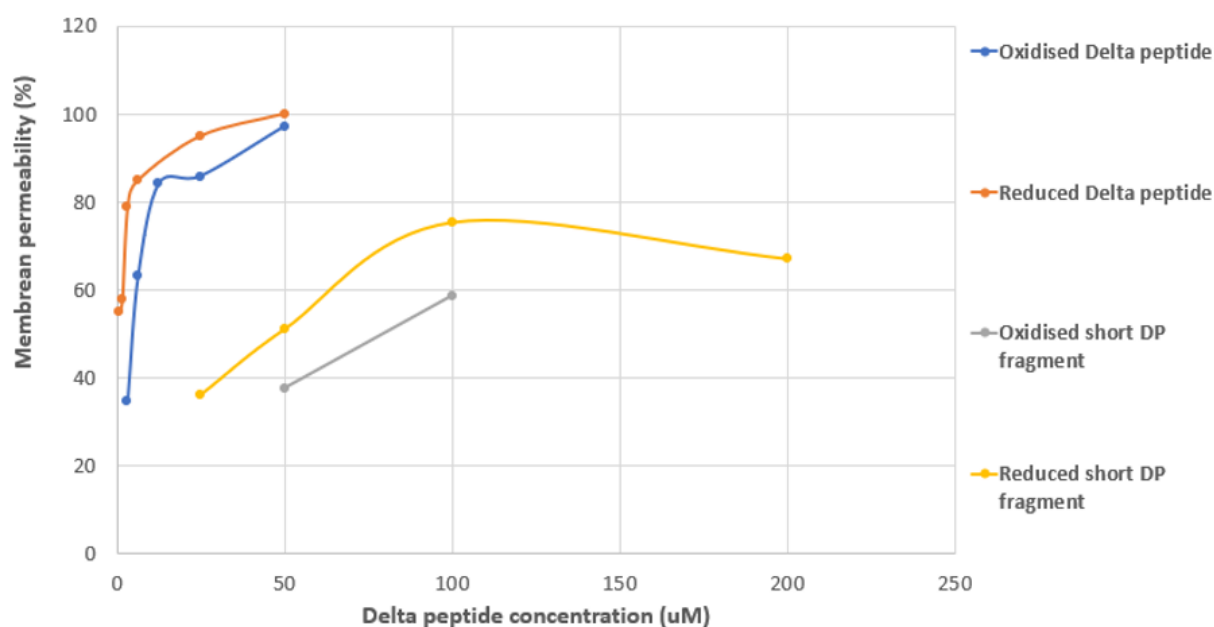


Figure 34- % membrane permeability caused by the short DP fragment in its reduced and oxidised states and full-length DP also in both oxidation states. (Short DP fragment experiments by Diego Cantoni)

The short DP fragment caused lower % membrane permeabilization than full-length DP in both oxidation states showing it is less active. As a result, higher concentrations were added. Fewer concentration points were collected using the short DP fragment due to experimental factors however it is still useful to compare the data to that of the full-length DP. % membrane permeabilization increased as the concentration of short DP fragment being added was increased until 100 μ M of reduced peptide was reached. From 100 μ M onwards the % membrane permeabilization occurring decreased. Not enough data points were able to be collected using the oxidised short DP fragment to be able to see if this would also happen when the peptide is oxidised.

% membrane permeabilization caused by all four DP samples can be directly compared when 50 μ M of peptide was added. This is shown in table 3 and highlights that the short DP fragment samples caused less membrane permeabilization than the full-length DP samples.

Table 3- % membrane permeabilization caused by 50µM of each DP sample.

| Peptide | % membrane permeabilization caused by 50µM |
|----------------------------|--|
| Reduced full-length DP | 100% |
| Oxidised full-length DP | 97% |
| Reduced short DP fragment | 51% |
| Oxidised short DP fragment | 38% |

4.4. Discussion

From the UV microscopy insertion assay images, it can be confirmed that DP interacts with GUV asolectin membranes. The green FITC signal from the labelled DP can be seen throughout the membrane overlapping with the red signal of the Nile-red bound membrane lipids. It can't be confirmed from this data that DP definitely inserts into the membrane. Some viral peptides interact with membranes and float on top of them like a raft. One such example of this is the M1 protein of the influenza virus which forms a coat in the viral envelope so it can bind to both RNA and the membrane at the same time.(49) This membrane interaction would present in the same way - the FITC signal sitting across the membrane. However, it does confirm that DP colocalises to the asolectin membranes and suggests an interaction occurs. This colocalization occurred with both the oxidised and reduced samples indicating the oxidation state of DP doesn't affect its ability to interact with GUVs. These findings support predictions that DP interacts with membranes and further strengthens the argument that it could be behaving as a Viroporin. It does however disagree with He et al.s findings that DP must be in its oxidised state to interact with membranes.(17)

DP insertion into asolectin membranes was further investigated using a dye leakage assay. Data from this confirmed that DP does insert into asolectin vesicle membranes rather than sitting across them like a raft. Adding DP caused the Sulforhodamine B dye to leak from the vesicles showing the peptide is inserting into the membranes. It also indicates that when DP inserts into the membrane it forms pores through which dye can leak. He et al. observed from experiments using synthetic DP that it must be oxidised with its C-terminal portion, including Trp25, present to insert into membranes. To investigate this, the dye leakage assay was performed under both reducing and oxidising conditions. Similarly, the assay was performed with the full-length DP grown and purified from the new construct DNA and a chemically produced short DP fragment (consisting of the 23 N-terminal residues of DP).

The trend in membrane permeabilization caused by both reduced and oxidised full-length DP was similar, a steep initial increase occurred followed by a plateau as the data levels off. The initial increases in fluorescence caused by doubling DP concentration are large, indicated by the steep curve on the % membrane permeabilization graph (figure 33). This indicates that at low concentrations DP inserts readily into asolectin membranes and causes large increases in membrane permeabilization. The plateau indicates that once the peptide concentration reaches 12.5 μ M, increasing it fails to cause significant increases in the amount of membrane permeabilization occurring. This plateau is likely because such a high level of membrane permeabilization has already occurred. These small increases between DP additions at high concentrations likely occur because a high level of membrane permeabilization occurs by 12.5 μ M. Any more peptide struggles to insert as the membrane is already highly permeabilised. This trend is also apparent when adding reduced DP. The plateaus could be because by 12.5 μ M DP the membrane is already fully permeabilised - no further increase in fluorescence intensity can occur as all the dye has already leaked from the vesicles. Alternatively, a saturation point could have been reached. This saturation point may be due to a lack of space in the membrane, as lots of DP has already inserted. Both of these hypotheses, would explain the levelling off at high concentrations.

The reduced DP shows a slightly higher level of insertion and peptide activity. At low concentrations, reduced DP additions exhibited a faster, steeper increase in the % dye leakage than oxidised DP did. This data indicates that at low concentrations DP is more active when in its reduced form. He et al. found, however, that the disulphide bond present only when DP is oxidised, was essential for membrane insertion. In this investigation reduced DP was able to fully permeabilise the membrane. 100% membrane permeabilization occurred when 50 μ M was added, indicated by no further increase in fluorescence intensity occurring upon the addition of triton at 10 minutes. The asolectin vesicles had been fully permeabilised and their rupture had no further effect on the fluorescence emission recorded. Oxidised DP didn't reach 100% membrane permeabilization but did achieve 97%. This is still a high % permeabilization and follows the same trend present in the reduced DP data.

The consensus of these DP dye leakage assays is that DP can insert into asolectin vesicle membranes in both its reduced and oxidised states. This indicates that the disulphide bond between Cys29 and Cys38 is not essential for DP activity as He et al. previously said.(17) It is also apparent that reduced DP is more active than oxidised, particularly at low concentrations. The oxidation state of DP is not essential for

membrane insertion at high concentrations as both oxidised and reduced DP can achieve complete or almost complete membrane permeabilization.

The short DP fragment was designed to deliberately exclude the C-terminus and Trp25 to investigate if they are, as He et al. found, essential for DP membrane insertion and activity.(17) When this was added to the asolectin vesicles the fluorescence measured increased showing the short DP fragment inserted into the membrane. This indicates that the C-terminus and Trp25 are not essential for insertion as was previously believed. Whilst the concentrations of peptide measured for the short DP fragment and full-length DP samples were slightly different due to their differences in activity, there are some regions of overlap and similar general trends in the data sets making them comparable. The 3 outlier points seen in the full-length DP assays were removed for comparison with the short DP fragment data as they clearly deviate from the expected shape of the curve and so don't represent the overall trend of the data. These outliers likely occurred due to hydrolysis of the lipids or experimental differences as some of the assays were performed on different days. Each time the lipid vesicles are defrosted, opened and refrozen there is opportunity for hydrolysis of the lipids to occur which alters the properties of the vesicles. Alternatively as some experiments were run on different days small differences may have been present altering the fluorescence readings slightly. As the experiments recorded were kinetics experiments they are highly susceptible to change and experimental errors. Such changes may include the laboratory temperature, speed of pipette mixing, how long vesicles had been at room temperature, accuracy pipetting the small volumes or moving the fluorimeter.

The % membrane permeabilization of the short DP fragment follows a similar general trend to the full-length peptide - Increasing DP concentration increased % membrane permeabilization caused by the peptide which then levelled off at high concentrations. When 100 μ M of the short DP fragment was added, the % membrane permeabilization levelled off as it had done with the full-length DP. However, by 150 μ M this had begun to decrease showing, less DP inserted into the vesicle membranes when very high concentrations were present. This wasn't seen for the oxidised sample or the full-length DP experiments however not enough concentrations were collected to be able to comment on this. Had assays been collected using higher concentrations of full-length DP and oxidised short DP fragment a similar effect may well have been seen.

Comparison of the % membrane permeabilisation caused by the short DP fragment and full-length DP in figure 34 clearly shows that full length DP caused greater membrane permeabilisation. This is apparent as despite higher concentrations being used, the curves of both reduced and oxidised short DP

fragments are lower than those of the full-length DP samples. This difference was quantified by comparing the % membrane permeabilisation caused by 50 μ M of each of the four peptide samples. 50 μ M of both full-length DP caused complete or almost complete membrane permeabilisation of the asolectin vesicles. The short DP fragments however did not. The reduced sample reached 51% but the oxidised sample only caused to 38% membrane permeabilisation. This data demonstrates that full-length DP is more active than the short DP fragment. Similarly addition of 100 μ M of full-length DP membrane permeabilisation at 100 μ M can be compared. At 100 μ M full-length DP caused 100% and 98% membrane permeabilization in reduced and oxidised samples respectively. However, the addition short DP fragment, even to higher concentrations was only able to achieve maximum % membrane permeabilizations of 67% (reduced) and 59% (oxidised). This indicates that full length DP was able to achieve better membrane permeabilization than the short DP fragment.

He et al. had previously found that the C-terminal portion and Trp25 were essential for membrane insertion and permeabilization of DP.(17) Other studies have also found that Tryptophan residues play an important role in aiding membrane insertion of antimicrobial peptides such as antimicrobial hexapeptide Ac-RRWWRF-NH₂.(50) The dye leakage assays performed in this report, on the other hand, show that this is not the case. Membrane insertion and permeabilization was achieved by both the full-length DP and short DP fragments indicating DP activity is not dependent on the C-terminal portion and Trp25. The difference in % membrane permeabilization suggests the C-terminal portion and Trp25 are likely involved in membrane permeabilization. Although the short DP fragment was able to insert, it constantly caused lower % membrane permeabilization than full-length DP and failed to achieve permeabilization higher than 67% and 58%. DP membrane permeabilization is, therefore, more effective when the C-terminus and Trp25 are intact. This demonstrates they must, as He et al. stated, be involved in DPs membrane permeabilization activity but they are not essential for it.(17)

The activity of DP can also be compared to other Viroporins using this dye leakage assay data. Gervais et al. conducted similar investigations into the activity of a Viroporin of the Hepatitis C virus called p7. In their investigations Gervais et al. used a high-throughput screening assay based on a liposome fluorescent dye permeability assay almost identical to the dye leakage assay performed here. Gervais et al. found that addition of 1 μ M of p7 in a liposome leakage assay resulted in 50% membrane permeabilization (compared to 100% permeabilization achieved through the addition of 0.5% Triton X-100). This is directly comparable to the dye leakage assays performed in this report as the assay was performed in a very similar way. In the DP dye leakage assay using the full-length peptide 0.78125 μ M of

both the reduced and oxidised peptide was needed to reach 50% membrane permeabilization. For the short DP fragment assay however, 50% membrane permeabilization was reached when 50 μ M of reduced short DP fragment as added and 75 μ M of oxidised short DP fragment. Very similar concentrations of full-length DP and p7 were required to achieve the same level of membrane permeabilization. Yet 50x more of the short DP fragment had to be added to achieve the same 50% membrane permeabilization. This indicates that DP and p7 likely behave similarly again supporting predictions that DP has Viroporin activity and further identifies that the short DP fragment was less active than full-length DP.(51)

5. Conclusion

This report has made many steps towards understanding DPs activity and solving its structure. The main developments were in investigating the activity of DP. Understanding of DPs structure and activity prior to this study was scarce with three main publications providing almost all the current knowledge available. Gallaher et al., He et al. and Pokhrel et al.s papers provided a good basis for the further investigations made in this report.

5.1 Structure

With such limited understanding of DPs structure available prior to investigations in this report, the information gained here from NMR and CD investigations although not extensive represents an important development. DP likely has an amphipathic α - helical structure. This is was initially apparent from the difficulties encountered dissolving DP for NMR experiments. However, because solubilisation was eventually achieved it can be concluded that DP isn't completely hydrophilic and so exists as an amphipathic helix.

The CD data further confirms this. The graphs produced from both the oxidised and reduced peptide in 40% methanol are very similar to the characteristic shape of the standard plot produced by an entirely α -helical 'pure protein' (figure 29). When the data was then analysed using the K2D3 database DP was predicted to have an almost exclusively α -helical secondary structure. This was also the case when DP with asolectin vesicles present was analysed. The graph was very close to the α -helical standard protein and the K2D3 predictions again showed a mainly α - helical peptide. It can be concluded from the CD data that DP exists as an α -helix when in 40% methanol irrespective of whether membranes are present or not. This shows that DP inserts into membranes as an α -helix. The CD data supports predictions made by Gallaher et al. that DP exists as an amphipathic helix due to its high frequency of residues that tend to form amphipathic helices.(16)

NMR investigations provided more insight into the structure of DP. The spectra collected show that DP is not a non-structured peptide as was previously believed.(17) NMR spectra collected from disordered proteins have sharper peaks indicating that DP does have secondary structure. The lack of spread on the spectra also shows the peptide is an α -helix and doesn't contain any β -sheet components. The NMR lipid experiments demonstrated structural changes occurring due to lipid addition. It can be seen that in the presence of membranes some peaks shifted and disappeared. These represent regions of DP whose

chemical environment changed and residues which interacted with the asolectin membranes. Although there wasn't time to perform a full peptide assignment in order to identify exactly which residues these altered peaks represent, the spectra provide a good basis for this to be done in the future. The potential for more developments to be made from this data is discussed further in 5.3.

Whilst DP's structure wasn't successfully solved, the data collected confirms basic understanding of DP's structure indicating it exists as an amphipathic α -helix. The preparations are also now in place for future work to be able to do this. Plasmid design along with successful optimisation of the growth and purification processes mean that DP can now be produced relatively easily and effectively. The optimised protocols can be used to produce cleaved, pure DP for future investigations. Optimisation of NMR settings and sample preparation are also important findings considering the problems encountered in achieving full solubilisation of DP.

5.2 Activity

Although the three studies mentioned above made some predictions and progress towards understanding the function of DP, its exact activity and mechanism of insertion were unknown. Data from this report brings us closer to elucidating DP's activity. The UV microscopy membrane insertion assay demonstrated that DP colocalises to asolectin membranes. This was confirmed by the NMR spectrum which showed 17 peaks shifting and 8 disappearing when asolectin vesicles were present indicating residues were interacting with the membranes. This proves Gallaher et al.'s predictions that based on the WWIHS score membrane insertion of DP is favourable in terms of free energy correct.(16) The experimental findings also go some way to support the implication of all three papers that DP behaves as a Viroporin, as in order to do this DP must be able to insert into membranes.

Whilst the NMR and UV microscopy insertion assay results confirm membrane interactions are occurring, they don't show the activity of DP once it's in the membrane. In order to provide some explanation as to the behaviour of DP in membranes the dye leakage assay data collected must be considered. The dye leakage assay demonstrated that DP inserts into asolectin membranes where it forms a pore allowing dye to leak from the vesicles into the surrounding buffer. This activity is as Pokhrel predicted - DP forms a pore in the membrane allowing cell contents, such as water, to leave the cell.(15) Similarly it confirms Gallaher et al.'s prediction that DP would behave as a Viroporin due to its sequence similarities with other Viroporins and its 3/4/7 amino acid repeat which is often conserved in lytic

peptides such as rotavirus peptide NSP4.(16) Membrane permeabilization occurred over a range of concentrations with the amount of membrane permeabilization occurring due to DP increasing as the concentration was sequentially doubled. In the case of the oxidised peptide 100% membrane permeabilization was even reached.

The experiments performed in this report also demonstrate that DP is active in both its oxidised and reduced state. He et al. had previously published that DP's membrane permeabilization activity is dependent on oxidation of Cys29 and Cys38. The UV microscopy insertion assay shows DP colocalises to asolectin membranes when in both oxidation states indicating the cysteine residues do not have to be oxidised for DP to insert into membranes. The NMR experiments were performed in the presence of 2mM DTT making the peptide reduced. When asolectin vesicles were added lipid interactions were seen as shifts and disappearance of some residue peaks confirming that DP is able to insert into membranes when in its reduced state. The successful membrane permeabilization activity of DP seen in the dye leakage assay irrespective of its oxidation state shows that not only is membrane insertion possible but DP is fully active in both states. A similar general trend in behaviour of DP was seen between the reduced and oxidised DP samples during the dye leakage assay. As peptide concentration was increased the amount of membrane permeabilization caused by DP also increased. This suggests that He et al.'s findings that DP is inactive when in its reduced state are not the case. Similarly, Pokhrel et al.'s identification of the Cys29-Cys38 disulphide bond as essential to pore formation and stability falls down here. The dye leakage assay shows that contrary to He et al.'s experimental findings and Pokhrel et al.'s predictions the oxidation state of DP doesn't dictate its ability to permeabilise membranes.(15)(17)

He et al. also found that fragments of DP which didn't contain the C-terminal portion or the tryptophan 15 residues from the C-terminus of the peptide were inactive. When the dye leakage assay was performed using the 23-residue short DP fragment containing neither Trp25 or the C-terminal portion however, DP was still active. Membrane permeabilization still occurred and the dye leaked from the vesicles. The fluorescence emission measured was consistently lower than that measured for the full-length peptide and 100% membrane permeabilization was never reached, even when high concentrations of short DP fragment were added. Lower fluorescence emission indicates reduced dye leakage occurred when the short DP fragment was added. This shows that DP insertion and activity is more effective when the whole peptide is present. This suggests insertion isn't solely down to an amphipathic helix at Trp18 to Ile40 as He et al. previously stated because membrane insertion and permeabilization was more effective when the full-length peptide was used. Although they are not

essential for membrane insertion and permeabilization as He et al. found, the C-terminal portion and Trp25 did increase the amount of membrane permeabilization DP caused during the dye leakage assays.(17)

From these investigations it can be confirmed that DP colocalises to asolectin membranes where it interacts with the lipids, inserts into membranes and permeabilises them. It is also clear that this occurs regardless of the peptide's oxidation state or the presence of its C-terminus or Trp25, although the latter two features may aid more effective permeabilization.

5.3 Future work

The BEST TROSY HSQC spectra collected showing the disappearance and shift of peaks due to asolectin addition is a significant result as it highlights that a structural change does occur when DP inserts into membranes. Had there been more time for the project, a double labelled growth could have been prepared. From this double labelled DP, triple resonance spectra would have been collected which could be used to produce an assignment. This assignment would identify which peaks correspond to which residues of DP. Using the assignment, it would be possible to identify which residues shifted and disappeared when asolectin vesicles were added. Residues involved in or located close to the region involved in structural changes would be identified and DPs mechanism of insertion more effectively understood.

Following the identification of regions undergoing structural changes, these areas could be investigated further. For example, to identify key residues involved in insertion or residues essential for structural changes to occur. Eventually, these residues or regions identified could become pharmaceutical targets to try and develop a targeted treatment for the Ebola virus which prevents DP insertion into patient's cell membranes.

Additionally, it would be interesting to find a way to investigate perform the experiments in this report under conditions more akin to DPs natural, physiological environment. Such experiments would give a more representative insight into DPs structure and activity when in its entirely native form and so not effected by the 40% methanol which had to be used in this report to solubilize DP. It would also demonstrate for certain whether the conditions used in these experiments (e.g. 40% methanol) effected the activity and structure of DP.

6. Bibliography

1. Volchkova, V. Klenk, H. et al. (1995) Delta-Peptide Is the Carboxy-Terminal Cleavage Fragment of the Nonstructural Small Glycoprotein sGP of Ebola Virus. *Virology*. 265: 164–171.
2. (1995) Outbreak of Ebola Viral Hemorrhagic Fever -- Zaire, *Centres Dis. Control Prev.* 44: 468–469.
3. Groseth, A. Feldmann H. et al. (2007) The ecology of Ebola virus. *Trends Microbiol.* 15: 408–416.
4. Deng, I. Duku, O. et al. (1978) Ebola haemorrhagic fever in Sudan, 1976. Report of a WHO/International Study Team. *Bull. World Health Organ.* 56: 247–270.
5. Baseler, L. Chertow, D. et al. (2017) The Pathogenesis of Ebola Virus Disease*. *Annu. Rev. Pathol. Mech. Dis.* 24: 387–418.
6. World Health Organisation (2021) Ebola virus disease. .
7. Fischer, R. Judson, S. et al. (2015) Ebola Virus Stability on Surfaces and in Fluids in Simulated Outbreak Environments. *Emerg. Infect. Dis.* 21: 1243.
8. Nielsen, C. Kidd, S. et al. (2015) Improving Burial Practices and Cemetery Management During an Ebola Virus Disease Epidemic — Sierra Leone, 2014.
9. Gire, S. Goba, A. et al. (2014) Genomic surveillance elucidates Ebola virus origin and transmission during the 2014 outbreak. *Science.* 345: 1369–1372.
10. Leroy, E. Baize, S. et al. (2000) Human asymptomatic Ebola infection and strong inflammatory response. *Lancet.* 355: 2210–2215.
11. Chertow, D. Kleine, C. et al. (2014) Ebola virus disease in West Africa--clinical manifestations and management. *N. Engl. J. Med.* 371: 2054–2057.
12. Mattia, J. Vandy, M. et al. (2016) Early clinical sequelae of Ebola virus disease in Sierra Leone: a cross-sectional study. *Lancet Infect. Dis.* 16: 331–338.
13. Jacobs, M. Rodger, A. et al. (2016) Late Ebola virus relapse causing meningoencephalitis: a case report. *Lancet.* 388: 498–503.
14. Pigot, D. Golding, N. et al. (2014) Mapping the zoonotic niche of Ebola virus disease in Africa.

- Elife. 3: 1–29.
15. Pokhrel, R. Pavadai, E. et al. (2019) Membrane pore formation and ion selectivity of the Ebola virus delta peptide. *Phys. Chem. Chem. Phys.* 21: 5578–5585.
 16. Gallaher, W. and Garry, R. (2015) Modeling of the Ebola virus delta peptide reveals a potential lytic sequence motif. *Viruses.* 7: 285–305.
 17. He, J. Melnik, L. et al. (2017) Ebola Virus Delta Peptide Is a Viroporin. *J. Virol.* 91: 1–14.
 18. Shuck, K. Lamb, R. et al. (2000) Analysis of the Pore Structure of the Influenza A Virus M2 Ion Channel by the Substituted-Cysteine Accessibility Method. *J. Virol.* 74: 7755–7761.
 19. Mould, J. Drury, J. et al. (2000) Permeation and activation of the M2 ion channel of influenza A virus. *J. Biol. Chem.* 275: 31038–31050.
 20. Nieva, J. and Carrasco, L. (2015) Viroporins: Structures and functions beyond cell membrane permeabilization. *Viruses.* 7: 5169–5171.
 21. Mbaye, M. Hou, Q. et al. (2019) A comprehensive computational study of amino acid interactions in membrane proteins. *Sci. Rep.* 9: 1–14.
 22. Gonzalez, M. Carrasco, L et al. (2003) Minireview Viroporins.
 23. Wimley, W. and White, S. (1996) Experimentally determined hydrophobicity scale for proteins at membrane interfaces. *Nat. Struct. Biol.* 3: 842–848.
 24. Yount, N. Yeaman, M. et al. (2004) Multidimensional signatures in antimicrobial peptides. *Proc. Natl. Acad. Sci. U. S. A.* 101: 7363–7368.
 25. Hyser, J. Collinson-Pautz, M. et al. (2010) Rotavirus disrupts calcium homeostasis by NSP4 viroporin activity. *Am. Soc. Microbiol.* 1: 1–11.
 26. Jarvis, D. (2009) Chapter 14 Baculovirus–Insect Cell Expression Systems. *Methods Enzymol.* 463: 191–222.
 27. Zhu, J. (2012) Mammalian cell protein expression for biopharmaceutical production. *Biotechnol. Adv.* 30: 1158–1170.
 28. Barnes, L. and Dickson, A. (2006) Mammalian cell factories for efficient and stable protein

- expression. *Curr. Opin. Biotechnol.* 17: 381–386.
29. Cregg, J. Cereghino, J. et al. (2000) Recombinant protein expression in *Pichia pastoris*. *Mol. Biotechnol.* 16: 23–52.
 30. Baneyx, F. (1999) Recombinant protein expression in *Escherichia coli*. *Curr. Opin. Biotechnol.* 10: 411–421.
 31. Mikami, S. Kobayashi, T. et al. (2008) A human cell-derived in vitro coupled transcription/translation system optimized for production of recombinant proteins. *Protein Expr. Purif.* 62: 190–198.
 32. McCue, J. (2009) Chapter 25 Theory and Use of Hydrophobic Interaction Chromatography in Protein Purification Applications. *Methods Enzymol.* 463: 405–414.
 33. Regnier, F. (1983) High-Performance Liquid Chromatography of Biopolymers. *Science* (80-.). 222: 245–252.
 34. Bornhorst, J. and Falke, J. (2000) [16] Purification of proteins using polyhistidine affinity tags. *Methods Enzymol.* 326: 245–254.
 35. Kostallas, G. Löfdahl, P. et al. (2011) Substrate Profiling of Tobacco Etch Virus Protease Using a Novel Fluorescence-Assisted Whole-Cell Assay. *PLoS ONE* 6: 16136.
 36. Hwang, P. Pan, J. et al. (2014) Targeted expression, purification, and cleavage of fusion proteins from inclusion bodies in *Escherichia coli*. *FEBS Lett.* 588: 247–252.
 37. Louis-Jeune, C. Andrade-Navarro, M. et al. (2012) Prediction of protein secondary structure from circular dichroism using theoretically derived spectra. *Proteins Struct. Funct. Bioinforma.* 80: 374–381.
 38. Torres, A. and Price, W. (2016) Common problems and artifacts encountered in solution-state NMR experiments. *Concepts Magn. Reson. Part A Bridg. Educ. Res.* 45A: 1–16.
 39. Seddon, A. Curnow, P. et al. (2004) Membrane proteins, lipids and detergents: not just a soap opera. *Biochim. Biophys. Acta - Biomembr.* 1666: 105–117.
 40. Yeagle, P. (2016) *The Membranes of Cells*.
 41. Le Maire, M. Champeil, P. et al. (2000) Interaction of membrane proteins and lipids with

- solubilizing detergents. *Biochim. Biophys. Acta - Biomembr.* 1508: 86–111.
42. (2015) DL-Proline | C₅H₉NO₂. PubChem. .
 43. Wishart, D. Bigam, C. et al. (1995) ¹H, ¹³C and ¹⁵N random coil NMR chemical shifts of the common amino acids. I. Investigations of nearest-neighbor effects. *J. Biomol. NMR.* 5: 67–81.
 44. Schanda, P. and Brutscher. B (2005) Very Fast Two-Dimensional NMR Spectroscopy for Real-Time Investigation of Dynamic Events in Proteins on the Time Scale of Seconds. *J. Am. Chem. Soc.* 127: 8014–8015.
 45. Dodero, V. Quirolo, Z. et al. (2011) Biomolecular studies by circular dichroism. *Front. Biosci.* 16: 61–73.
 46. Hwang, S. Shao, Q. et al. (2011) Methanol Strengthens Hydrogen Bonds and Weakens Hydrophobic Interactions in Proteins – A Combined Molecular Dynamics and NMR study. *J. Phys. Chem. B.* 115: 6653–6660.
 47. Hirota, N. Mizuno, K. et al. (1998) Group additive contributions to the alcohol-induced α -helix formation of melittin: implication for the mechanism of the alcohol effects on proteins. *J. Mol. Biol.* 275: 365–378.
 48. Roccatano, D. Colombo, G. et al. (2002) Mechanism by which 2,2,2-trifluoroethanol/water mixtures stabilize secondary-structure formation in peptides: A molecular dynamics study. *Proc. Natl. Acad. Sci.* 99: 12179–12184.
 49. Sha, B. and Luo. M. (1997) Structure of a bifunctional membrane-RNA binding protein, influenza virus matrix protein M1. *Nature.* 4: 239–244.
 50. Jing, W. Hunter, H. et al. (2003) The structure of the antimicrobial peptide Ac-RRWWRF-NH₂ bound to micelles and its interactions with phospholipid bilayers. *J. Pept. Res.* 61: 219–229.
 51. Gervais, C. Do, F. et al. (2011) Development and Validation of a High-throughput Screening Assay for the Hepatitis c Virus p7 Viroporin. *J. Biomol. Screen.* 16: 363–369.